Innovation, Sciences et Développement économique Canada
Office de la Propriété Intellectuelle du Canada

Innovation, Science and Economic Development Canada
Canadian Intellectual Property Office

CA 3107778 A1 2020/01/30

(21) 3 107 778

(12) DEMANDE DE BREVET CANADIEN
CANADIAN PATENT APPLICATION

(13) A1

(86) Date de dépôt PCT/PCT Filing Date: 2019/07/20
(87) Date publication PCT/PCT Publication Date: 2020/01/30
(85) Entrée phase nationale/National Entry: 2021/01/26
(86) N° demande PCT/PCT Application No.: US 2019/042715
(87) N° publication PCT/PCT Publication No.: 2020/023323
(30) Priorités/Priorities: 2018/07/26 (US62/703,534); 2019/05/10 (US62/846,549)

(51) Cl.Int./Int.Cl. *C07D 487/04* (2006.01), *A61K 47/54* (2017.01), *A61K 47/55* (2017.01), *A61K 49/00* (2006.01), *A61P 31/16* (2006.01), *C07D 519/00* (2006.01), *C07H 15/04* (2006.01), *C07H 15/26* (2006.01), *C07K 5/02* (2006.01), *C07K 14/11* (2006.01), *C12N 9/24* (2006.01)

(71) Demandeur/Applicant:
PURDUE RESEARCH FOUNDATION, US

(72) Inventeurs/Inventors:
LOW, PHILIP STEWART, US;
LIU, XIN, US

(74) Agent: BERESKIN & PARR LLP/S.E.N.C.R.L.,S.R.L.

(54) Titre : CONJUGUES MEDICAMENTEUX CIBLANT UN LIGAND, DE TYPE PETITE MOLECULE, PERMETTANT UNE CHIMIOTHERAPIE ET UNE IMMUNOTHERAPIE CONTRE LA GRIPPE

(54) Title: SMALL MOLECULE LIGAND-TARGETED DRUG CONJUGATES FOR ANTI-INFLUENZA CHEMOTHERAPY AND IMMUNOTHERAPY

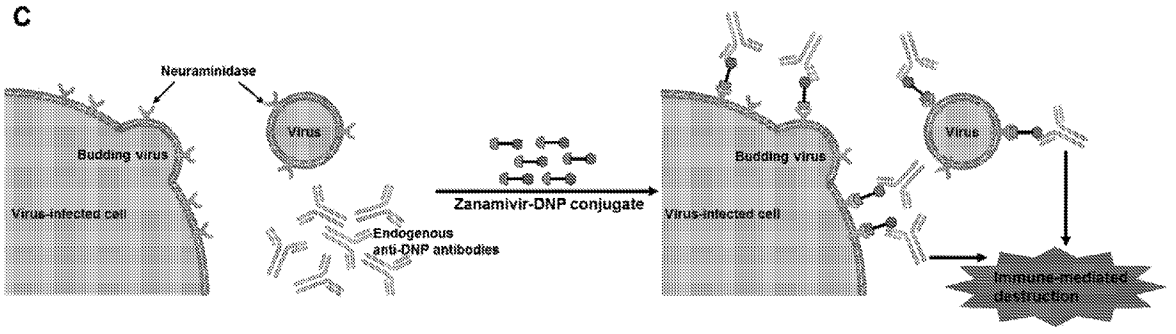

FIGURE 20C

(57) Abrégé/Abstract:
Disclosed herein is a small molecule targeted drug conjugate for anti-influenza chemotherapy and immunotherapy. The disclosed drug conjugate may form an adaptor to recruit additional CAR T cells or other immune cells for precise elimination of influenza virus-infected cells in a subject. Concurrently administered antibodies or pre-existing immunity in influenza-virus infected subject works well with the targeted conjugate to eliminate virus infected cells, saving valuable time for rescuing late stage patients.

(12) INTERNATIONAL APPLICATION PUBLISHED UNDER THE PATENT COOPERATION TREATY (PCT)

(19) World Intellectual Property Organization
International Bureau

(43) International Publication Date
30 January 2020 (30.01.2020)

WIPO | PCT

(10) International Publication Number
WO 2020/023323 A1

(51) International Patent Classification:
A61K 47/55 (2017.01) *C07D 309/28* (2006.01)
A61P 31/16 (2006.01)

(21) International Application Number:
PCT/US2019/042715

(22) International Filing Date:
20 July 2019 (20.07.2019)

(25) Filing Language: English

(26) Publication Language: English

(30) Priority Data:
62/703,534 26 July 2018 (26.07.2018) US
62/846,549 10 May 2019 (10.05.2019) US

(71) Applicant: **PURDUE RESEARCH FOUNDATION** [US/US]; 1801 Newman Road, West Lafayette, Indiana 47906 (US).

(72) Inventors: **LOW, Philip Stewart**; 5850 Farm Ridge Rd., West Lafayette, Indiana 47906 (US). **LIU, Xin**; 2812 Peachleaf Drive, West Lafayette, Indiana 47906 (US).

(74) Agent: **HOU, YONGHAO**; 1801 Newman Rd., West Lafayette, Indiana 47906 (US).

(81) Designated States *(unless otherwise indicated, for every kind of national protection available)*: AE, AG, AL, AM, AO, AT, AU, AZ, BA, BB, BG, BH, BN, BR, BW, BY, BZ, CA, CH, CL, CN, CO, CR, CU, CZ, DE, DJ, DK, DM, DO, DZ, EC, EE, EG, ES, FI, GB, GD, GE, GH, GM, GT, HN, HR, HU, ID, IL, IN, IR, IS, JO, JP, KE, KG, KH, KN, KP, KR, KW, KZ, LA, LC, LK, LR, LS, LU, LY, MA, MD, ME, MG, MK, MN, MW, MX, MY, MZ, NA, NG, NI, NO, NZ, OM, PA, PE, PG, PH, PL, PT, QA, RO, RS, RU, RW, SA, SC, SD, SE, SG, SK, SL, SM, ST, SV, SY, TH, TJ, TM, TN, TR, TT, TZ, UA, UG, US, UZ, VC, VN, ZA, ZM, ZW.

(84) Designated States *(unless otherwise indicated, for every kind of regional protection available)*: ARIPO (BW, GH, GM, KE, LR, LS, MW, MZ, NA, RW, SD, SL, ST, SZ, TZ, UG, ZM, ZW), Eurasian (AM, AZ, BY, KG, KZ, RU, TJ, TM), European (AL, AT, BE, BG, CH, CY, CZ, DE, DK, EE, ES, FI, FR, GB, GR, HR, HU, IE, IS, IT, LT, LU, LV, MC, MK, MT, NL, NO, PL, PT, RO, RS, SE, SI, SK, SM, TR), OAPI (BF, BJ, CF, CG, CI, CM, GA, GN, GQ, GW, KM, ML, MR, NE, SN, TD, TG).

Declarations under Rule 4.17:
— *as to applicant's entitlement to apply for and be granted a patent (Rule 4.17(ii))*
— *as to the applicant's entitlement to claim the priority of the earlier application (Rule 4.17(iii))*

Published:
— *with international search report (Art. 21(3))*

(54) **Title:** SMALL MOLECULE LIGAND-TARGETED DRUG CONJUGATES FOR ANTI-INFLUENZA CHEMOTHERAPY AND IMMUNOTHERAPY

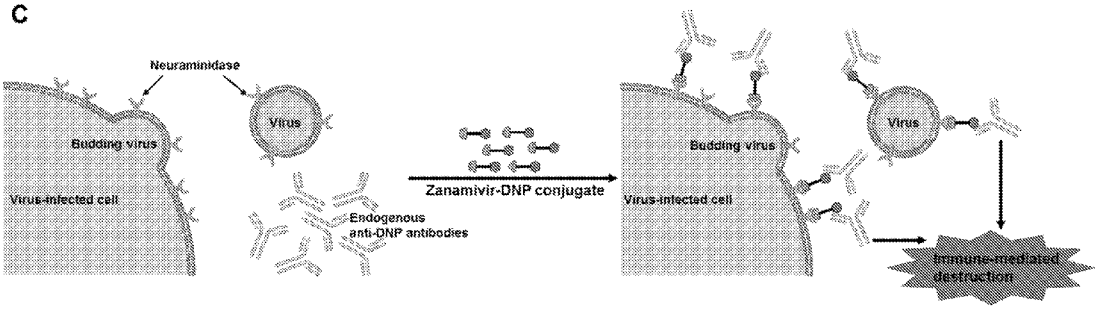

FIGURE 20C

(57) **Abstract:** Disclosed herein is a small molecule targeted drug conjugate for anti-influenza chemotherapy and immunotherapy. The disclosed drug conjugate may form an adaptor to recruit additional CAR T cells or other immune cells for precise elimination of influenza virus-infected cells in a subject. Concurrently administered antibodies or pre-existing immunity in influenza-virus infected subject works well with the targeted conjugate to eliminate virus infected cells, saving valuable time for rescuing late stage patients.

WO 2020/023323 A1

Small molecule ligand-targeted drug conjugates for anti-influenza chemotherapy and immunotherapy

FIELD OF INVENTION

This disclosure provides a targeted delivery of anti-influenza therapy. Particularly, a small molecule ligand that specifically binds to influenza virus is conjugated to a payload of drug to invoke either direct killing or immunomodulation of influenza virus infected cells.

BACKGROUND

Caused by Influenza virus infection, the acute febrile respiratory disease influenza (also known as "flu") is still one of the most life-threatening disseminated diseases. According to Influenza Fact Sheet released by World Health Organization (WHO), Influenza spreads worldwide in seasonal epidemics, resulting in about 3 to 5 million yearly cases of severe illness and about 250,000 to 500,000 yearly deaths.[1] In the united states, there are between 12,000 and 56,000 deaths and between 140,000 to 710,000 hospitalizations are directly associated with influenza per year.[2] In addition to causing high morbidity and mortality, influenza imposes a substantial social economic burden arising from the productivity lost and medical prevention and treatment. The total annual cost associated with influenza has been over $10 billion in the U.S.[3]

Current anti-influenza chemotherapy for influenza

Because influenza virus constantly changes via antigen shift and drift, vaccines often become ineffective against mutating strains. Therefore, anti-influenza chemotherapy still plays an important role in the prophylaxis and treatment of influenza.[4] At present, two classes of Anti-influenza drugs, M2 ion channel inhibitor and neuraminidase inhibitor, have been approved by U.S. Food and Drug Administration (FDA). M2 ion channel inhibitors include amantadine and rimantadine. The mechanism of action of these drugs results from blocking the acid-activated viral M2 ion channel, and as a consequence inhibiting the release of viral ribonucleoprotein from virion to host cytosol.[4] However, both H1N1 and H3N2 viruses currently circulating in humans are resistant to these inhibitors. Thus, Centers for Disease Control and Prevention (CDC) advises against their use due to the rapid emergence of drug resistance.[5] The commonly used neuraminidase inhibitors include oseltamivir and zanamivir. They act as competitive inhibitors competing with sialic acid to bind to the active site of neuraminidase.[4] While these inhibitors are

effective against both influenza A and influenza B viruses, they have two major limitations. First, only small benefits were observed for neuraminidase inhibitors in terms of symptom severity alleviation and sickness duration reduction (0.6~0.7 day out of 7 days).[6] Second, this class of antivirals also suffer from the drug resistant problem. An increase in the number of oseltamivir-resistant strains has been noted since 2007 to 2008 season. In light of the limitations of the current anti-influenza chemotherapies, there is an urgent need to develop new anti-influenza drugs with novel mechanisms of action.[7]

SUMMARY OF THE INVENTION

This disclosure provide a conjugate comprising a targeting ligand (TL) for an envelope protein of an influenza virus, a linker (L) and a payload of drug (D), wherein the TL is a molecule that binds to the envelope protein, the linker is covalently bound to both the D and the TL, and the D is an imaging agent, a therapeutic drug, an immune modulator or the combination thereof.

In some preferred embodiment the aforementioned linker comprises a spacer and a cleavable or noncleavable bridge between the TL and the D.

In some preferred embodiment the aforementioned envelope protein of the influenza virus is Neuraminidase (NA) or Hemagglutinin (HA).

In some preferred embodiment the aforementioned TL is zanamivir.

In some preferred embodiment the aforementioned TL is selected from the group consisting of oseltamivir, zanamivir, peramivir and laninamivir.

In some preferred embodiment, the aforementioned conjugate comprises an imaging agent used to quantify the intensity of the influenza infection.

In some preferred embodiment the aforementioned imaging agent comprises a chelation complex containing technetium-99m (^{99m}Tc).

In some preferred embodiment, the aforementioned conjugate has a binding affinity to the NA at about 1 nM to about 15nM.

In some preferred embodiment the aforementioned D is selected from the group consisting of Tubulysin B hydrazide, pimodivir, Ozanimod and SN38.

In some preferred embodiment the aforementioned conjugate is one of the following:

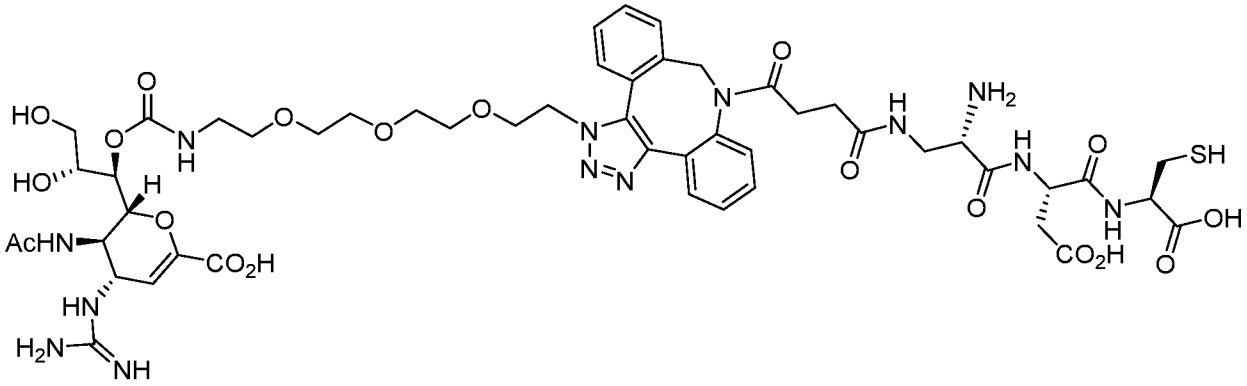

zanamivir-EC20,

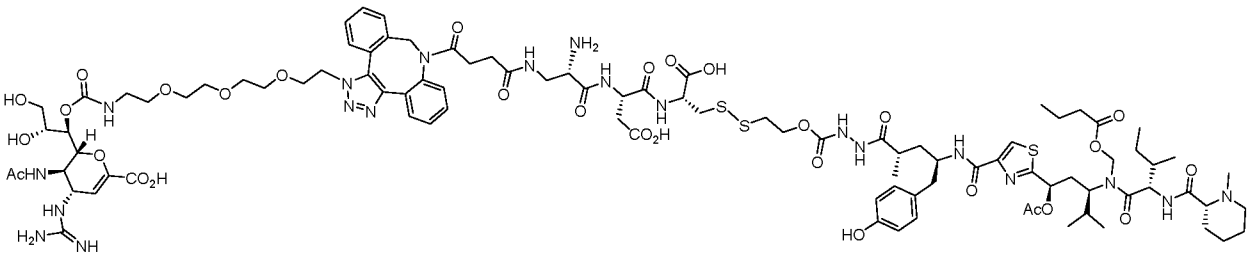

zanamivir-tubulysin B hydrazide,

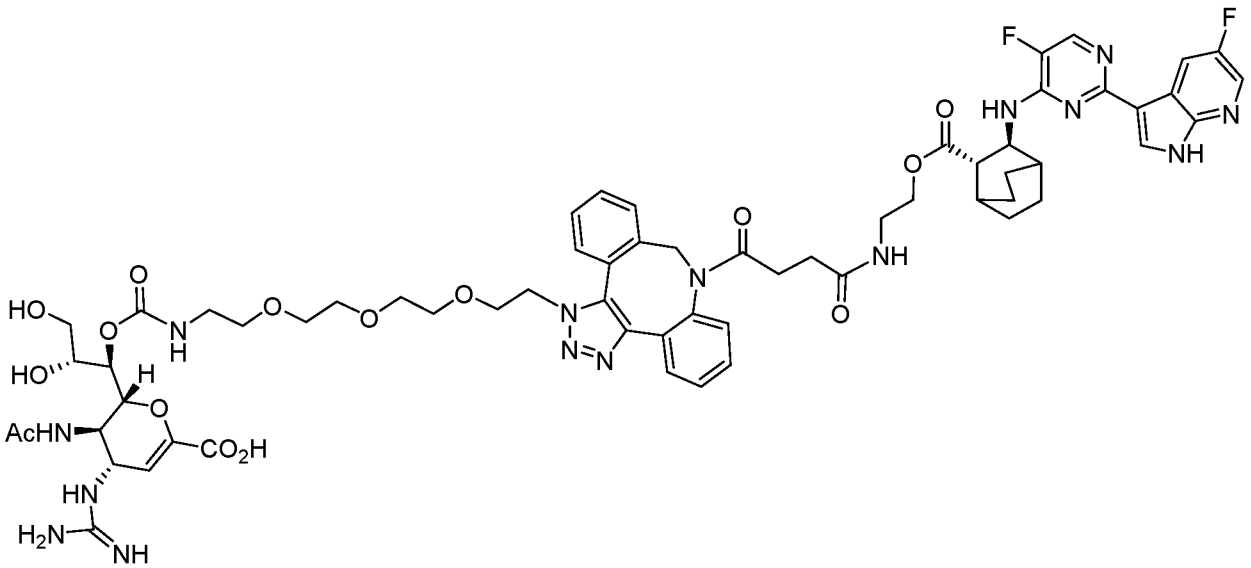

zanamivir-pimodivir,

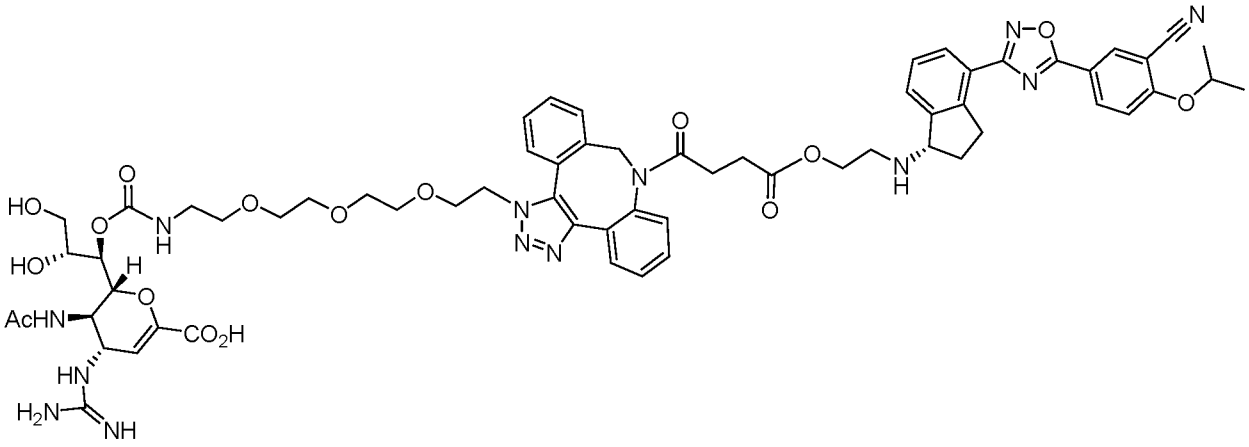

zanamivir-ozanimod,

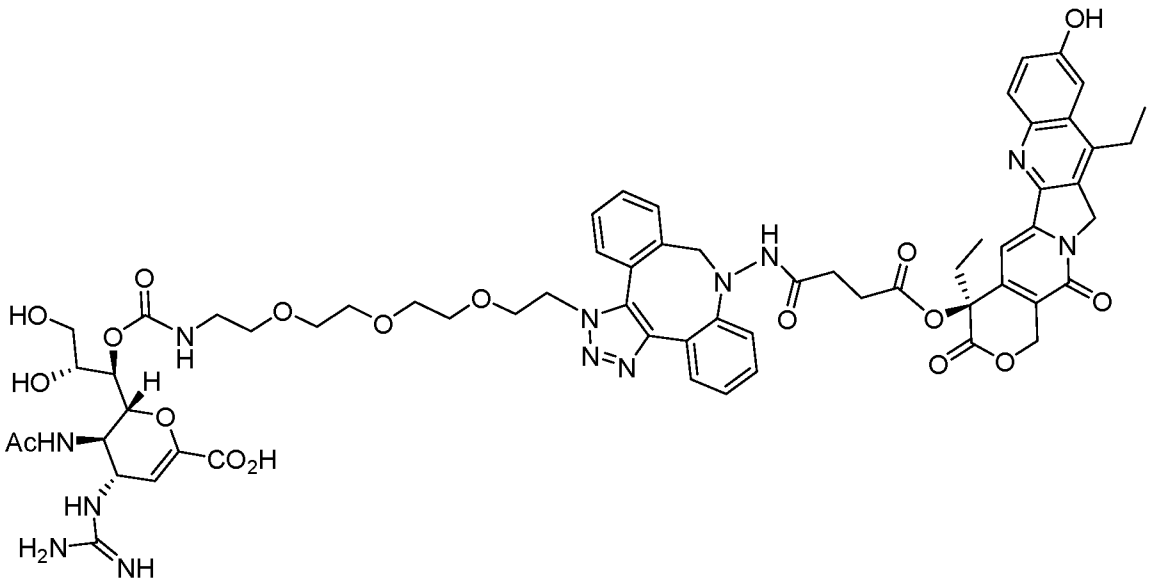

zanamivir-SN38,

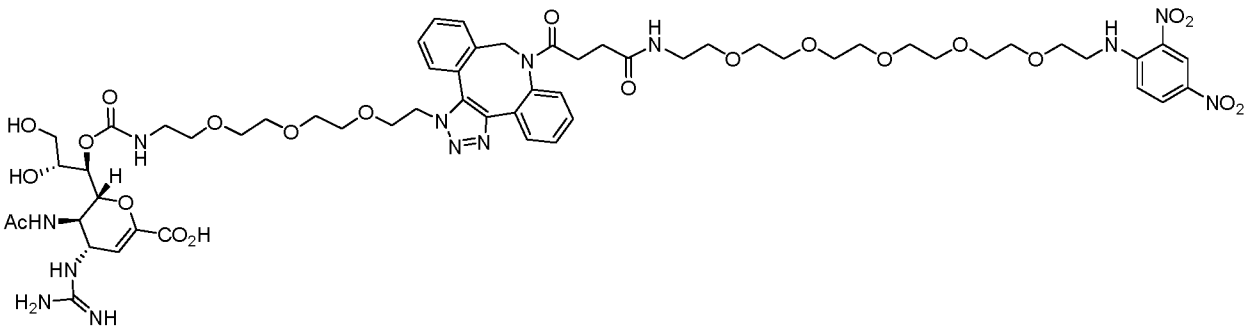

zanamivir-DNP,

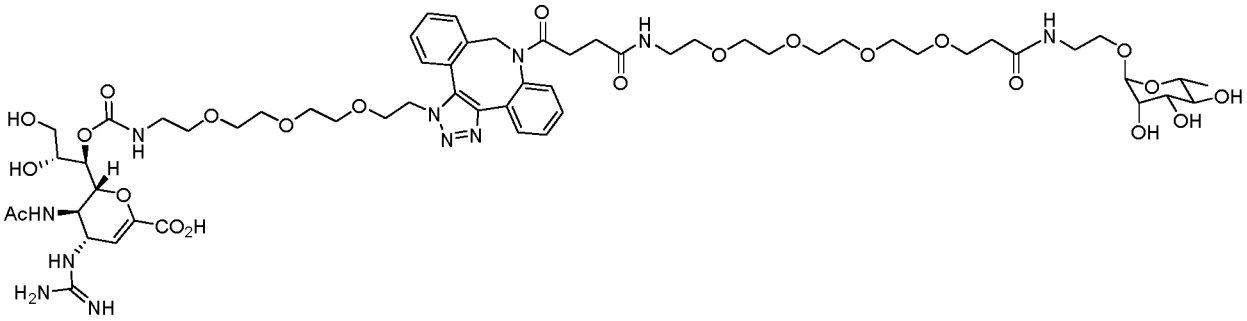

zanamivir-rhamnose,

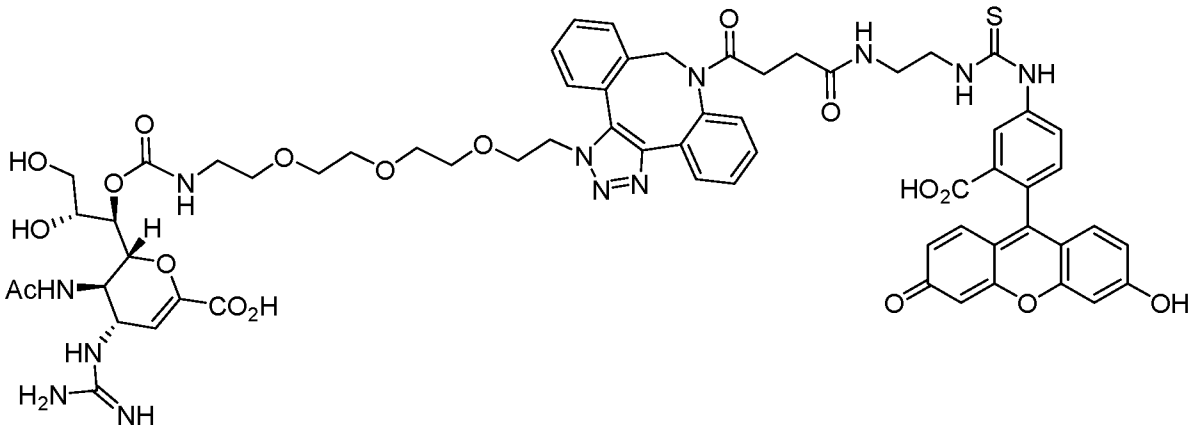

zanamivir-FITC, or

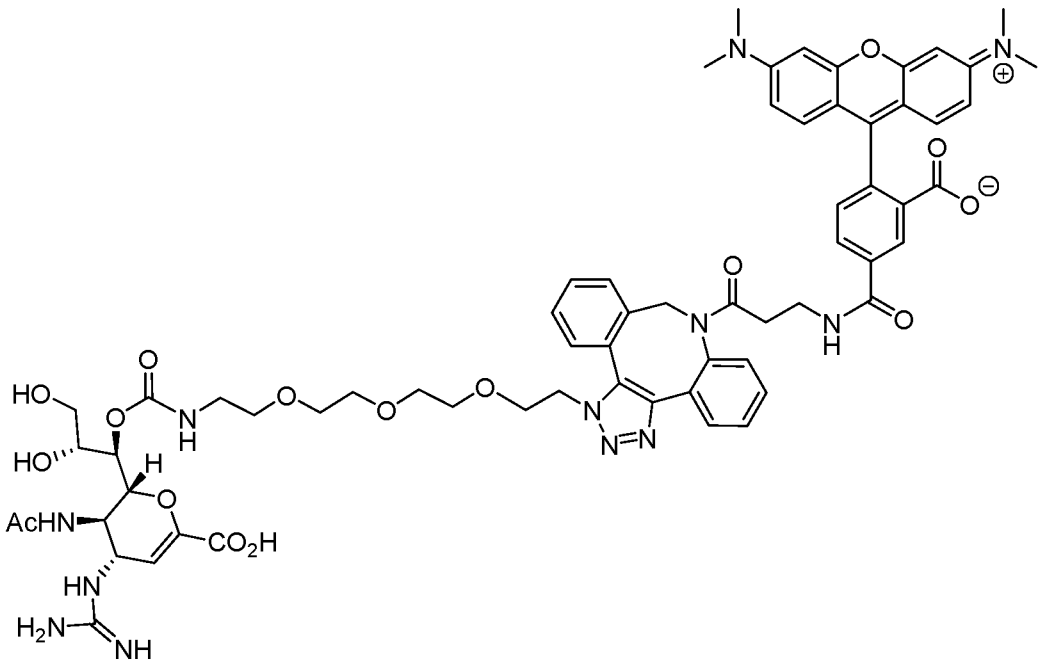

zanamivir-rhodamine.

In some preferred embodiment the aforementioned cleavable bridge contains a disulfide or acid labile bond.

In some preferred embodiment the aforementioned acid labile bond comprises an ester, hydrazone, oxime, acetal, ketal, phenolic ether, or Schiff base bond.

This disclosure further provides a method to treat influenza virus infection in a subject, the method comprising providing a conjugate to the subject, wherein said conjugate comprises a targeting ligand (TL) of NA of the influenza virus, a linker (L) and a payload of drug (D), wherein the TL is a molecule that binds NA, the L is covalently bound to both the D and the TL, and the D is an imaging agent, a therapeutic drug, an immune modulator or the combination thereof.

In some preferred embodiment, the aforementioned method uses zanamivir as the TL.

In some preferred embodiment, the aforementioned method used therapeutic drug to kill influenza virus infected cells in the subject, or to inhibit influenza virus replication.

In some preferred embodiment, the aforementioned method uses therapeutic drug selected from the group consisting of Tubulysin B hydrazide, pimodivir, and SN38.

In some preferred embodiment, the aforementioned method used a therapeutic drug comprising an adaptor molecule (i.e. fluorescein covalently bound to the TL), and an anti-fluorescein CAR T cell, wherein upon binding to the adaptor molecule, said CAR-T cell kills influenza virus infected cell that expresses neuraminidase that binds with TL, and thereby inhibits influenza virus replication in the subject.

In some preferred embodiment, the aforementioned method used immune modulator to dampen influenza virus induced early cytokine storm.

In some preferred embodiment, the aforementioned method used immune modulator ozanimod or a hapten recognized by an autologous antibody.

In some preferred embodiment, the aforementioned hapten is comprised of dinitrophenyl (DNP), trinitrophenyl (TNP), rhamnose, or an alpha-galactosyl moiety.

In some preferred embodiment the aforementioned method used the zanamivir conjugate to elicit immune responses leading to the clearance of antibody-coated virus or virus infected cells

via antibody dependent cellular phagocytosis (ADCP), antibody dependent cellular cytotoxicity (ADCC) or complement-dependent cytotoxicity (CDC).

In some preferred embodiment the aforementioned method used an antigen or another moiety to conjugate with zanamivir, wherein the subject has pre-existing immunity to the antigen or the moiety or the subject is concurrently administered with an effective dose of antibody to the antigen or the moiety. For example, this antigen or moiety can be a toxin (e.g. tetanus toxoid).

This disclosure further provides a system comprising at least two components, a first component comprising a conjugate containing a targeting ligand (TL) for an envelope protein of an influenza virus, a linker (L) and a payload of drug (D), wherein the TL is a molecule that binds the envelop protein, the L is covalently bound to both the D and the TL, and the D is a fluorescein; a second component comprising an anti-fluorescein CAR-T cell that binds the first component's fluorescein, wherein said system is promoted to kill an influenza virus-infected cell.

Representative zanamivir-DNP conjugate's in vitro binding assay has shown its high binding affinity for both N1 and N2 classes of neuraminidase. The conjugate is much more potent than zanamivir or oseltanmivir; it is effective even when added after the infection has developed much further in the patient; it can cure the infection with a single injection of our drug, and is effective against all strains of the flu.

These and other features, aspects and advantages of the present invention will become better understood with reference to the following figures, associated descriptions and claims.

BRIEF DESCRIPTION OF THE DRAWINGS

Fig.1 Action mechanism of zanamivir-therapeutic drug conjugate (a) schematic of the drug conjugate (b) proposed mechanism of action.

Fig. 2 Therapeutic drug payloads selected for zanamivir-targeted therapeutic drug conjugates.

Fig.3 Action mechanism of zanamivir-hapten conjugate–targeted immunotherapy (a) schematic of zanamivir-DNP conjugate (b) proposed mechanism of action.

Fig. 4 Design of the targeting ligand based on zanamivir. The 7-OH group of zanamivir is highlighted in yellow.

Fig. 5 Crystal structure of zanamivir complexed with neuraminidase.

Fig. 6 Binding of zanamivir-rhodamine conjugate to influenza virus A/Puerto Rico/8/34 (H1N1) infected MDCK cells. (a) Confocal microscope images of drug group. Influenza virus infected MDCK cells incubated with 50 nM zanamivir-rhodamine conjugate; (b) Confocal microscope images of competition group. Influenza virus infected MDCK cells incubated with 50 nM zanamivir-rhodamine conjugate in the presence of 5 μM zanamivir; (c) Binding saturation curve.

Fig. 7 Binding of ^{99m}Tc chelated zanamivir-EC20 head conjugate to influenza virus A/Puerto Rico/8/34 (H1N1) infected MDCK cells. (a) Binding saturation curve; (b) Structure of ^{99m}Tc chelated zanamivir-EC20 head conjugate.

Fig. 8 Biodistribution of ^{99m}Tc chelated zanamivir-EC20 head conjugate in influenza virus A/Puerto Rico/8/1934 (H1N1) infected mice/uninfected mice.

Fig. 9 In vitro cytotoxicity of zanamivir-tubulysin B hydrazide conjugate and its component parts on neuraminidase transfected HEK 293 cells. The cytotoxicity of zanamivir-tubulysin B hydrazide conjugate (red circles), free tubulysin B hydrazide (orange triangles) and zanamivir-tubulysin B hydrazide conjugate in the presence of 100-fold excess of zanamivir (blue squares) are graphed.

Fig. 10 Competitive binding of zanamivir-DNP conjugate to neuraminidase transfected HEK 293 cells. (a) log(does)-response curve of zanamivir-DNP conjugate; (b) log(does)-response curve of zanamivir. zanamivir-rhodamine conjugate was used as the labelled ligand.

Fig. 11 Flow cytometry analysis demonstrating the ability of zanamivir-DNP conjugate to bind simultaneously to cell surface neuraminidase and antiDNP antibody. (a) Schematic depiction of flow cytometry-based antibody recruitment assay; (b) Flow cytometry analysis using neuraminidase transfected HEK293 cells (293tn NA); (c) Flow cytometry analysis using non-transfected HEK293 cells (293tn).

Fig. 12 In vivo protection efficacy of zanamivir-DNP conjugate against influenza virus A/Puerto Rico/8/1934 (H1N1) infection in BALB/c mice when administered 2h after infection. (a) Body weight curve; (b) survival curve.

Fig. 13 proposed scheme of targeted CAR-T therapy for influenza infected cells.

Fig. 14. *In vitro* anti-FITC CAR-T killing profile with fluorescein adaptor-mediated FITC-zanamivir conjugates for cells expressing influenza surface protein NA. (A) CAR T: 293 NA=5:1 has 41% killing of 293NA cells; (B) CAR T:293 NA=10:1 has 61% killing of 293NA cells.

Fig. 15. No binding of Zanamivir-FITC to normal 293T cells.

Fig. 16. The cytotoxicity against NA is specifically induced by Zanamivir-FITC.

Fig. 17. *in vitro* assay using real virus

Fig. 18. LDH assay of T cell Killing Influenza Infected MDCK versus CAR-T killing of influenza infected MDCK.

Fig. 19. Proposed mouse model for testing CAR T cell therapy of influenza-infected mouse.

Fig. 20. Mechanism of action anti-influenza immunotherapy includes: **A**. a small molecule ligand targeted drug conjugate: **B.** the structure of zanamivir–DNP conjugate: zanamivir (target ligand) is conjugated to Hapten (2,4-dinitrophneyl group) through a linker; **C**. upon the conjugate binding to the viral neuraminidase, the innate antibodies to DNP inhibits influenza virus replication. Thus the system redirects anti-dinitrophenyl (anti-DNP) antibodies to the influenza virus/virus-infected cells, induces the immune-mediated destruction of influenza virus/virus-infected cells.

Fig. 21. Various in-vitro binding assays in Influenza virus A/Puerto Rico/8/34 (H1N1) infected MDCK cells. **A**. Zanamivir-Rhodamine conjugate binding; **B**. free zanamivir binding and C. zanamivir-DNP-conjugate binding.

Fig. 22. Various in-vitro binding assays in Influenza virus A/Aichi/2/1968 **(H3N2)**infected MDCK cells. **A**. Zanamivir-Rhodamine conjugate binding; **B**. free zanamivir binding and C. zanamivir-DNP-conjugate binding.

Fig. 23. Anti-DNP antibody recruiting assay conducted in Influenza virus A/Puerto Rico/8/34 (H1N1) infected MDCK cells. **A.** assay flow chart; **B.** cell stain result from various conjugate addition (PE-red, TO-RPO-3 lolide-blue to show cell nucleus) and binding curve

Fig. 24. Anti-DNP antibody recruiting assay conducted in Influenza virus A/Aichi/2/1968 **(H3N2)**infected MDCK cells. **A.** assay flow chart; **B.** cell stain result from various conjugate addition (PE-red, TO-RPO-3 lolide-blue to show cell nucleus) and binding curve.

Fig. 25. Complement-dependent cytotoxicity assay (CDC). **A**. flow scheme of completment-dependent cytotoxicity assay conducted in NA transfected 293 cells. B. only 10nM drug conjugate is needed to mediate the maximum cell killing.

Fig. 26. Antibody-dependent phagocytosis assay (ADCP). **A.** ADCP work flow. **B**. THP-1 cells (human macrophage) were treated with PMA and labeled with DiD before use. 293tnNA (GFP+) were incubated with THP-1 cells (ratio 1:1) with various concentrations of zanamivir-DNP conjugate, and anti-DNP antibody (100nM) at 4 ^{o}C for 30 min. The ADCP effect was analysed by flow cytometry.

Fig. 27. Mouse protection study procedure: mice were immunized by subcutaneous injection of 2,4-Dinitrophenyl-Keyhole limpet Hemocyanin (DNP-KLH); Mice were infected with a lethal dose of influenza virus (100 LD50, A/Puerto Rico/8/1934 (H1N1)) at week 5; Treatment with zanamivir-DNP conjugate and other drugs starts after the infection and the mice were monitored for 2 weeks; Mice were counted as dead when losing either 25% of their initial weight or when they were moribund. B. Operation on a mouse.

Fig. 28. Dose escalation study (intranasal administration) Mice (5 mice/group) were infected with 50 uL H1N1 PR8 virus (100 LD_{50}, 4.2 x 10^{5} PFU) at day 0. Mice were intranasally given PBS/zanamivir/zanamivir-DNP conjugate 24h post-infection, twice daily for five days. Mice were counted as dead when losing either 25% of their initial weight or when they were

moribund. **A.** graphing of body weight percentage **B.** Percentage of survival mice according to the definition.

Fig. 29. Comparing the efficacy between zanamivir-DNP conjugates and its components (intranasal administration). Procedure: Mice (5 mice/group) were infected with 50 uL H1N1 PR8 virus (100 LD_{50}, 4.2 x 10^5 PFU) at day 0. Mice were intranasally given zanamivir-DNP conjugate and its components 24h post-infection, twice daily for five days. Mice were counted as dead when losing either 25% of their initial weight or when they were moribund. **A.** graphing of body weight percentage **B.** Percentage of survival mice according to the definition.

Fig. 30. Delayed-start-to-treat study (intranasal administration) procedure: DNP-KLH immunized mice were infected with 50 uL H1N1 PR8 virus (100 LD_{50}, 4.2 x 10^5 PFU) at day 0. Mice were intranasally given 1.5 umol/kg zanamivir-DNP conjugate 48h/72h/96h post-infection, twice daily for 7 days. Mice were counted as dead when losing either 25% of their initial weight or when they were moribund. **A.** graphing of body weight percentage **B.** Percentage of survival mice according to the definition.

Fig. 31. One dose treatment (intranasal administration) procedure: Mice (5 mice/group) were infected with 50 uL H1N1 PR8 virus (100 LD_{50}, 4.2 x 10^5 PFU) at day 0. Mice were intranasally given PBS/zanamivir-DNP conjugate 24h post-infection for only one time. Mice were counted as dead when losing either 25% of their initial weight or when they were moribund. **A.** graphing of body weight percentage **B.** Percentage of survival mice according to the definition.

Fig. 32. Bio-distribution and SPECT/CT imaging. **A.** new zanamivir-E20 head conjugate structure. **B.** cell bound radioactivity according to procedure below:

- Mice were infected by influenza virus (H1N1) 3d before the experiment.
- The mice were intravenous inject with 10 nmol zanamivir-EC20 head conjugate (150 μCi).
- The radioactivity was counted 4h post-injection.

C. binding curve of zanamivir-E20 head in the presence of competitor 100x free zanamivir. **D.** SPECT/CT imaging post injection of conjugate without (left) and with 100x free zanmivir according to the procedure below:

- Mice were infected by influenza virus (H1N1) 3d before the experiment.
- The mice were intravenous injected with 50 nmol zanamivir-EC20 head conjugate (750 μCi).
- The SPECT/CT imaging was performed 4h post-injection

Fig. 33. Dose escalation study (intraperitoneally administration) according to the following procedure: Mice (5 mice/group) were infected with 50 uL H1N1 PR8 virus (100 LD_{50}, 4.2 x 10^5 PFU) at day 0. Mice were intraperitoneally given PBS/zanamivir/zanamivir-DNP conjugate 24h post-infection, twice daily for five days. Mice were counted as dead when losing either 25% of their initial weight or when they were moribund. **A.** graphing of body weight percentage **B.** Percentage of survival mice according to the definition.

Fig. 34. Comparing the efficacy between zanamivir-DNP conjugates and its components (intraperitoneally administration) according to the following procedure: Mice (5 mice/group) were infected with 50 uL H1N1 PR8 virus (100 LD_{50}, 4.2 x 10^5 PFU) at day 0. Mice were intraperitoneally given PBS/zanamivir/zanamivir-DNP conjugate 24h post-infection, twice daily for five days. Mice were counted as dead when losing either 25% of their initial weight or when they were moribund. **A.** graphing of body weight percentage **B.** Percentage of survival mice according to the definition.

Fig. 35. Antibody-dependent cellular toxicity assay (ADCC). **A**. The ADCC Reporter Bioassay uses engineered Jurkat cells stably expressing the FcγRIIIa receptor and an NFAT (nuclear factor of activated T-cells) response element driving expression of firefly luciferase as effector cells. Antibody biological activity in ADCC MOA is quantified through the luciferase produced as a result of NFAT pathway activation. **B**. ADCC work scheme and results for DNP-Zanamivir.

Fig. 36. In vitro antiviral assay for H1N1 and H3N2 infected MDCK cells. **A.** A/Puerto Rico/8/34 (H1N1) and **B.** A/Aichi/2/1968 (H3N2).

FIG. 37. Single dose treatment (intranasal administration) for H3N2 virus infected mice. **A.** Treatment effects measured by body weight maintenance. **B.** treatment effects measured by survival percentage.

Fig. 38. Single dose treatment (intraperitoneally administration) for H1N1 PR8 virus infected mice. **A.** Treatment effects measured by body weight maintenance. **B.** treatment effects measured by survival percentage.

Fig. 39. Single dose treatment (intraperitoneally administration) for H3N2 virus infected mice.

A. Treatment effects measured by body weight maintenance. **B.** treatment effects measured by survival percentage.

Fig. 40. Anti-DNP antibody and zana-DNP treated unimmunized mice infected by H1N1 PR8 virus. Unimmunized mice were intravenously given different doses of anti-DNP antibody one day after infected with lethal dose of H1N1 PR8 virus, and immediately treated by single dose of intraperitoneally administered zanamivir-DNP conjugate. **A.** Treatment effects measured by body weight maintenance. **B.** treatment effects measured by survival percentage.

Fig. 41. Synthesis scheme of zanamivir-rhamnose conjugate, a different conjugate that utilizes innate immune system produced anti-rhamnose to markup influenza virus infected cells and induce immune attacks to influenza viruses infected cells.

Fig. 42. Competitive binding of zanamivir-DNP rhamnose conjugate to neuraminidase transfected HEK293 cells using zanamivir-rhodamine conjugate as the labelled ligand. A. Zanamivir Kd about 0.77nM. B. Zanamivir-rhamnose Kd about 3.57nM.

Fig. 43. Immunotherapy study with zanamivir-rhamnose conjugate. Rhamnose-OVA immunized mice (5 mice/group) were infected with 50 uL H1N1 PR8 virus (100 LD_{50}, 4.2 x 10^5 PFU) at day 0. Mice were intranasally given 1.5/0.5/0.17 umol/kg zanamivir-rhamnose conjugate/zanamivir/PBS 24h post-infection, twice daily for 5 days and mice were counted as dead when losing either 25% of their initial weight or when they were moribund. **A.** Treatment

effects measured by body weight maintenance. **B.** treatment effects measured by survival percentage.

DETAILED DESCRIPTION

While the concepts of the present disclosure are illustrated and described in detail in the figures and the description herein, results in the figures and their description are to be considered as exemplary and not restrictive in character; it being understood that only the illustrative embodiments are shown and described and that all changes and modifications that come within the spirit of the disclosure are desired to be protected.

Unless defined otherwise, the scientific and technology nomenclatures have the same meaning as commonly understood by a person in the ordinary skill in the art pertaining to this disclosure.

Influenza Virus in General

Influenza virus is an enveloped virus. All influenza subtypes are very similar in overall structure. The virus particle is 80–120 nanometers in diameter and usually roughly spherical, although filamentous forms can occur. These filamentous forms are more common in influenza C, which can form cordlike structures up to 500 micrometers long on the surfaces of infected cells. However, despite these varied shapes, the viral particles of all influenza viruses are similar in composition. These are made of a viral envelope containing two main types of glycoproteins, wrapped around a central core. The central core contains the viral RNA genome and other viral proteins that package and protect this RNA. RNA tends to be single stranded but in special cases, it is double stranded. Unusually for a virus, its genome is not a single piece of nucleic acid; instead, it contains seven or eight pieces of segmented negative-sense RNA, each piece of RNA containing either one or two genes, which code for a gene product (protein). For example, the influenza A genome contains 11 genes on eight pieces of RNA, encoding for 11 proteins: hemagglutinin (HA), neuraminidase (NA), nucleoprotein (NP), M1, M2, NS1, NS2 (NEP: nuclear export protein), PA, PB1 (polymerase basic 1), PB1-F2 and PB2.

Hemagglutinin (HA) and neuraminidase (NA) are the two large glycoproteins on the outside of the viral particles. HA is a lectin that mediates binding of the virus to target cells and

entry of the viral genome into the target cell, while NA is involved in the release of progeny virus from infected cells, by cleaving sugars that bind the mature viral particles. Thus, these proteins are targets for antiviral drugs. Furthermore, they are antigens to which antibodies can be raised. Influenza A viruses are classified into subtypes based on antibody responses to HA and NA. These different types of HA and NA form the basis of the *H* and *N* distinctions in, for example, *H5N1*. There are 16 H and 9 N subtypes known, but only H 1, 2 and 3, and N 1 and 2 are commonly found in humans.

Small molecule ligand-targeted drug conjugate for antiviral therapy

Small molecule ligand-targeted drug conjugate, which combines the receptor-specific ligand with therapeutic payload, has shown promise in the treatment of many diseases especially in cancer chemotherapy. By specifically delivering the therapeutic payload to cells that are recognized by targeting ligand, these drug conjugates demonstrate high selectivity toward malignant cells as well as reduced associated collateral toxicity. To date, many cancers have been tackled by small molecule ligand-targeted drug conjugates that target overexpressing receptors on tumor cells. These overexpressing receptors include folate receptor (FR), prostate-specific membrane antigen (PSMA), cholecystokinin 2 receptor (CCK2R), carbonic anhydrase IX (CA IX), etc. [8]

For enveloped virus, the last step of its replication involves assembling of viral components on the infected cell membrane and budding from the infected cell surface.[9] Meanwhile, some virus envelope glycoproteins, such as HIV gp120 and influenza neuraminidase/hemagglutinin, are expressed on the exterior surface of infected cells.[10] In light of the fact that these exogenous viral proteins are exclusively expressed on the infected cells, they have the potential to be targeted by ligand targeted drug conjugates.

Design of zanamivir-therapeutic drug conjugates

The general scheme of the instant disclosure is to provide a specific targeting ligand conjugated to an effective payload of therapeutic drug or modulator to treat virus infections. The targeting ligand will specifically recognize the envelop protein of the virus, which is exclusively expressed on the surface of the infected cells. In some occasions, the payload of therapeutic drug or modulator can be an adapted chimeric antigen receptor-expressing T cell (CAR T cell). For

example, if the payload of drug is a fluorescein adaptor, an anti-fluorescein CAR T cell can be administered along with the targeted ligand guided payload drug to either kill the virus infected cells, or inhibit the replication of the virus in the infected cells. For a detailed description of an adaptor molecule-mediated CAR T cell therapy and its makes thereof, please see US Application 15/296,666, filed on Oct. 16, 2016, the entire contents of which is incorporated herein by reference.

Here we designed a series of small molecule ligand targeted drug conjugates targeting influenza virus envelop protein, particularly neuraminidase (NA). Without being bound by any theory, it is contemplated that other small molecule ligands that specifically target Hemagglutinin (HA) may also work under this principle. For example, compounds that inhibit HA mediated influenza virus entry may be considered as potential targeting ligands effecting on HA of infected cells.

Accordingly, high affinity neuraminidase inhibitor zanamivir was herein repurposed to carry and deliver the therapeutic drugs specifically into the virus infected cells as well as the virus replication sites (e.g. nose, throat, and lungs). This presents a unique mechanism of action by which one can kill the virus infected cells prior to the progeny virus release, hinder the viral replication, or dampen the early cytokine storm induced by the virus infection (Fig. 1).

The therapeutic drug payloads selected for this project are shown in Figure 2 (1) Tubulysin B hydrazide is an antimitotic tetrapeptide that inhibits tubulin polymerization. It either kills the influenza virus infected cells by inducing cell apoptosis, or inhibits the transportation of viral components by destructing the microtubule network of influenza virus infected cells.[11] (2) Pimodivir is a RNA-dependent RNA polymerase (RdRp) inhibitor that blocks m^7GTP binding pocket in the PB2 subunit of influenza A viral polymerase complex. It interferes with virus replication by inhibiting PB2 cap-snatching activity.[12, 13] In view of the fact that the high morbidity and mortality caused by influenza are the result of both virus induced tissue destruction and hyper-induction of proinflammatory cytokine production (cytokine storm), two immunomodulatory drugs, Ozanimod and SN38, are selected in order to improve the outcome of influenza treatment.[14, 15] (3) Ozanimod is an investigational immunomodulatory drug acting as a sphingosine-1-phosphate (S1P) receptor agonist.[16] Researchers found that S1P receptor agonists can blunt but not abolish the excess virus induced cytokine production, providing significant protection against influenza virus infection in mice.[17, 18] (4) SN38 is a topoisomerase I inhibitor, which is the active

metabolite of irinotecan (an analog of camptothecin).[19] SN 38 was demonstrated to limit the overexpression of influenza virus induced inflammatory genes through inhibiting the recruitment of RNA polymerase II to innate immune genes.[20] In addition, SN38 can also kill the influenza virus infected cells by inducing cell apoptosis.

When these molecules including but not limited to Tubulysin B hydrazide, Pimodivir, Ozanimod, or SN38 are conjugated with the targeting ligand of virus envelop protein, they can play various roles of killing virus infected cells, or inhibiting the virus replication within the infected cells.

Design of Zanamivir-hapten conjugate–targeted immunotherapy for the treatment of influenza

Other than therapeutic drugs that can directly kill influenza virus infected cells or inhibit the replication of the virus within infected cells, immunotherapy can be effective to elicit immune system to fight the specific infection by antibodies existing in the body. One possible candidate for such immunotherapy is to wake up the circulating anti-DNP antibodies by making a conjugate of TL with dinitrophenyl (DNP).

Because of the potential targeting ability of zanamivir to influenza virus or virus infected cells, a zanamivir-dinitrophenyl (DNP) conjugate was also developed in our lab (Fig. 3). As shown in Figure 3b, zanamivir-DNP conjugate is believed to form a bispecific molecular "bridge" between influenza virus/virus infected cells and endogenous circulating anti-DNP antibodies. This "marking" step initiates the immune response leading to the clearance of the antibody-coated virus or virus infected cell via mechanisms such as antibody-dependent cellular phagocytosis (ADCP), antibody-dependent cellular cytotoxicity (ADCC) and complement-dependent cytotoxicity (CDC).[21-23]

There are two major advantages of zanamivir-DNP conjugate–targeted immunotherapy over influenza vaccines. First, current influenza vaccines are prepared based on predicting which subtypes of the virus will likely appear in the next season. Because this prediction occasionally fails, the vaccines can not precisely match the virus. However, zanamivir is effective for all 11 influenza NA subtypes with high affinities, and there are very few zanamivir resistant viruses are

found in the clinic.[7] Second, since anti-DNP antibodies are already present in the human bloodstream, the pre-vaccination is not necessary for this therapy.[24]

Without being bound by any theory, it is contemplated that zanamivir conjugated to any other moieties such as trinitrophenyl (TNP), rhamnose, or an alpha-galactosyl may recruit their respective antibodies to the influenza infected cells to elicit antibody-dependent immune responses. Thus, immunotherapy disclosed herein can target influenza virus infected cells that by zanamivir conjugate markings.

Influenza virus induced tumor types for targeted CAR T cell therapy

In connection with our newly developed adapted CAR T cell therapy, as described in US application 15/296, 666 or its related applications (the contents of which are expressly incorporated herein by reference), targeted delivery of CAR T cells to influenza virus infected cells to execute CAR T cells immune response functions is contemplated in this disclosure.

Fig. 13 depicts the CAR T cell strategy treating influenza virus infected cells. In Fig. 13, a zanamivir-FITC conjugate is produced and attached to an influenza virus-infected cell that expresses virus neuraminidase on the surface. It is noted that zanamivir-FITC may serve at least two different functions in this process, one is to serve as an imaging agent to illustrate the infection intensity of influenza virus; the other is to mark the virus-infected cells with zanamivir, an NA inhibitor that can block the virus budding from the envelop. The presence of zanamivir-FITC conjugate at the infected cell surface may direct a T cell adapted with anti-FITC antibody to virus infected cell and form immunological synapse. As a person skill in the art may know, such anti-FITC CAR T cells can be activated by the binding to zanamivir-FITC conjugate. Activated CAR T cell therefore may secret cytokines and subsequently kill virus-infected cells, preventing virus replication.

Without being limited by any theory, the advantages of using small molecule targeted drug or immune regulator conjugate to treat influenza infected cells can be seen from multiple facets. Currently vaccines are manufactured based on annual predicting of which strains will likely circulate during the next season. However, such strategy occasionally fails and thus causes vaccines ineffective for the predominant strain of virus in epidemic. The exemplified zanamivir, which is an NA inhibitor effective for all 11 influenza NA subtypes, blocks the virus budding from

the infected cells. Thus the effectivity suits for all subtypes of influenza virus. At the same time, zanamivir conjugated payload drug, either a therapeutic agent, or an immunotherapy modulator, or an adaptor molecule (i.e. fluorescein) mediated anti-fluorescein CAR T cell, specifically mark influenza infected cells to elicit necessary immune response to clear the virus infected cells.

Examples:

Example 1. Design of the targeting ligand

Influenza neuraminidase (NA) is a transmembrane glycoprotein anchored in the lipid raft domain of influenza virus envelope. NA accounts for 20% (about 80) of the membrane glycoproteins and the head of NA is a homo-tetramer. It assists in the release of progeny virus from the infected cells by cleaving sialic acids from membrane glycoproteins or glycolipids (In the virus budding process, influenza virus hemagglutinin can bind to sialic acid receptors on the host cell membrane, which hinders the release of newly formed virus.).[9] Since neuraminidases are expressed on both the influenza virus surface and the surface of infected cell membrane, it was selected by our group as the potential target for the design of targeting ligand to target influenza virus and virus infected cells.

To date, four neuraminidase inhibitors have been developed as anti-influenza drugs: oseltamivir (Tamiflu; Glide/Roche), zanamivir (Relenza; GlaxoSmithKline), peramivir (Rapivab; BioCryst) and laninamivir (Inavir; Daiichi Sankyo).[25] Because zanamivir is an inhibitor derived from the naturally occurring sialic acid with minimal functionalization, rare zanamivir-resistant virus is found in the clinic.[7] Therefore, zanamivir was selected as the candidate for the targeting ligand design among neuraminidase inhibitors. Honda et al. reported that C-7 alkyl-modified analogues of zanamivir retained their inhibitory activities against neuraminidase (Fig. 4), which indicates that the C-7 position is tolerant to be modified as the linker attachment site.[26] Honda's conclusion is supported by the result of X-ray crystallographic structure of zanamivir complexed with neuraminidase: the 7-OH group of zanamivir is exposed to the solvent surface area and makes no direct interaction with the active site of neuraminidase (Fig. 5).[27] Moreover, several research groups also used the C7 position as the linkage site to build a set of multimeric analogues of zanamivir and zanamivir derivatives with improved anti-influenza activity.[28] Taken together, we design a new NA targeting ligand based on zanamivir by modifying its 7-OH group as the linkage site (Fig. 4).

Example 2. Compound synthesis

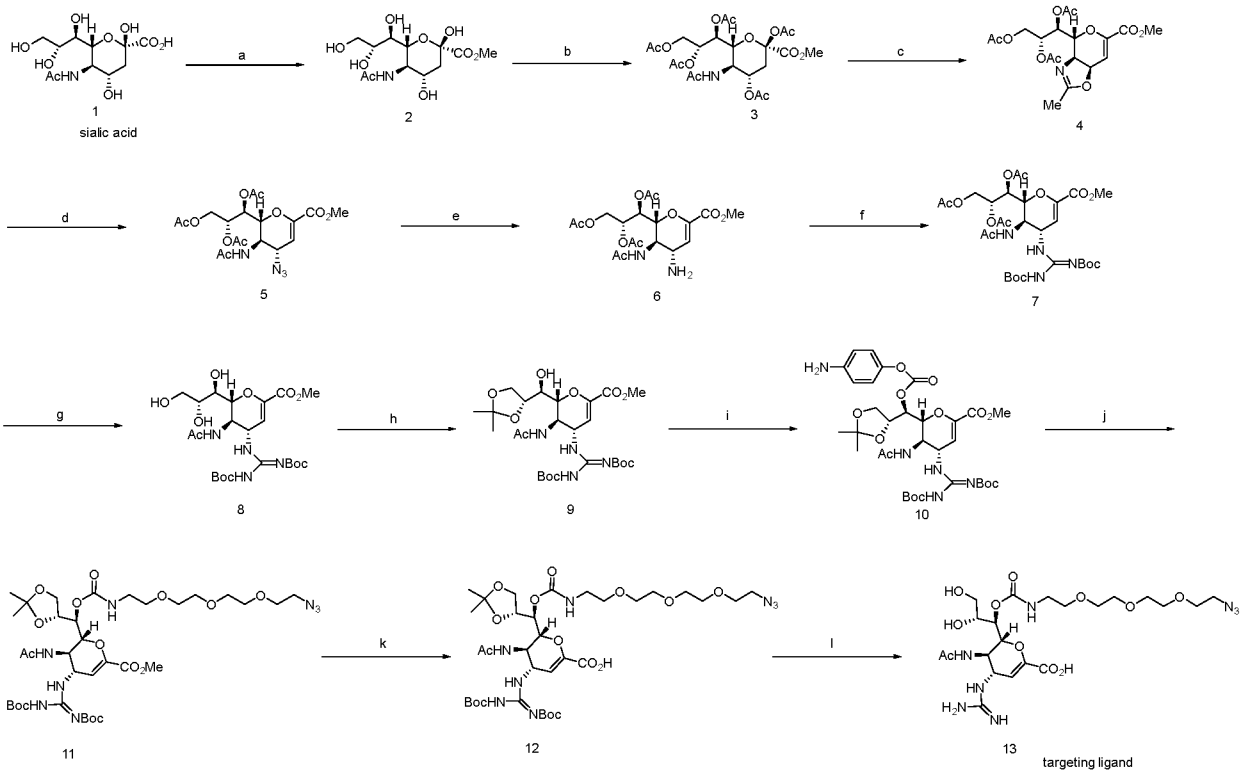

Scheme 1 Synthesis of targeting ligand Reagents and conditions: (a) amberlite IR-120B (H^+ form), MeOH; (b) acetic anhydride, 4-(dimethylamino)pyridine (DMAP), pyridine; (c) trimethylsilyl trifluoromethanesulfonate, ethyl acetate; (d) azidotrimethylsilane, tert-butyl alcohol; (e) triphenylphosphine, H_20, THF; (f) N,N'-bis(tertbutoxycarbonyl)-1H-pyrazole-1-carboxamidine, triethylamine, THF; (g) sodium methoxide solution, MeOH; (h) 2,2-dimethoxypropane, p-toluenesulfonic acid, acetone; (i) 4-nitrophenylchloroformate, DMAP, pyridine; (j) azido-dPEG®$_3$-amine, DMAP, pyridine; (k) 1M NaOH (aq), THF; (l) TFA.

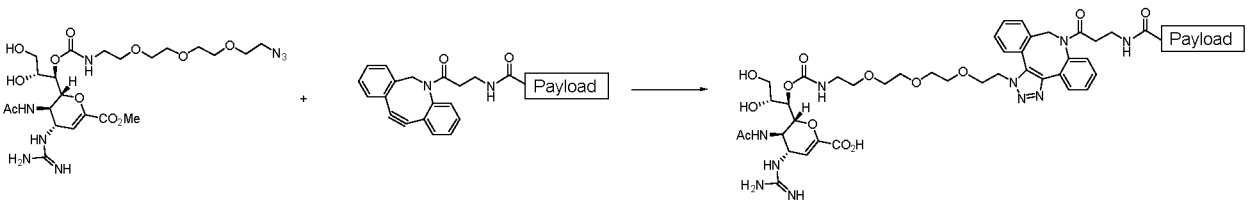

Scheme 2 General synthetic scheme of small molecule drug conjugate.

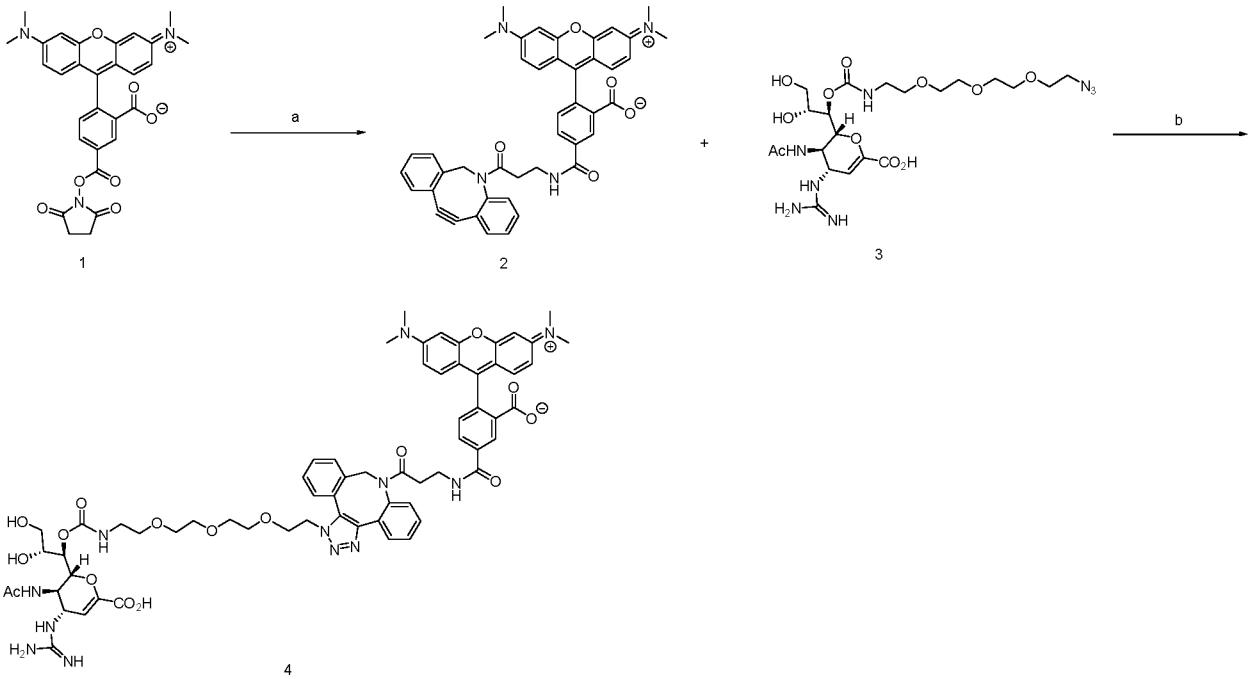

Scheme 3 Synthesis of zanamivir-rhodamine conjugate Reagents and conditions: (a) DBCO-amine, DIPEA, DMF; (b) DMSO.

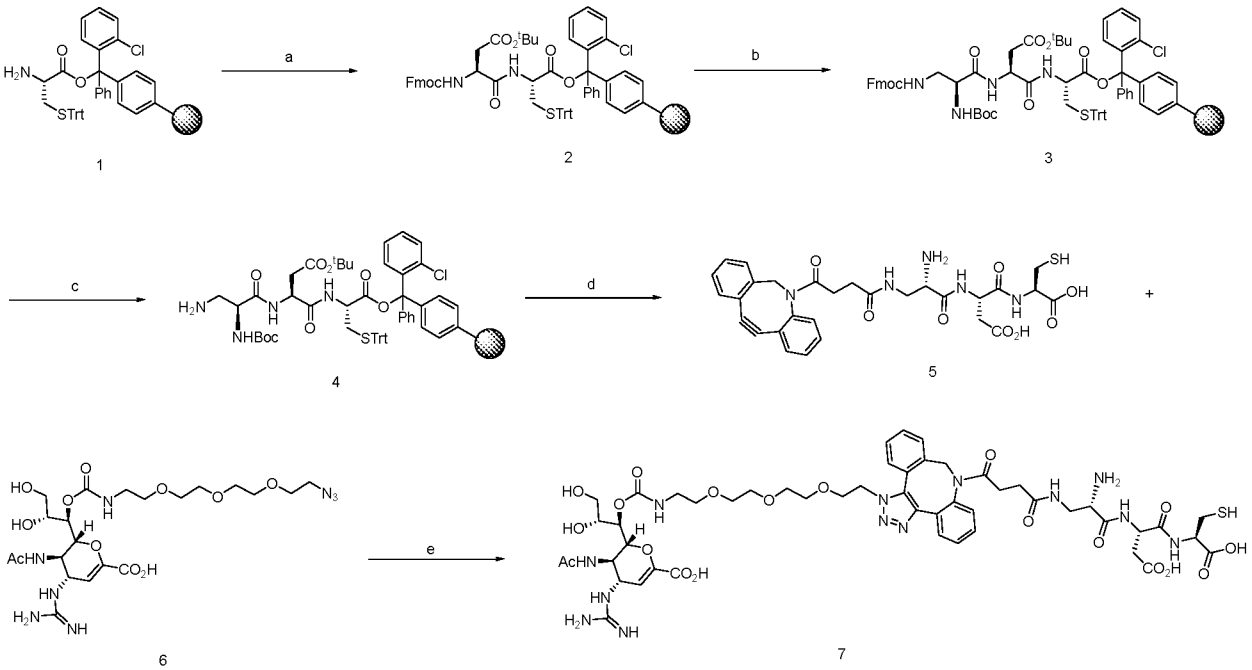

Scheme 4 Synthesis of zanamivir-EC20 conjugate Reagents and conditions: (a) 1. Wet resin with DMF, 2. Fmoc-Asp(OtBu)-OH, PyBop, DIPEA, DMF; (b) 1. 20% piperidine in DMF, 2. Fmoc-DAPA-OH, PyBop, DIPEA, DMF; (c) 20% piperidine in DMF; (d) 1. DBCO-acid, PyBop, DIPEA, DMF, 2. TFA/TIPS/EtSH/H_2O (92.5:2.5:2.5:2.5); (e) DMSO.

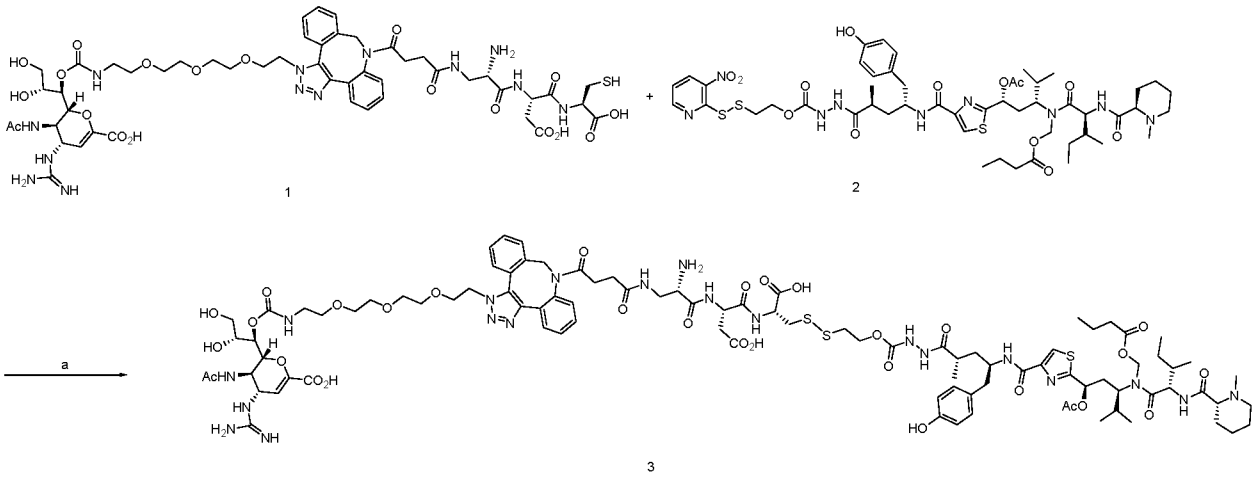

Scheme 5 Synthesis of zanamivir-tubulysin B hydrazide conjugate Reagents and conditions: (a) THF/$NaHCO_3$ buffer.

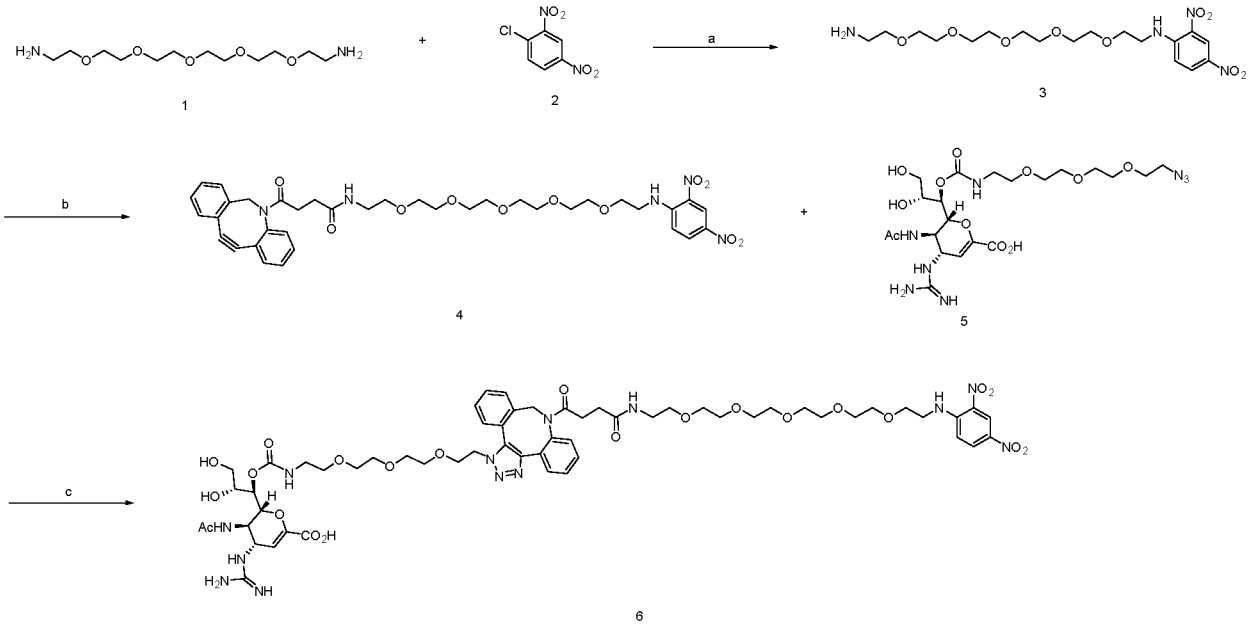

Scheme 6 Synthesis of zanamivir-DNP conjugate Reagents and conditions: (a)TEA, EtOH; (b) DBCO-NHS, DIPEA, DMSO; (c) DMSO.

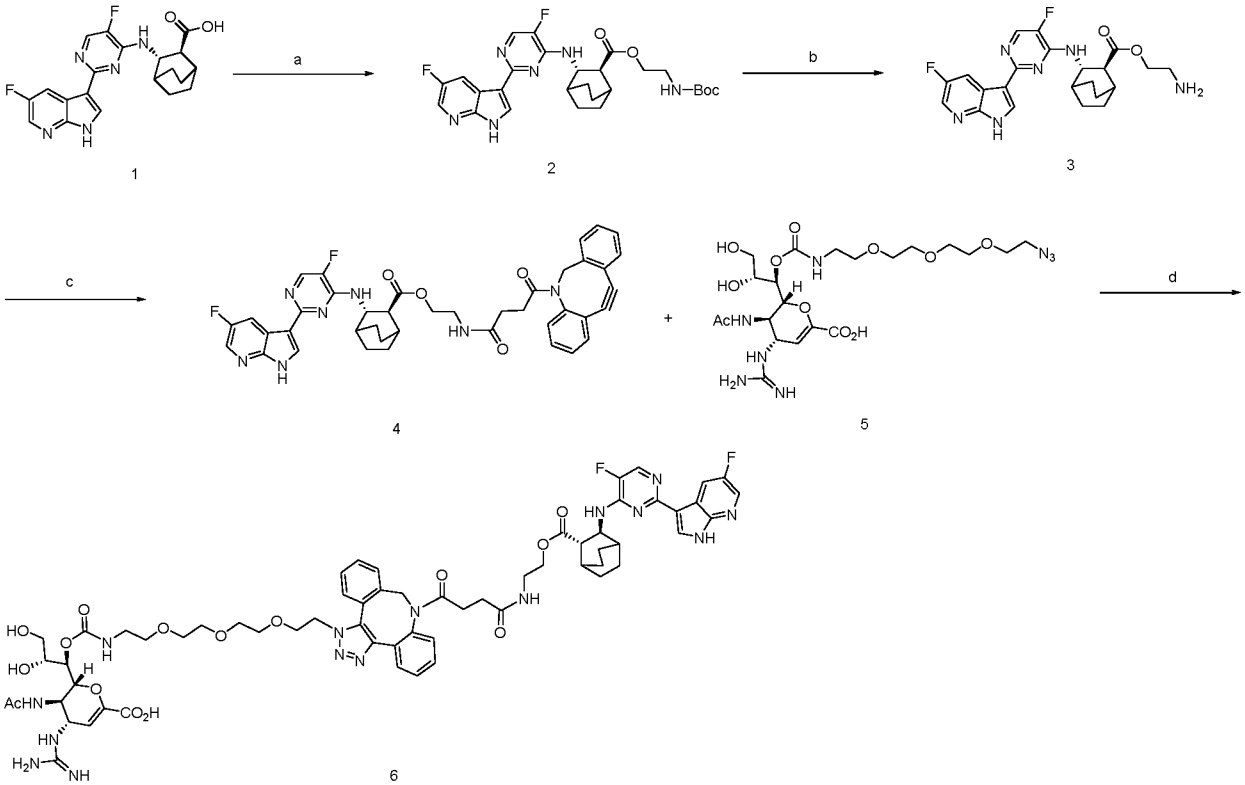

Scheme 7 Synthesis of zanamivir-pimodivir conjugate Reagents and conditions: (a) N-Boc-diethanolamine, EDC, DMAP, DCM; (b) 20% TFA in DCM; (c) DBCO-NHS, DIPEA, DMSO; (d) DMSO.

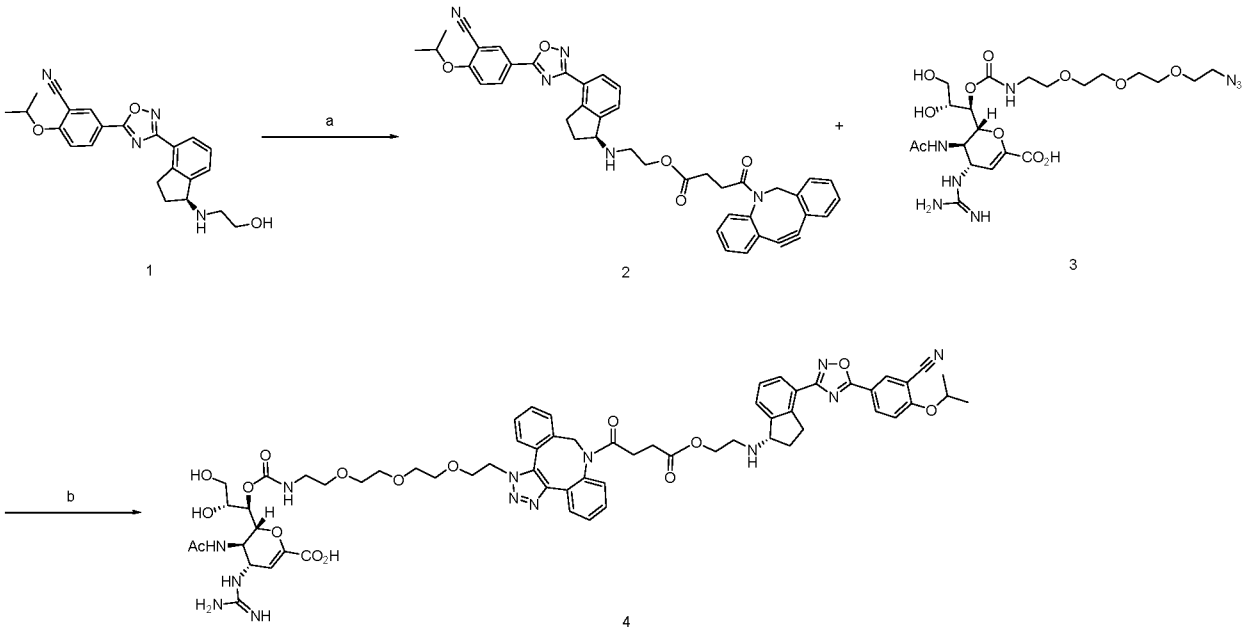

Scheme 8 Synthesis of zanamivir-ozanimod conjugate Reagents and conditions: (a) DBCO-acid, EDC, DMAP, DCM; (b) DMSO.

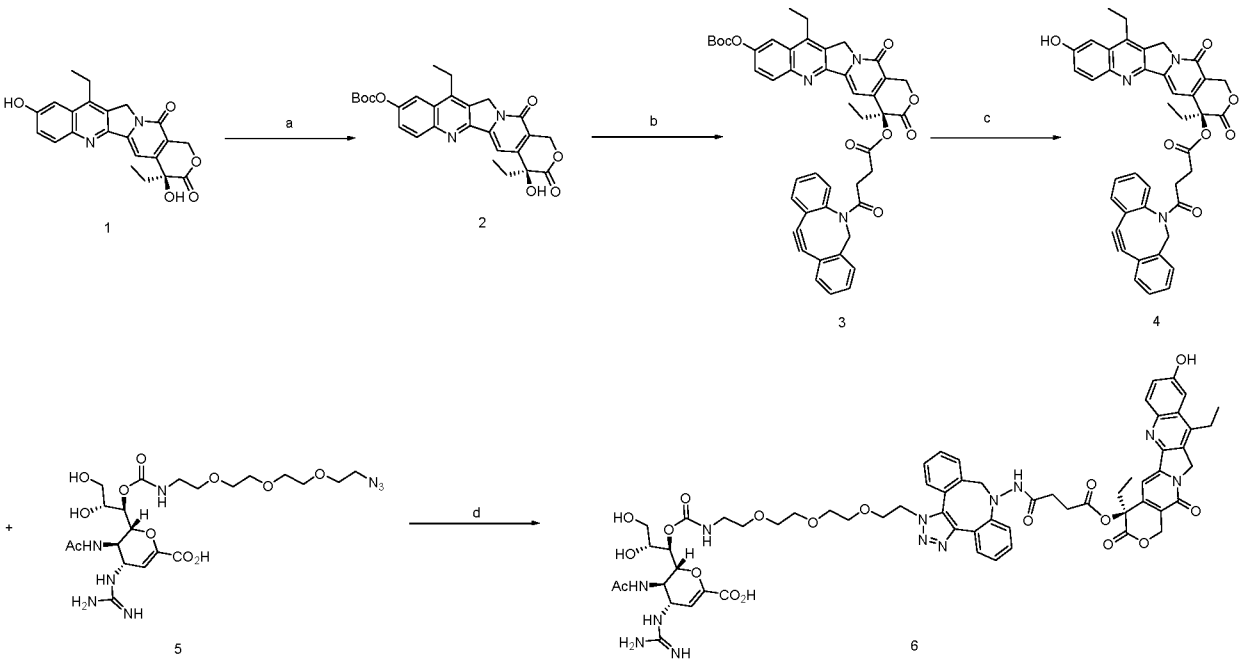

Scheme 9 Synthesis of zanamivir-SN38 conjugate Reagents and conditions: (a)di-tertbutyl decarbonate, pyridine, DCM; (b) DBCO-acid, EDC, DMAP, DCM; (c) 20% TFA in DCM; (d) DMSO.

Example 3. Small molecule ligand-targeted drug conjugates for anti-influenza chemotherapy

In Vitro binding to influenza virus infected MDCK cells

(1) Confocal microscope study with zanamivir-rhodamine conjugate

Method: MDCK cells were seeded in confocal plates and incubated overnight. In the next day when the cells reached 80% confluence, they were infected with 100 $TCID_{50}$ influenza virus A/Puerto Rico/8/34 (H1N1). On the third day, the infected MDCK cells were incubated with 50 nM zanamivir-rhodamine conjugate in the presence or absence of 5 μM zanamivr. After incubated for 1h at 37 °C, the cells were washed with the cell culture medium and sent to the confocal microscope.

As shown in Figure 6a, a strong fluorescent signal is observed when influenza virus infected MDCK cells were incubated with 50 nM zanamivir-rhodamine conjugate. The fluorescent

emission signal disappears when the binding of zanamivir-rhodamine conjugate to neuraminidase is competed by 100 fold excess of zanamivir (Fig. 6b), which indicates that the cell uptake of the conjugate was receptor mediated. In short, this result demonstrates that zanamivir-rhodamine conjugate can bind to and be internalized into the influenza virus infected MDCK cells.

(2) Binding affinity study with zanamivir-rhodamine conjugate

Method: MDCK cells were seeded in 24-well plates and incubated overnight. In the next day when the cells reached 80% confluence, they were infected with 100 $TCID_{50}$ influenza virus A/Puerto Rico/8/34 (H1N1). On the third day, the infected MDCK cells were incubated with various concentrations of zanamivir-rhodamine conjugate in the presence or absence of 100-fold excess of zanamivr. After incubated for 1h at 37 °C, the cells were washed with the cell culture medium and the remaining fluorescence was quantitated by fluorescence spectroscopy. Apparent K_d was calculated by plotting cell bound fluorescence intensity versus the concentration of zanamivir-rhodamine conjugate added using GraphPad Prism 4.

As shown in Figure 6c, the binding of zanamivir-rhodamine conjugate to neuraminidase expressed on virus infected cells was found to be saturated with K_d of 10.98 nM, and this binding of zanamivir-rhodamine conjugate can be competed by 100 fold excess of zanamivir.

Based on the confocal and binding affinity studies above, the zanamivir derivative is proved to be a good candidate as a targeting ligand for the influenza virus neuraminidase.

Example 4. *in Vivo* biodistribution

(1) Bind affinity study with ^{99m}Tc chelated zanamivir-EC20 head conjugate

Method: MDCK cells were seeded in 24-well plates and incubated overnight. In the next day when the cells reached 80% confluence, they were infected with 100 $TCID_{50}$ influenza virus A/Puerto Rico/8/34 (H1N1). On the third day, the infected MDCK cells were incubated with various concentrations of ^{99m}Tc chelated zanamivir-EC20 head conjugate in the presence or absence of 100-fold excess of zanamivr. After incubated for 1h at 37 °C, the cells were washed with the cell culture medium and the radioactivity of the remaining ^{99m}Tc chelated zanamivir-EC20 head conjugate was quantitated by gamma counter. Apparent K_d was calculated by plotting cell bound radioactivity versus the concentration of radiotracer using GraphPad Prism 4.

The binding of technetium-99m (^{99m}Tc) chelated zanamivir-EC20 head conjugate to neuraminidase expressed on virus infected cells was found to be saturated with K_d of 15.09 nM, and this binding of ^{99m}Tc chelated zanamivir-EC20 head conjugate can be competed by 100 fold excess of zanamivir (Fig. 7a). This binding affinity value is consistent with the value measured by zanamivir-rhodamine conjugate, which further proves that the zanamivir derivative is a good targeting ligand for influenza virus neuraminidase.

(2) Biodistribution study with ^{99m}Tc chelated zanamivir-EC20 head conjugate

Method: BALB/c mice (6-7 weeks old) were first intranasally infected with 50 μL influenza virus A/Puerto Rico/8/1934 (H1N1) to develop influenza symptom. 3 days later, the mice were intravenously injected with 100 μL 10 nmol zanamivir-EC20 head conjugate (contains 20 pM ^{99m}Tc chelated conjugate) in the presence or absence of 100-fold excess of zanamivir. 5h post-injection, major tissues/organs were removed and the amount of radioactivity was determined by gamma counter.

In order to test the ability of zanamivir derivative to specially deliver therapeutic or imaging agents to influenza virus infected lung, the biodistribution profiles of ^{99m}Tc chelated zanamivir-EC20 head conjugate in virus infected mice/uninfected mice were measured. As shown in Figure 8, the conjugate exhibits the highest uptake in the lung of virus infected mice, the major organ in which influenza virus proliferate. Moreover, there is no lung uptake of ^{99m}Tc chelated zanamivr-EC20 conjugate from the mice in either competition group or uninfected group, indicating that the lung uptake of the conjugate was receptor mediated. Apart from the virus infected lung, kidney is the only organ that shows significant radioactive signal. However, the signals were not abolished in competition group and uninfected group, indicating that the accumulation of ^{99m}Tc chelated zanamivir-EC20 head conjugate in kidney was not neuraminidase mediated. Taken together, this result provides the strong evidence that the zanamivir derivative designed in this project can be used as the targeting ligand to specifically deliver therapeutic or imaging agents to the virus infected lung.

Example 5. *in-vitro* cytotoxic study with zanamivir-tubulysin B hydrazide conjugate

Method: Neuraminidase transfected HEK 293 cells were seed at 96 well plates and incubated with zanamivir-tubulysin B hydrazide conjugate, free tubulysin B hydrazide or zanamivir-tubulysin B

hydrazide conjugate in the presence of 100-fold excess of zanamivir for 2h at 37 °C. Cells were then washed with fresh medium and incubated for another 48h at 37 °C. The cell viability was measured using ATP detection (CellTiter Glo, Promege Inc. Madison, WT). EC_{50} values were calculated by plotting % luminescence intensity versus log concentration of drugs using GraphPad Prism 4.

To determine the cytotoxicity and targeting specificity of zanamivir-tubulysin B hydrazide conjugate, an in-vitro cytotoxic assay using neuraminidase transfected HEK293 cells was performed. As shown in Figure 9, The EC_{50} of zanamivir-tubulysin B hydrazide conjugate was 5.2 nM, which is comparable to that of free tubulysin B hydrazide (9.9 nM). Blocking of neuraminidase binding sites with 100-fold excess of zanamivir reduced the cytotoxicity > 30-fold, suggesting that most of the cell killing is receptor mediated.

Example 6. Small molecule ligand-targeted drug conjugates for anti-influenza chemotherapy and immunotherapy

Competitive binding of zanamivir-DNP conjugate to neuraminidase transfected HEK293 cells using zanamivir-rhodamine conjugate as the labelled ligand

Method: Neuraminidase transfected HEK 293 cells were seed at 24 well plates and incubated overnight. In the next day the cells were incubated with a single concentration of labeled ligand (15 nM zanamivir-rhodamine conjugate) as well as with various concentrations of zanamivir-DNP conjugate or zanamivir. After incubated for 1h, the cells were washed with the cell culture medium and the remaining fluorescence was quantitated by fluorescence spectroscopy. Apparent K_d was calculated by plotting cell bound fluorescence intensity versus the log concentration of zanamivir-DNP conjugate or zanamivir added using the competition binding equation in GraphPad Prism 4.

The binding affinity of zanamivir-DNP conjugate to cell membrane bound neuraminidase was mesured in a competitive binding experiment. Figure 10 shows that the bindng affinity of zanamivir-DNP conjugate and zanamivir were measured at 12.81 and 0.45 nM, respective. Even though the binding affinity of the targeting ligand drops 28-fold upon being attached with DNP moiety, its binding affinity is still in a low nanomolar range, which indicates that zanamivir-DNP conjugate has the potential to be used as the ligand targeted hepten conjugate.

Example 7. Anti-DNP antibody recruiting assay with zanamivir-DNP conjugate

As shown in Figure 11, zanamivir-DNP conjugate was able to specifically bind to neuraminidase on the neuraminidase transfected HEK293 cell membrane (293tn NA) and recruit antiDNP antibody at around 10nM. No binding was observed in non-transfected HEK293 cells (293tn).

Methods: 293tn NA (Neuraminidase transfected) and control (non-transfected 293tn) cells were incubated with different concentrations of zanamivir-DNP conjugate at 4 °C for 30min, followed by PBS washing for 3 times. After that, cells were stained with antiDNP-biotin and Streptavidin-PE at 4 °C for 30min. Cells were washed by PBS for 3 times and submitted to flow cytometry.

Example 8. Mouse protection study

Method: BALB/c mice (4 weeks old) were immunized with DNP-KLH on week 1 and week 3 twice. On week 4, both the immunized and unimmunized mice were intranasally infected with 50 μL 100 LD_{50} influenza virus A/Puerto Rico/8/1934 (H1N1) to develop the influenza symptom. 2h later, mice were intranasally given PBS/zanamivir/zanamivir-DNP conjugate (1.5 μmol/kg) one time a day for five days. Mice were counted as dead when losing either 25% of their initial weight or when they were moribund.

As shown in Figure 12, zanamivir-DNP conjugate (red invert triangles) has a superior effect to zanamivir (green triangles) at dose of 1.5 μmol/kg. There was no body weight loss or influenza symptom observed for zanamivir-DNP conjugate treated immunized mice (Fig. 12a, red line). Zanamivir-DNP conjugate protected all immunized mice from lethal virus challenge (Fig. 12b, red line). In contrast, zanamivir only rescued 60% of the immunized mice (Fig. 12b, green line). It is worth mentioning that the efficacy of zanamivir-DNP conjugate dropped dramatically when it was given to the unimmunized mice (blue line), which underlines the importance of the immunological function of zanamivir-DNP conjugate.

Example 9. Influenza virus induced tumor types for targeted CAR T therapy

In this example, *in vitro* study of CAR T cell killing NA expressing HEK 293 cells is demonstrated.

Figure 14 shows that HEK 293 cells that express NA (293NA) are used to mimic influenza virus infected cells. Figure 14 A and B respectively show

CAR-T (100,000 cells) : 293NA (20,000) = 5 : 1, causes 41% killing

CAR-T (200,000 cells) : 293NA (20,000) = 10 : 1, causes 61% killing

Example 10. No binding of Zanamivir-FITC to normal 293T cells

Figure 15 shows zanamivir-FITC does not bind to normal 293 T cells. Because of the specific binding between zanamivir and NA on a cell surface, if 293 cells are not transfected with NA expression, zanamivir-FITC will not be on the cell surface, thus normal 293 cells are not detected when gated in flow cytometer. Only cells expressing NA on its surface will be detected by zanamivir-FITC conjugate. Therefore, Zanamivir-FITC may serve as a probe to identify NA expressing cells.

Example 11. The cytotoxicity against NA is specifically induced by Zanamivir-FITC

Figure 16 shows anti-FITC CAR T executes its cytotoxicity against HEK 293NA cells specifically.

three different groups (HEK-293+FITC-zanamivir, 293NA+EC17, 293NA+Free zanamivir) were co-cultured with human CAR-T cells and the % of killing were tested by LDH.

In this table/figure 16, HEK-293 are normal 293T cells that do not express NA, while 293NA are 293T cells that express NA. FITC-zanamivir is the adaptor designed for the CAR-T to target cells that express NA (in nature, influenza infected cells; in this experiment, 293NA). For EC17, the FITC side can bind to CAR-T cells, but the other side do not bind to 293NA. Therefore, the three groups can be considered as: 1. non-target cells with correct adaptor; 2.target cells with wrong adaptor; 3.target cells with free drug. The results of the three groups were expected to be no killing and the experimental results in Fig. 16 support the hypothesis (The 3-5% killing from 293NA+EC17 group could be variation, and it is not significant compared to the 40-60% killing from the experimental group (293NA+FITC-zanamivir) in Fig. 14.

Example 12. *in vitro* essay using real virus

Similar to Example 10, MDCK cells infected by real virus can be identified by zanamivir-rhodamine conjugate to check the expression level of NA, as shown in Figure 17.

Typically, confluent MDCK cells were infected with 100TCID$_{50}$ influenza virus (H1N1). In exemplified Figure 17, cells are stained with 100nM zanamivir-rhodamine conjugate to check the expression level of NA on the cell surface.

After the influenza virus infection to MDCK cells for about 15 hours, these cells are co-cultured with CAR-T cells for a number of hours. Then the efficacy of the CAR-T killing effect is checked by at least two different ways: one is to check the cell lysis such as LDH assay. Figure 18 provides zanamivir-FITC conjugate adapted anti-FITC CAR –T cells to kill H1N1 infected MDCK. The left panel shows a literature report of regular T cell killing of MDCK cells at maximum rate of 10% after co-cultured for 18 hours, whereas adapted CAR-T cells caused about 8.4% killing of influenza infected MDCK cells after only 7 hours of co-culture. Further, adapted CAR-T cells do not have non-infected MDCK killing, indicating the CAR T is very specific to infected T cells. The other way of checking CAR T killing effect is to measure the virus titer in the supernatant (for example, using qPCR to measure viral genetic material to quantify viral replication).

Example 13. In vivo mouse model to study influenza induced tumor types for targeted CAR-T therapy

Figure 19 provides a mouse model for studying influenza virus induced tumor type, using targeted adaptor mediated anti-FITC CAR-T therapy described in previous examples. Influenza virus infected NSG mice are first studied to determine the LD$_{50}$ of the virus titer. After establishing proper virus titer and infected NSG mice, zanamivir-FITC conjugated adapter and anti-FITC CAR-T cells are applied to the infected NSG mice to rescue. It is expected that mice survival will increase upon the zanamivir-FITC conjugate and anti-FITC CAR-T rescue.

Example 14. The binding affinity of zanamivir-DNP conjugate for both influenza A group 1 neuraminidase (represented by N1) and group 2 neuraminidase (represented by N2)

Figure 21 provides in-vitro binding assay of influenza virus A/Puerto Rico/8/34 (H1N1) infected MDCK cells.

Figure 22 provides in-vitro binding assay of influenza virus A/Aichi2/1968 (H3N2) infected MDCK cells.

Example 15. The ability of the zanamivir-DNP conjugate to induce the killing of influenza virus-infected cells through CDC and ADCP effects

Figs. 23-24 show that anti-DNP antibody can be recruited to virus infected MDCK cells for both H1N1 and H3N2 strains.

Figs. 25 shows complement dependent cytotoxicity assay of zanamivir-DNP conjugate, in which only 10nM drug conjugate is needed for achieving maximum killing. This indicates zanamivir-DNP conjugate is much more potent than zanamivir alone.

Fig. 26 shows zanamivir-DNP conjugate may bring anti-DNP antibody to achieve antibody dependent phagocytosis (ADCP).

Example 16. A series of live mouse studies demonstrating:

a. Efficacy of intranasal administration of drug in treating influenza virus infection (Figs. 27-29)
b. Dose escalation study showing optimal dose following intranasal administration (Fig. 27)
c. Dose frequency study showing that a single dose is sufficient to yield complete cures following intranasal administration (Fig. 28, 31)
d. That treatment can be delayed until 72 hours after detection of flu symptoms and complete cures can still be achieved following intranasal administration (Fig. 29-30)
e. The same drug can be administered via intraperitoneal injection and still achieve complete cures (Figs. 33-34)
f. In all of the above assays, our drug outperforms zanamivir dramatically (Figs. 27-34)
g. BioD data and spect/CT imaging showing specificity for infected lung tissue (Fig. 32)

Example 17. Ligand-targeted Immunotherapy for the treatment of Influenza analyzed with antibody dependent cellular cytotoxicity Reporter bioassay (Figure 35A-B)

In this Example, an ADCC reporter bioassay is applied to monitor the zanamivir-DNP conjugate inducted ADCC response via a firefly luciferase reporter assay (ADCC Reporter Bioassays, V Variant, Catalog #: G7010, Promega). Briefly, engineered Jurkat cells are used to stably express FcγRIIIa receptor and an NFAT (nuclear factor of activated T-cells) response

element driving expression of firefly luciferase is used as effector cells shown in Figure 35A. Antibody biological activity in ADCC Mode of Action is quantified through the luciferase produced as a result of NFAT pathway activation, which indicates the engagement of zanamivir-DNP conjugate in mediating ADCC effect to the target cell, as outlined in Figure 35B. This example shows that zanamivir-DNP conjugate serves important roles for mediating ADCC effects.

Example 18. Ligand-targeted Immunotherapy for the treatment of Influenza analyzed with in vitro antiviral assay for H1N1 and H3N2 infected MDCK cells (Figure 36 A-B)

In this Example, MDCK cells infected with either H1N1 or H3N2 virus were studied for zanamivir-DNP conjugate protection effect. As shown in Figure 36A (H1N1) and 36B (H3N2), the EC50 represents the inhibitor concentrations for 50% protection of virus infected MDCK.

To assure that zanamivir-DNP conjugate can still inhibit the neuraminidase activity necessary for its suppression of influenza virus proliferation, we compared the potency of zanamivir and zanamivir-DNP conjugate in suppressing propagation of influenza virus in an MDCK-influenza virus co-culture.

Example 19. Single dose treatment (intranasal administration) for H3N2 virus infected mice (Figure 37A-B)

In this Example, DNP-KLH immunized mice (5 mice/group) were infected with 50 uL A/Aichi/2/1968 (HA, NA), x-31b (H3N2) virus (100 LD_{50}) at day 0.

Mice were intranasally given zanamivir-DNP conjugate/zanamivir/PBS 24h post-infection for only one time and mice were counted as dead when losing either 25% of their initial weight or when they were moribund.

As shown in Figure 37A and B, intranasally administered zanamivir-DNP provides good protection 14 days of post infection (all mice were cured), whereas zanamivir alone does not provide the same protection.

Example 20. Single dose treatment (intraperitoneally administration) for H1N1 virus infected mice (Figure 38A-B)

In this Example DNP-KLH immunized mice (5 mice/group) were infected with 50 uL A/Puerto Rico/8/34 (100 LD_{50}, 4.2×10^5 PFU) at day 0.

Mice were intraperitoneally given zanamivir-DNP conjugate/zanamivir/PBS 24h post-infection for only one time and mice were counted as dead when losing either 25% of their initial weight or when they were moribund.

As shown in Figure 38A and B, intraperitoneally administered zanamivir-DNP provides good protection 14 days of post infection (all mice were cured), whereas zanamivir alone does not provide the same protection.

Example 21. Single dose treatment (intraperitoneally administration) for H3N2 virus infected mice (Figure 39A-B)

In this Example DNP-KLH immunized mice (5 mice/group) were infected with 50 uL A/Aichi/2/1968 (HA, NA), x-31b (H3N2) virus (100 LD_{50}) at day 0.

Mice were intraperitoneally given zanamivir-DNP conjugate/zanamivir/PBS 24h post-infection for only one time and mice were counted as dead when losing either 25% of their initial weight or when they were moribund.

As shown in Figure 39A-B, intraperitoneally administered zanamivir-DNP provides good protection 14 days of post infection (all mice were cured), whereas zanamivir alone does not provide the same protection.

Example 22. Anti-DNP antibody treated unimmunized mice infected by H1N1 virus (Figure 40A-B)

In this Example, unimmunized mice were intravenously given anti-DNP antibody one day after infected with lethal dose of H1N1 virus and immediately treated by various doses of intraperitoneally administered zanamivir-DNP conjugate.

In the pilot study, mice (3 mice/group) were infected with 50 uL A/Puerto Rico/8/34 virus (100 LD_{50}, 4.2 x 10^5 PFU) at day 0.

Mice were intravenously given anti-DNP antibody (polyclonal rabbit IgG) 24h post-infection for only one time and intranasally given zanamivir-DNP conjugate 24h post-infection for only one time.

Mice were counted as dead when losing either 25% of their initial weight or when they were moribund.

As shown in Figure 40A-B, if concurrently administered 24 hours post infection, as low as 1mg/kg of intravenously administered anti-DNP antibody along with 1.5umol/kg intranasally administered zana-DNP conjugate are able to provide necessary protection to lethal dose of H1N1 virus infection.

Example 23. Synthesis scheme of zanamivir-rhamnose conjugate (Figure 41)

In this Example, a different conjugate zanamivir-rhamnose is synthesized to be used in induction of immune response to influenza virus infection. The synthesis scheme is provided in Figure 41.

Example 24. Competitive binding of zanamivir-rhamnose conjugate to neuraminidase transfected HEK293 cells using zanamivir-rhodamine conjugate as the labelled ligand (Figure 42A-B)

In this Example, Neuraminidase transfected HEK 293 cells were seed at 24 well plates and incubated overnight. In the next day the cells were incubated with a single concentration of labeled ligand (15 nM zanamivir-rhodamine conjugate) as well as with various concentrations of zanamivir-rhamnose conjugate or zanamivir. After incubated for 1h, the cells were washed with the cell culture medium and the remaining fluorescence was quantitated by fluorescence spectroscopy. Apparent K_d was calculated by plotting cell bound fluorescence intensity versus the log concentration of zanamivir-DNP conjugate or zanamivir added using the competition binding equation in GraphPad Prism 4. K_d about 3.57 nM is plotted for zanamivir-rhamnose conjugate as compared to free zanamivir K_d about 0.77 nM, and zanamivir-rhodamine conjugate K_d about 11.71 nM.

Example 25. Immunotherapy study with zanamivir-rhamnose conjugate (Figure 43A-B)

In this Example, mouse protection by zanamivir-rhamnose conjugate is observed in a dose escalation study. Briefly, rhamnose-OVA immunized mice (5 mice/group) were infected with 50 uL A/Puerto Rico/8/34 virus (100 LD_{50}, 4.2 x 10^5 PFU) at day 0.

Mice were intranasally given 1.5/0.5/0.17 umol/kg zanamivir-rhamnose conjugate/zanamivir/PBS 24h post-infection, twice daily for 5 days and mice were counted as dead when losing either 25% of their initial weight or when they were moribund.

As shown in Figures 43A-B, as little as 0.17umol/kg zanamivir-rhamnose conjugate b.i.d was able to provide at least 50% protection for A/Puerto Rico/8/34 (H1N1) virus lethally infected mice.

References

1. Organization, W. H. Influenza (Seasonal). Fact Sheet No 211. 2014. In 2014.

2. Control, C. f. D.; Prevention. Estimating seasonal influenza-associated deaths in the United States. *Disponibile su:* http://www. *cdc. gov/flu/about/disease/us_flu-related_deaths. htm* **2015**.

3. Bush, G. W. *The national security strategy of the United States of America*. Wordclay: 2009.

4. De Clercq, E. Antiviral agents active against influenza A viruses. *Nature reviews Drug discovery* **2006,** 5, 1015.

5. Control, C. f. D.; Prevention. Influenza antiviral drug resistance: questions & answers. In 2008.

6. Ebell, M. H.; Call, M.; Shinholser, J. Effectiveness of oseltamivir in adults: a meta-analysis of published and unpublished clinical trials. *Family practice* **2012,** 30, 125-133.

7. Von Itzstein, M. The war against influenza: discovery and development of sialidase inhibitors. *Nature reviews Drug discovery* **2007,** 6, 967.

8. Srinivasarao, M.; Galliford, C. V.; Low, P. S. Principles in the design of ligand-targeted cancer therapeutics and imaging agents. *Nature reviews Drug discovery* **2015,** 14, 203.

9. Lamb, R. A.; Krug, R.; Knipe, D. Fields virology. *Fields virology* **2001,** 1.

10. Nayak, D. P.; Balogun, R. A.; Yamada, H.; Zhou, Z. H.; Barman, S. Influenza virus morphogenesis and budding. *Virus research* **2009,** 143, 147-161.

11. Murray, B. C.; Peterson, M. T.; Fecik, R. A. Chemistry and biology of tubulysins: antimitotic tetrapeptides with activity against drug resistant cancers. *Natural product reports* **2015,** 32, 654-662.

12. Clark, M. P.; Ledeboer, M. W.; Davies, I.; Byrn, R. A.; Jones, S. M.; Perola, E.; Tsai, A.; Jacobs, M.; Nti-Addae, K.; Bandarage, U. K. Discovery of a novel, first-in-class, orally bioavailable azaindole inhibitor (VX-787) of influenza PB2. *Journal of medicinal chemistry* **2014,** 57, 6668-6678.

13. Byrn, R. A.; Jones, S. M.; Bennett, H. B.; Bral, C.; Clark, M. P.; Jacobs, M. D.; Kwong, A. D.; Ledeboer, M. W.; Leeman, J. R.; McNeil, C. F. Preclinical activity of VX-787, a first-in-class, orally bioavailable inhibitor of the influenza virus polymerase PB2 subunit. *Antimicrobial agents and chemotherapy* **2015,** 59, 1569-1582.

14. Liu, Q.; Zhou, Y.-h.; Yang, Z.-q. The cytokine storm of severe influenza and development of immunomodulatory therapy. *Cellular & molecular immunology* **2016,** 13, 3.

15. Oldstone, M. B.; Teijaro, J. R.; Walsh, K. B.; Rosen, H. Dissecting influenza virus pathogenesis uncovers a novel chemical approach to combat the infection. *Virology* **2013,** 435, 92-101.

16. Scott, F.; Clemons, B.; Brooks, J.; Brahmachary, E.; Powell, R.; Dedman, H.; Desale, H.; Timony, G.; Martinborough, E.; Rosen, H. Ozanimod (RPC1063) is a potent sphingosine-1-phosphate receptor-1 (S1P1) and receptor-5 (S1P5) agonist with autoimmune disease-modifying activity. *British journal of pharmacology* **2016,** 173, 1778-1792.

17. Walsh, K. B.; Teijaro, J. R.; Wilker, P. R.; Jatzek, A.; Fremgen, D. M.; Das, S. C.; Watanabe, T.; Hatta, M.; Shinya, K.; Suresh, M. Suppression of cytokine storm with a sphingosine analog provides protection against pathogenic influenza virus. *Proceedings of the National Academy of Sciences* **2011,** 108, 12018-12023.

18. Teijaro, J. R.; Walsh, K. B.; Cahalan, S.; Fremgen, D. M.; Roberts, E.; Scott, F.; Martinborough, E.; Peach, R.; Oldstone, M. B.; Rosen, H. Endothelial cells are central orchestrators of cytokine amplification during influenza virus infection. *Cell* **2011,** 146, 980-991.

19. Pommier, Y. Topoisomerase I inhibitors: camptothecins and beyond. *Nature Reviews Cancer* **2006,** 6, 789.

20. Rialdi, A.; Campisi, L.; Zhao, N.; Lagda, A. C.; Pietzsch, C.; Ho, J. S. Y.; Martinez-Gil, L.; Fenouil, R.; Chen, X.; Edwards, M. Topoisomerase 1 inhibition suppresses inflammatory genes and protects from death by inflammation. *Science* **2016,** 352, aad7993.

21. Lu, Y.; You, F.; Vlahov, I.; Westrick, E.; Fan, M.; Low, P. S.; Leamon, C. P. Folate-targeted dinitrophenyl hapten immunotherapy: effect of linker chemistry on antitumor activity and allergic potential. *Molecular pharmaceutics* **2007,** 4, 695-706.

22. Lu, Y.; Sega, E.; Leamon, C. P.; Low, P. S. Folate receptor-targeted immunotherapy of cancer: mechanism and therapeutic potential. *Advanced drug delivery reviews* **2004,** 56, 1161-1176.

23. McEnaney, P. J.; Parker, C. G.; Zhang, A. X. Antibody-Recruiting Small Molecules: Synthetic Constructs as Immunotherapeutics. In *Annual Reports in Medicinal Chemistry*, Elsevier: 2017; Vol. 50, pp 481-518.

24. Sheridan, R. T.; Hudon, J.; Hank, J. A.; Sondel, P. M.; Kiessling, L. L. Rhamnose Glycoconjugates for the Recruitment of Endogenous Anti-Carbohydrate Antibodies to Tumor Cells. *ChemBioChem* **2014,** 15, 1393-1398.

25. Wu, X.; Wu, X.; Sun, Q.; Zhang, C.; Yang, S.; Li, L.; Jia, Z. Progress of small molecular inhibitors in the development of anti-influenza virus agents. *Theranostics* **2017,** 7, 826.

26. Honda, T.; Masuda, T.; Yoshida, S.; Arai, M.; Kaneko, S.; Yamashita, M. Synthesis and anti-influenza virus activity of 7-O-alkylated derivatives related to zanamivir. *Bioorganic & medicinal chemistry letters* **2002,** 12, 1925-1928.

27. Xu, X.; Zhu, X.; Dwek, R. A.; Stevens, J.; Wilson, I. A. Structural characterization of the 1918 influenza virus H1N1 neuraminidase. *Journal of virology* **2008,** 82, 10493-10501.

28. Feng, E.; Ye, D.; Li, J.; Zhang, D.; Wang, J.; Zhao, F.; Hilgenfeld, R.; Zheng, M.; Jiang, H.; Liu, H. Recent Advances in Neuraminidase Inhibitor Development as Anti-influenza Drugs. *ChemMedChem* **2012,** 7, 1527-1536.

CLAIMS

1. A conjugate comprising a targeting ligand (TL) for an envelope protein of an influenza virus, a linker (L) and a payload of drug (D), wherein the TL is a molecule that binds to the envelope protein, the linker is covalently bound to both the D and the TL, and the D is an imaging agent, a therapeutic drug, an immune modulator or the combination thereof.
2. The conjugate according to claim 1, wherein the linker comprises a spacer and a cleavable or noncleavable bridge between the TL and the D.
3. The conjugate according to claim 1, wherein the envelope protein of the influenza virus is Neuraminidase (NA) or Hemagglutinin (HA).
4. The conjugate according to claim 1, wherein the TL is zanamivir.
5. The conjugate according to claim 1, wherein the TL is selected from the group consisting of oseltamivir, zanamivir, peramivir and laninamivir.
6. The conjugate according to claim 1, wherein the D is selected from the group consisting of Tubulysin B hydrazide, pimodivir, Ozanimod and SN38.
7. The conjugate according to claim 4 comprises

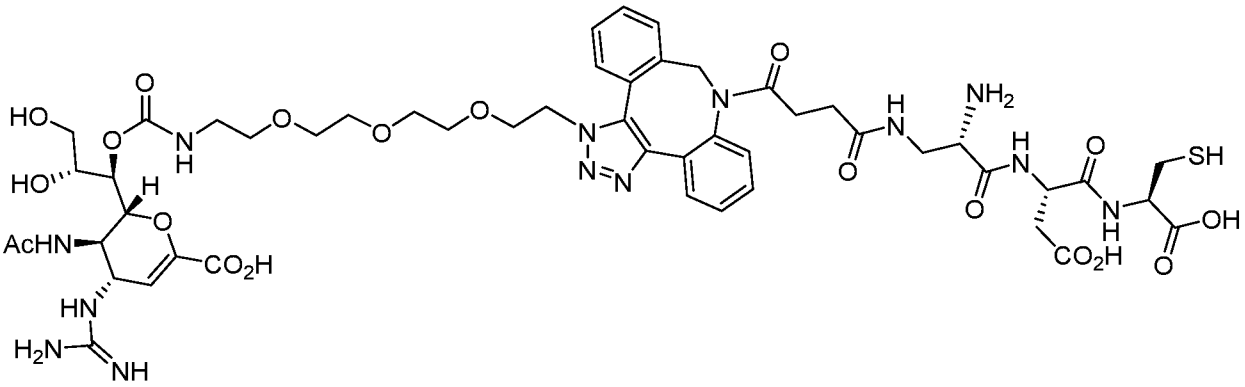

zanamivir-EC20,

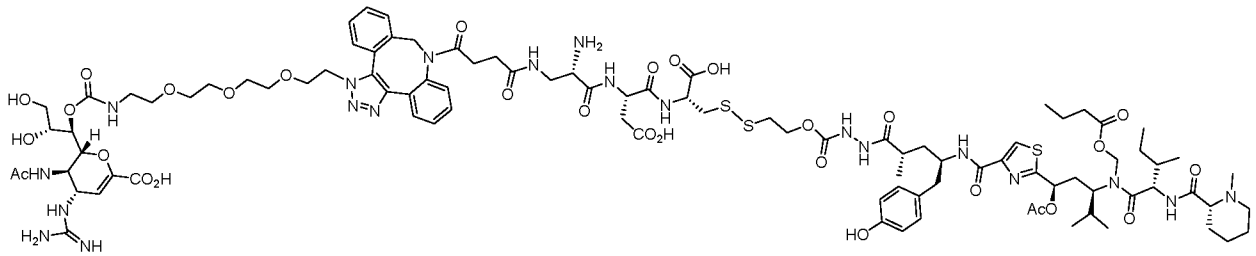

zanamivir-tubulysin B hydrazide,

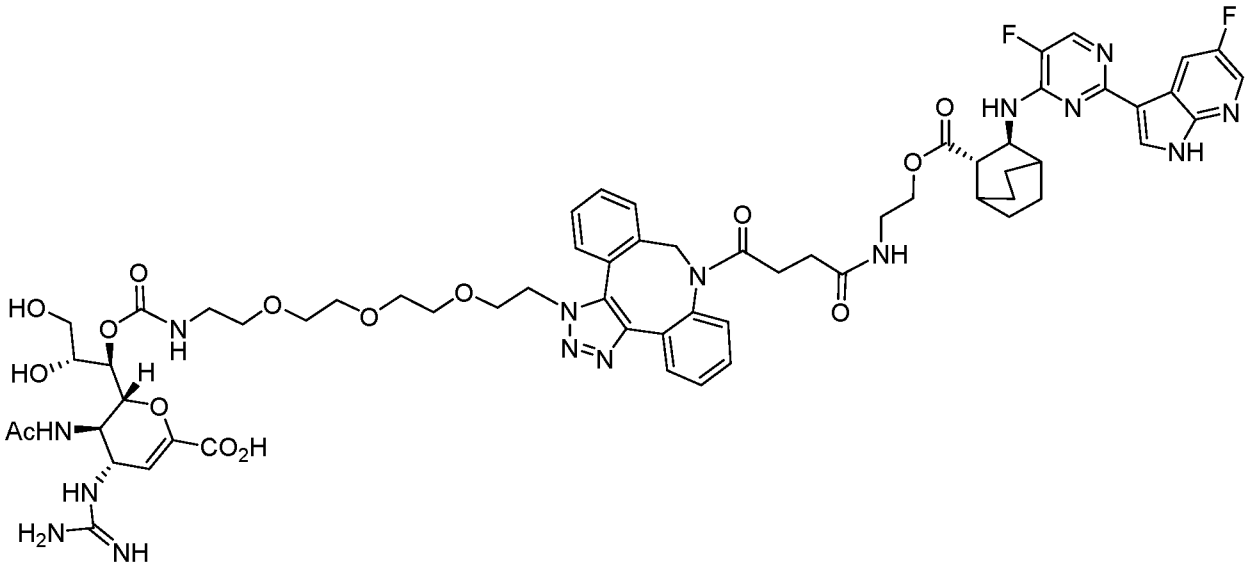

zanamivir-pimodivir,

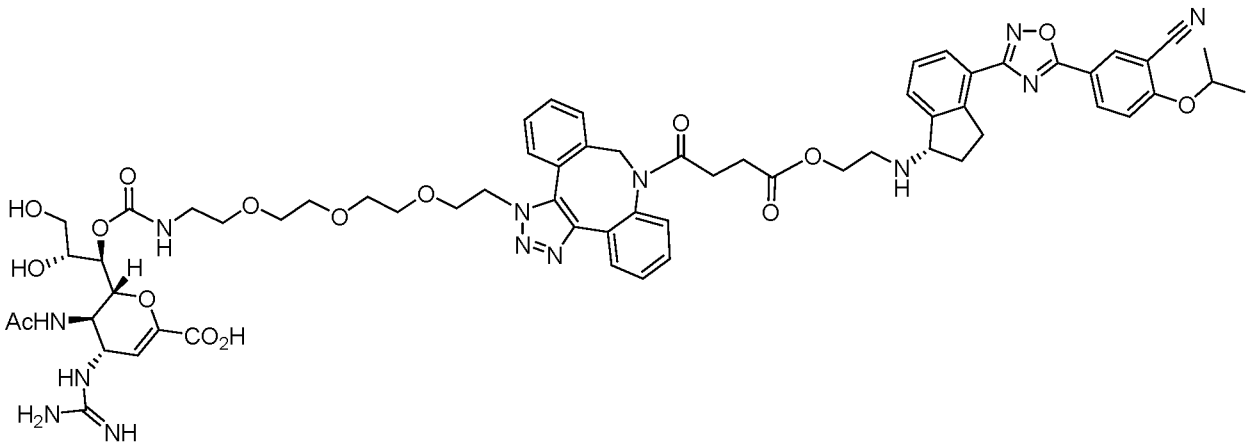

zanamivir-ozanimod,

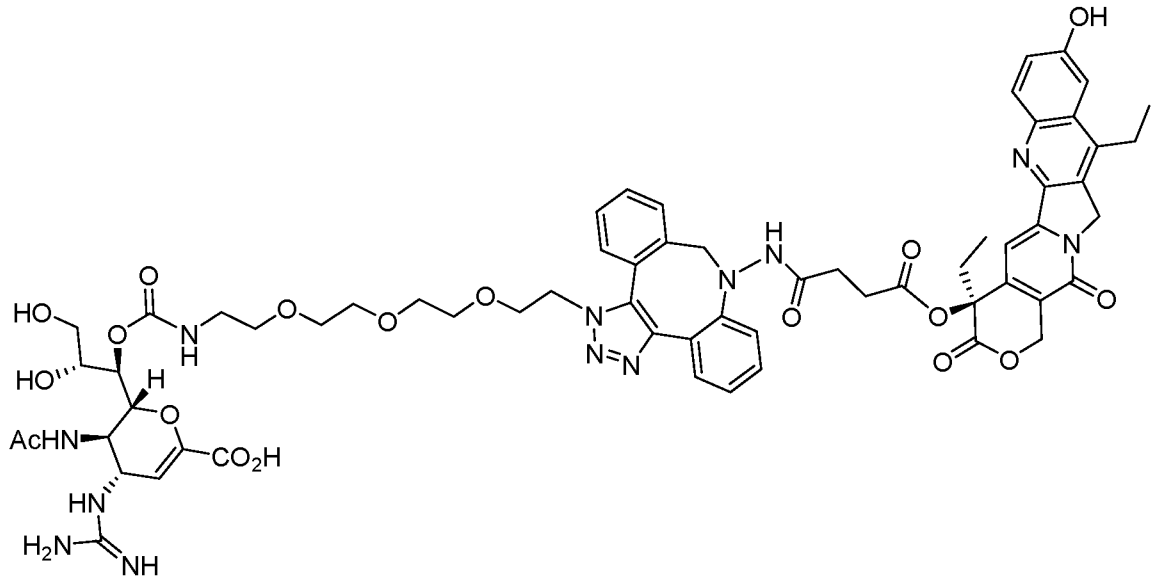

zanamivir-SN38,

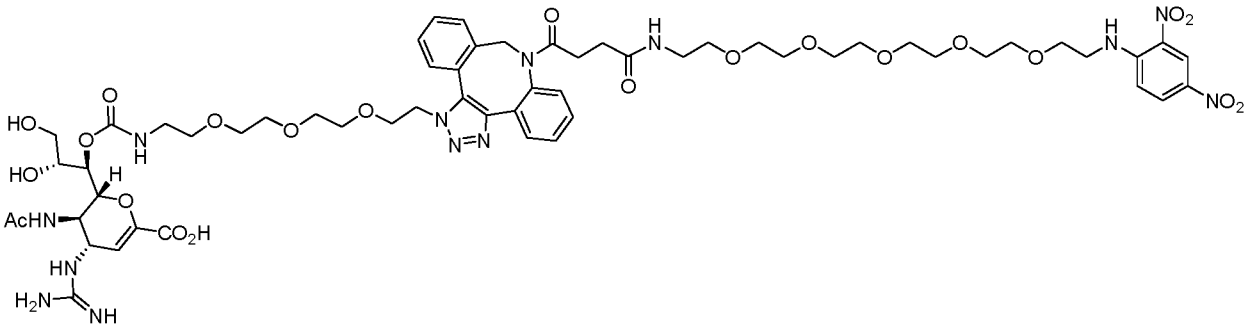

zanamivir-DNP,

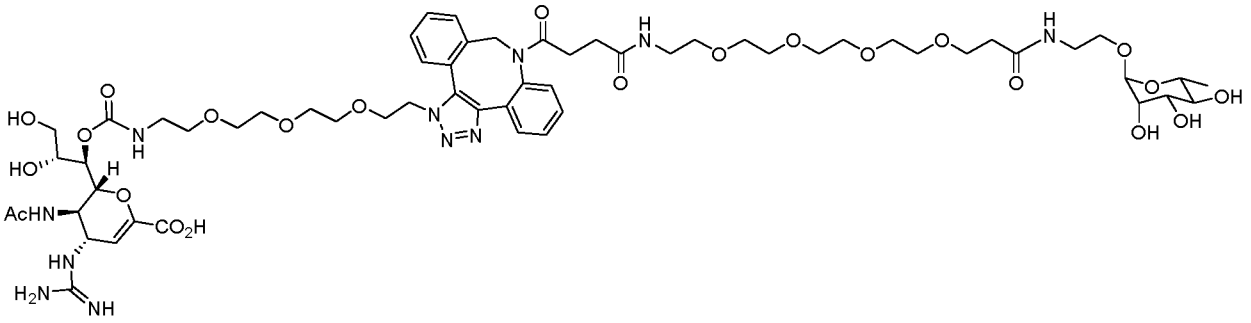

zanamivir-rhamnose,

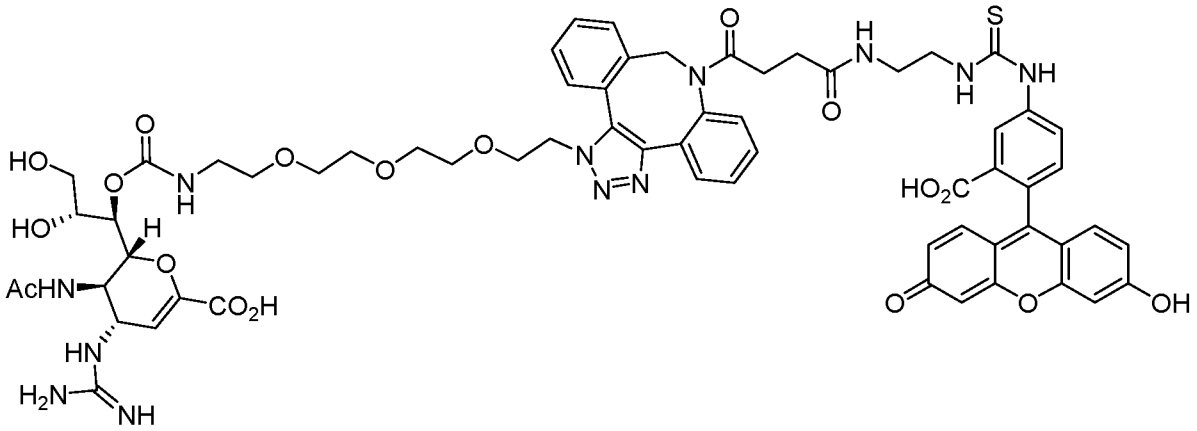

zanamivir-FITC, or

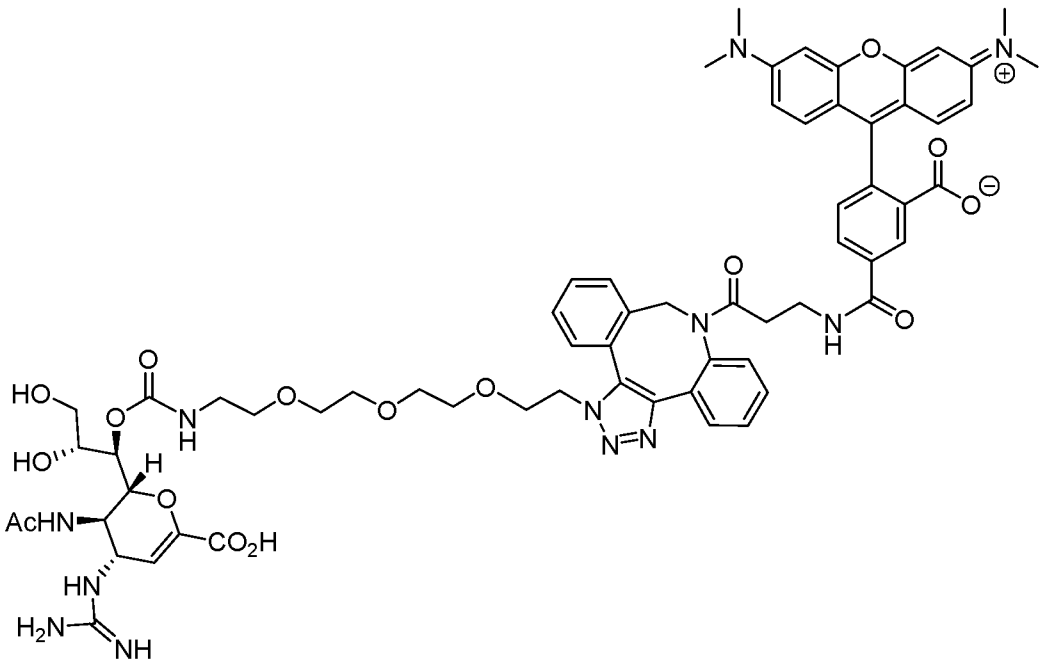

zanamivir-rhodamine.

8. The conjugate according to claim 2, wherein the cleavable bridge contains a disulfide or acid labile bond.
9. The conjugate according to claim 8, wherein the acid labile bond comprises an ester, hydrazone, oxime, acetal, ketal, phenolic ether, or Schiff base bond.
10. A method to treat influenza virus infection in a subject, comprising providing a conjugate to the subject, wherein said conjugate comprises a targeting ligand (TL) of NA of the

influenza virus, a linker (L) and a payload of drug (D), wherein the TL is a molecule that binds NA, the L is covalently bound to both the D and the TL, and the D is an imaging agent, a therapeutic drug, an immune modulator or the combination thereof.

11. The method according to claim 10, wherein the TL is zanamivir.
12. The method according to claim 10, wherein the therapeutic drug kills influenza virus infected cells in the subject, or inhibits influenza virus replication.
13. The method according to claim 10, wherein the therapeutic drug is selected from the group consisting of Tubulysin B hydrazide, pimodivir, and SN38.
14. The method according to claim 10, wherein the therapeutic drug comprising an adaptor molecule (i.e. fluorescein bound to the TL), and an anti-fluorescein CAR T cell, wherein upon binding to the adaptor, said CAR-T cell kills influenza virus infected cell or inhibits influenza virus replication in the subject.
15. The method according to claim 10, wherein the immune modulator dampens influenza virus induced early cytokine storm.
16. The method according to claim 10, wherein the immune modulator is ozanimod or a hapten recognized by an autologous antibody.
17. The method according to claim 16, wherein the hapten is comprised of dinitrophenyl (DNP), trinitrophenyl (TNP), rhamnose, or an alpha-galactosyl moiety.
18. The conjugate according to claim 1, where the conjugate comprises an imaging agent used to quantify the intensity of the influenza infection.
19. The conjugate according to claim 18, wherein the imaging agent comprises a chelation complex containing technetium-99m (^{99m}Tc).
20. The conjugate according to claim 4, wherein the conjugate has a binding affinity to the NA at about 1 nM to about 15nM.
21. The method according to claim 11, wherein the zanamivir conjugate elicits immune responses leading to the clearance of antibody-coated virus or virus infected cells via antibody dependent cellular phagocytosis (ADCP), antibody dependent cellular cytotoxicity (ADCC) or complement-dependent cytotoxicity (CDC).
22. A system comprising at least two components, a first component comprising a conjugate containing a targeting ligand (TL) for an envelope protein of an influenza virus, a linker (L) and a payload of drug (D), wherein the TL is a molecule that binds the envelop protein,

the L is covalently bound to both the D and the TL, and the D is a fluorescein; a second component comprising an anti-fluorescein CAR T cell that binds to the first component's fluorescein, wherein said system is promoted to kill an influenza virus-infected cell.

23. The method according to claim 10, wherein D is an antigen or a moiety that the subject has pre-existing immunity.
24. The method according to claim 23, further comprising a step of concurrently administering to the subject an effective dose of antibody to said antigen or moiety.
25. The method according to claim 23 wherein said antigen or moiety is a bacteria toxin.

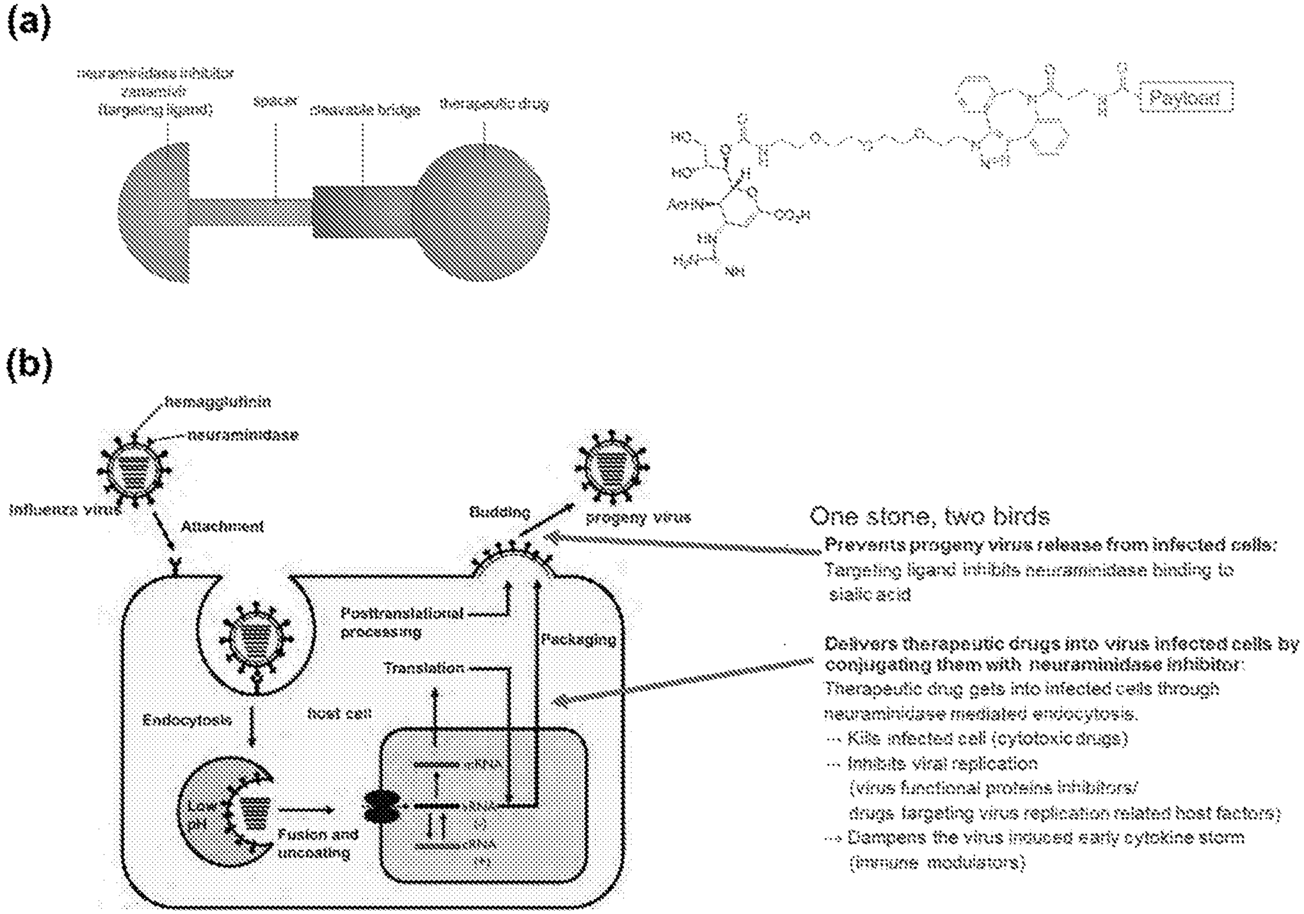
(a)
neuraminidase inhibitor
zanamivir
(targeting ligand)
spacer
cleavable bridge
therapeutic drug
Payload
(b)
hemagglutinin
neuraminidase
Influenza virus
Attachment
Endocytosis
host cell
Low pH
Fusion and uncoating
Posttranslational processing
Translation
Packaging
Budding
progeny virus
One stone, two birds
Prevents progeny virus release from infected cells:
Targeting ligand inhibits neuraminidase binding to sialic acid
Delivers therapeutic drugs into virus infected cells by conjugating them with neuraminidase inhibitor:
Therapeutic drug gets into infected cells through neuraminidase mediated endocytosis.
→ Kills infected cell (cytotoxic drugs)
→ Inhibits viral replication
(virus functional proteins inhibitors/
drugs targeting virus replication related host factors)
→ Dampens the virus induced early cytokine storm
(immune modulators)

FIGURE 1

1. Tubulysin B hydrazide (microtubule inhibitor)
1. kills virus infected cell (cytotoxic drug)
2. inhibits virus replication (drug targeting virus replication related host factor)
Tubulysin B hydrazide
Zanamivir-tubulysin B hydrazide conjugate
2. Pimodivir (VX787) (RNA-dependent RNA polymerase (RdRp) inhibitor)
inhibits virus replication (drug targeting virus functional protein)
Pimodivir (VX787)
Zanamivir-Pimodivir conjugate

FIGURE 2A

3. Ozanimod (RPC1063) (sphingosine-1-phosphate Receptor 1 agonist)
dampens virus induced early cytokine storm (immune modulator)

Ozanimod (RPC1063)

Zanamivir-ozanimod conjugate

4. SN38 (topoisomerase I inhibitor)
1. kills virus infected cell (cytotoxic drug)
2. dampens virus induced early cytokine storm (immune modulator)

SN38

Zanamivir-SN38 conjugate

FIGURE 2B

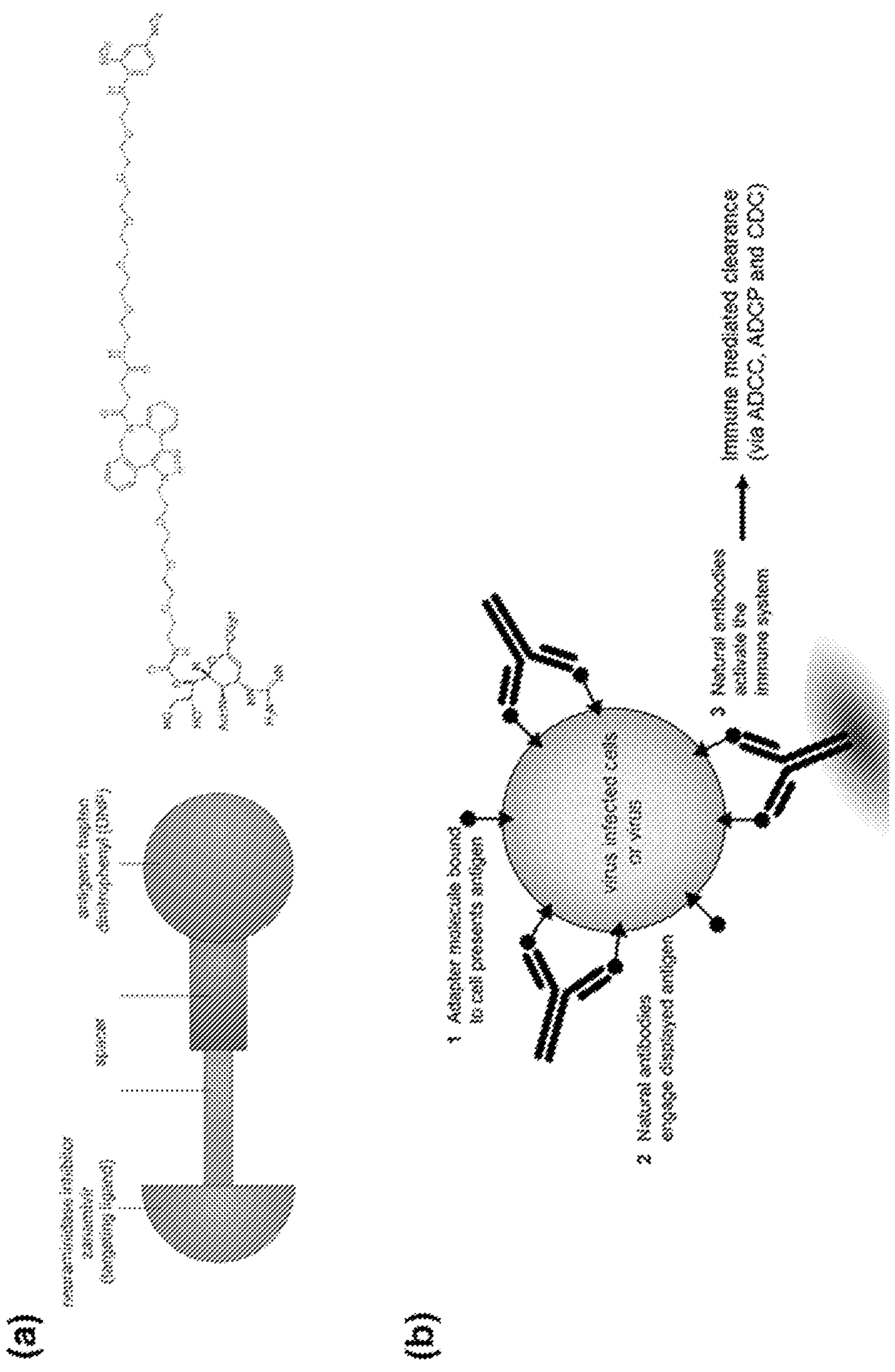
(a)
(b)
1 Adapter molecule bound to cell presents antigen
2 Natural antibodies engage displayed antigen
virus infected cells or virus
3 Natural antibodies activate the immune system
Immune mediated clearance (via ADCC, ADCP and CDC)

FIGURE 3

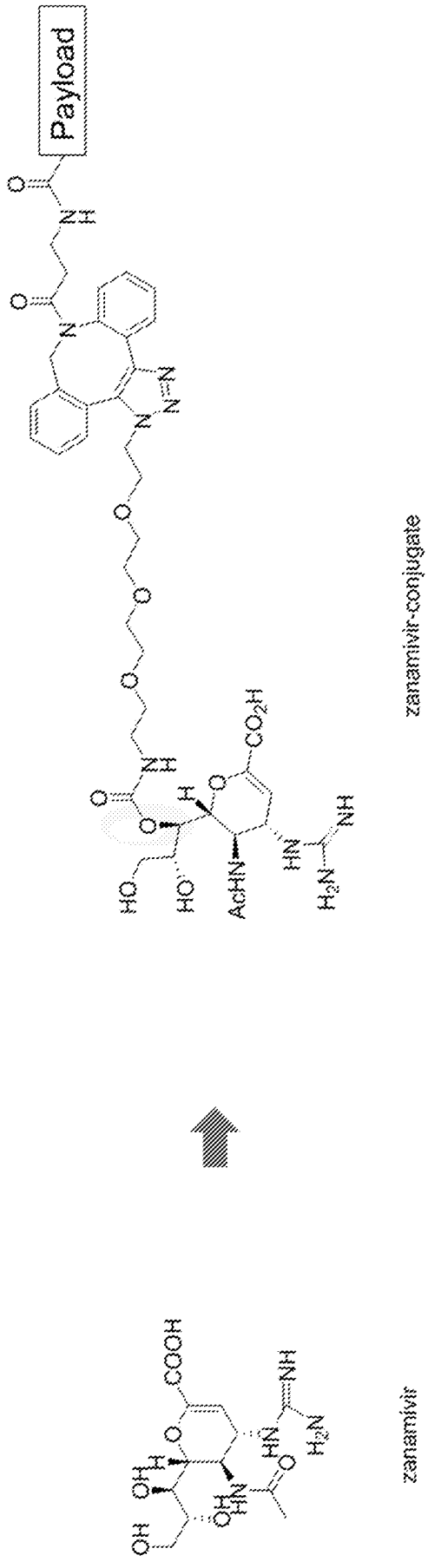

FIGURE 4

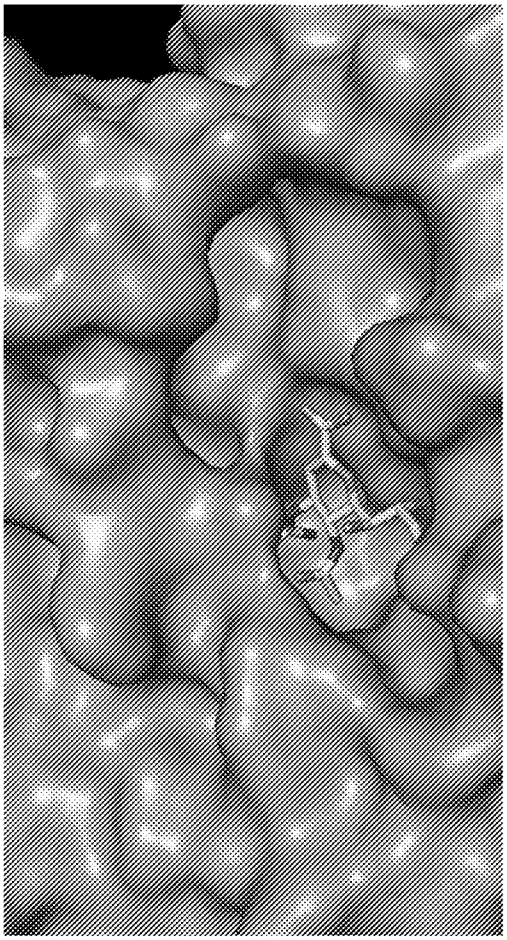

FIGURE 5

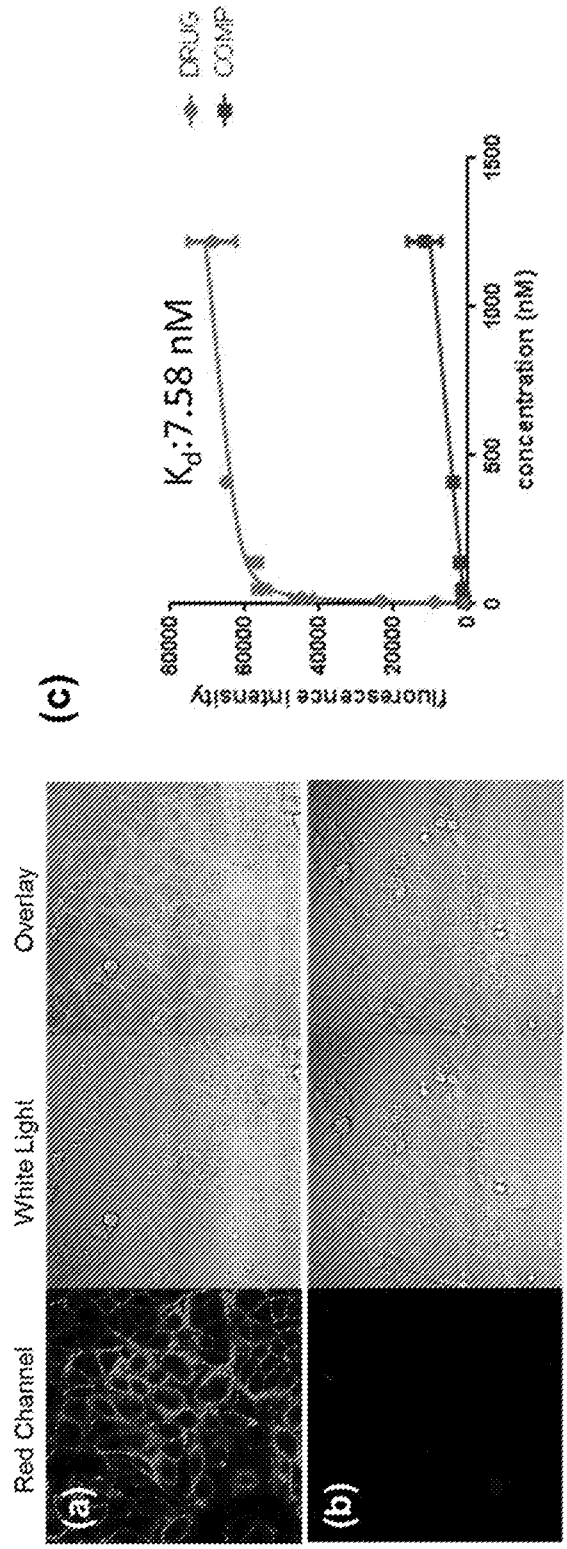
Red Channel
White Light
Overlay
(a)
(b)
(c)
DRUG
COMP
K_d:7.58 nM
fluorescence intensity
concentration (nM)
0
200000
400000
600000
800000
0
500
1000
1500

FIGURE 6

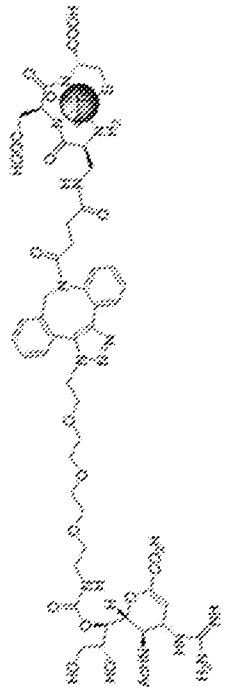

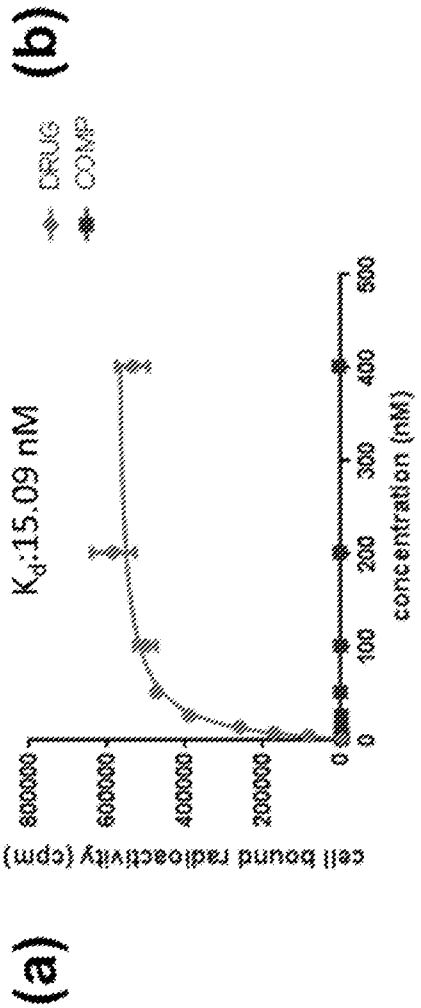
(a)
cell bound radioactivity (cpm)
800000
600000
400000
200000
0
100
200
300
400
500
concentration (nM)
K_d:15.09 nM
DRUG
COMP
(b)

FIGURE 7

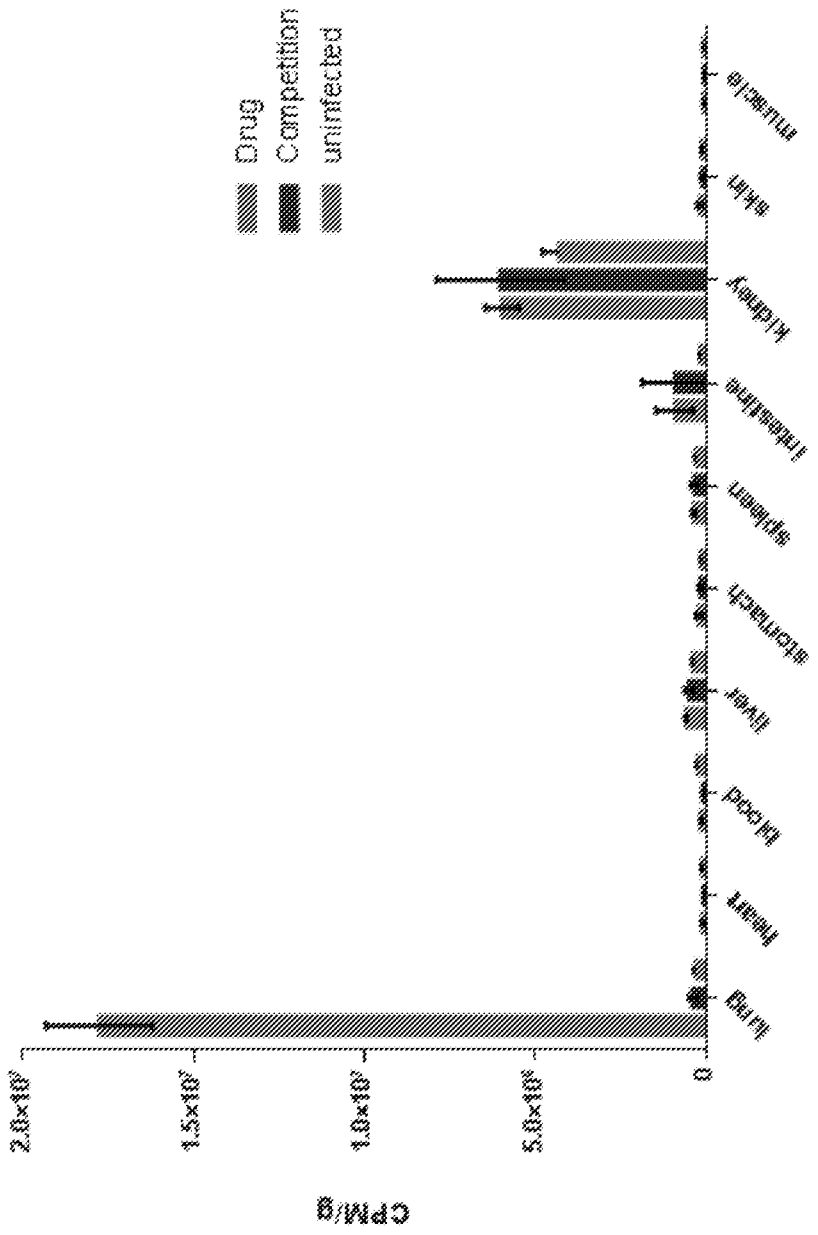
Drug
Competition
uninfected
CPM/g
2.0x10⁷
1.5x10⁷
1.0x10⁷
5.0x10⁶
0

FIGURE 8

	EC_{50} (nM)
Zanamivir-tubulysin conjugate	5.155
Free tubulysin	9.865
Zanamivir-tubulysin+ 100 × zanamivir	180

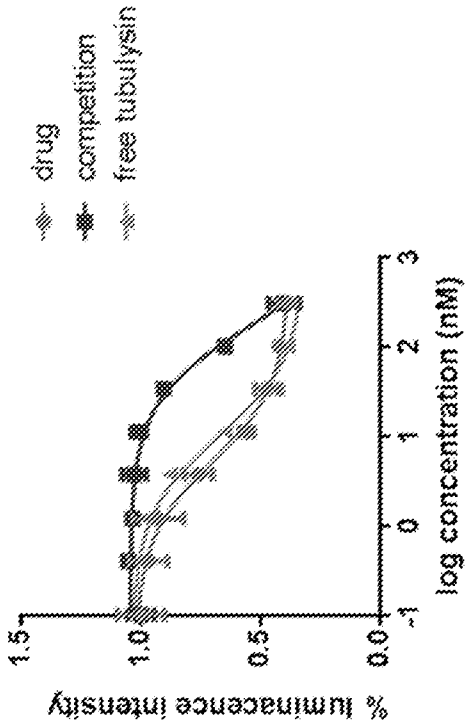

FIGURE 9

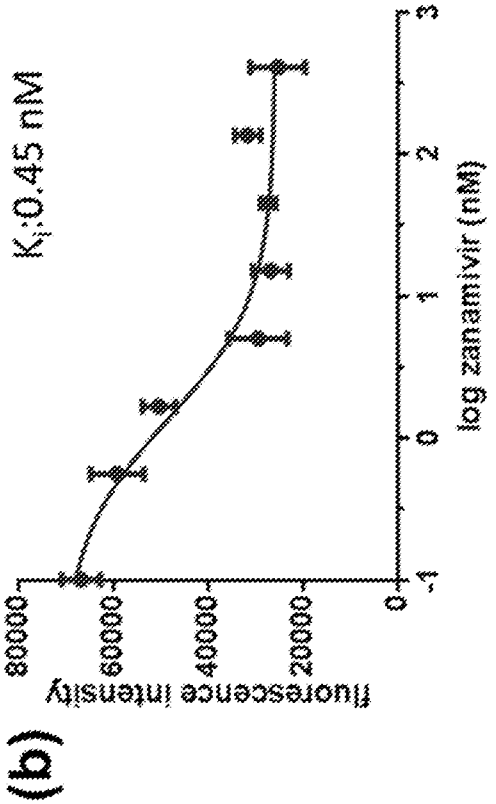
(b)
K_i:0.45 nM
fluorescence intensity
80000
60000
40000
20000
0
-1
0
1
2
3
log zanamivir (nM)

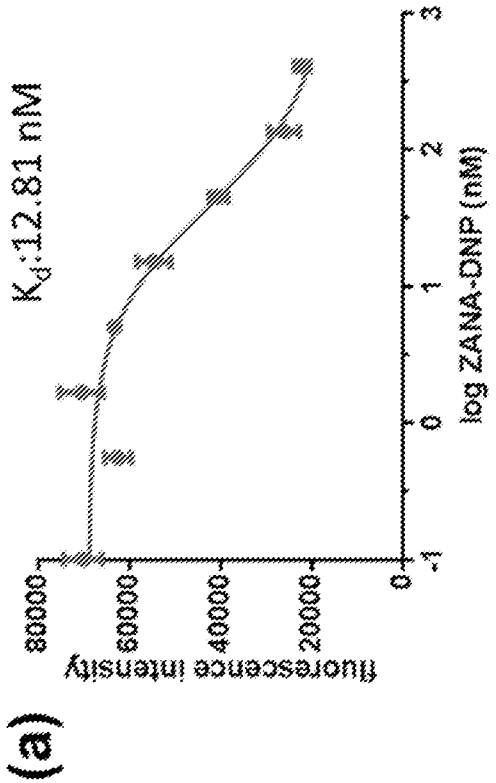
(a)
K_d:12.81 nM
fluorescence intensity
80000
60000
40000
20000
0
-1
0
1
2
3
log ZANA-DNP (nM)

FIGURE 10

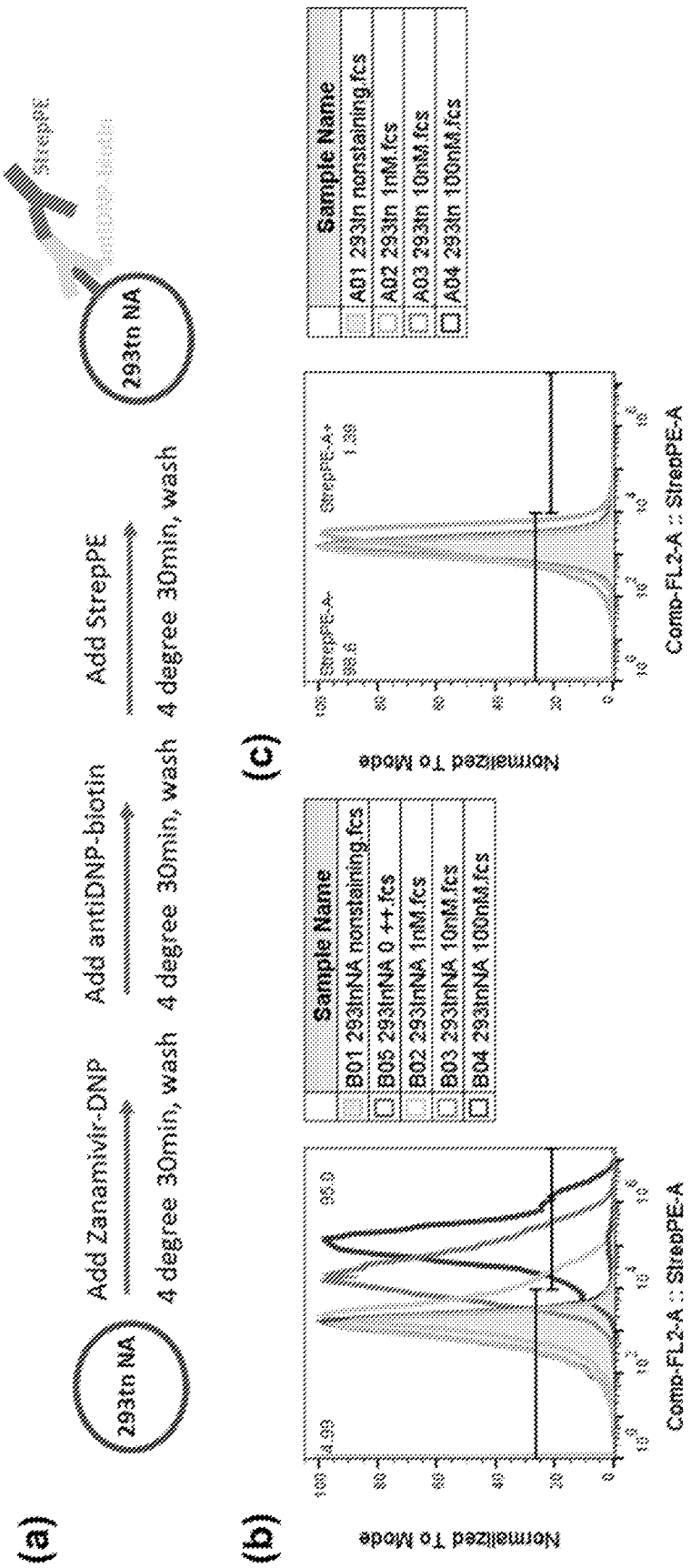
(a)
293tn NA
Add Zanamivir-DNP
4 degree 30min, wash
Add antiDNP-biotin
4 degree 30min, wash
Add StrepPE
4 degree 30min, wash
293tn NA
StrepPE
(b)
Normalized To Mode
Comp-FL2-A :: StrepPE-A
Sample Name
B01 293tnNA nonstaining.fcs
B05 293tnNA 0 ++.fcs
B02 293tnNA 1nM.fcs
B03 293tnNA 10nM.fcs
B04 293tnNA 100nM.fcs
(c)
Normalized To Mode
Comp-FL2-A :: StrepPE-A
Sample Name
A01 293tn nonstaining.fcs
A02 293tn 1nM.fcs
A03 293tn 10nM.fcs
A04 293tn 100nM.fcs

FIGURE 11

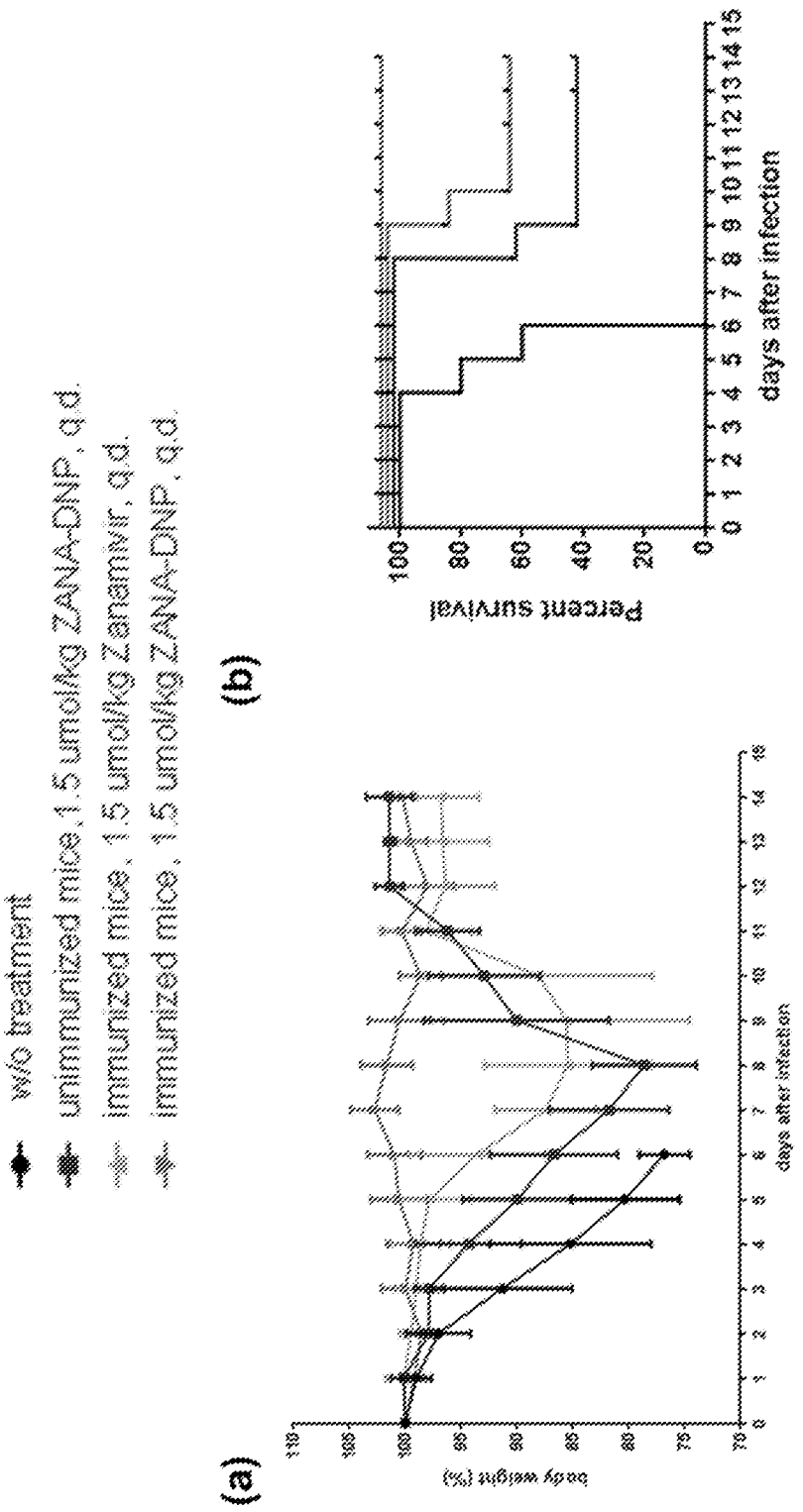
w/o treatment
unimmunized mice,1.5 umol/kg ZANA-DNP, q.d.
immunized mice, 1.5 umol/kg Zanamivir, q.d.
immunized mice, 1.5 umol/kg ZANA-DNP, q.d.
(a)
(b)
Percent survival
days after infection

FIGURE 12

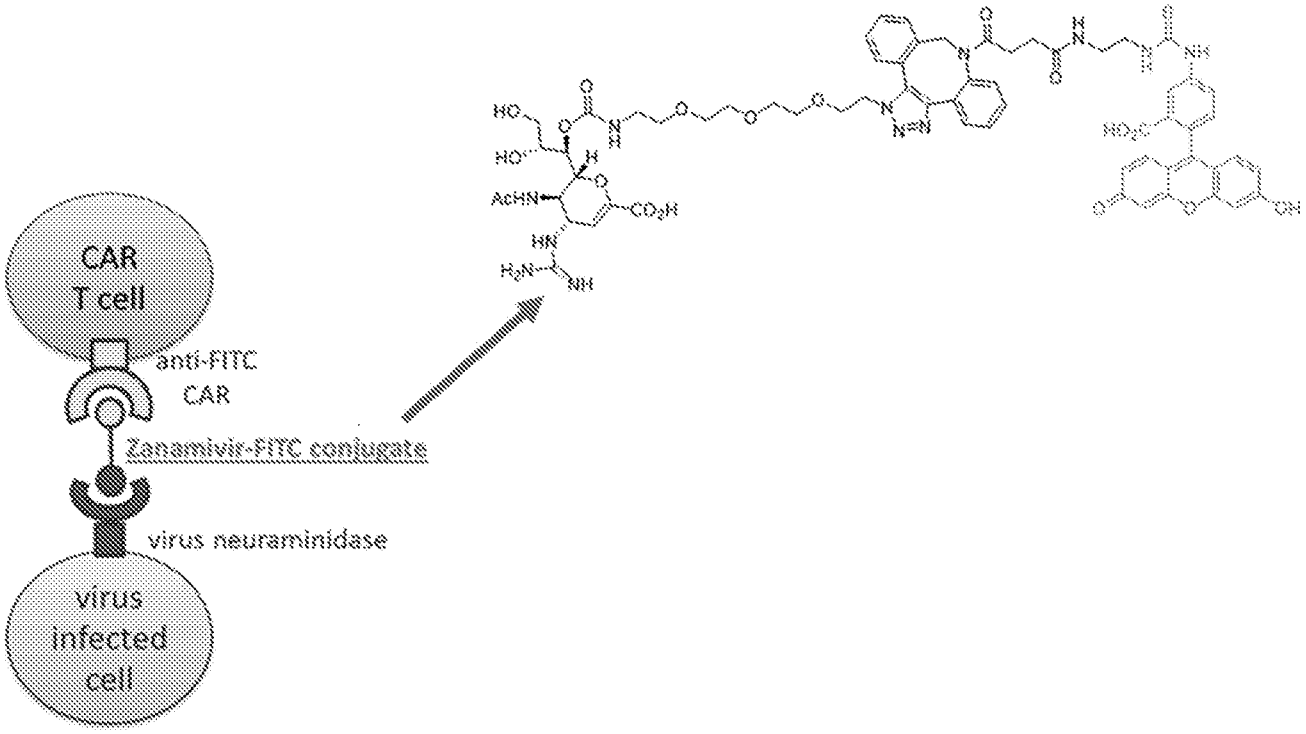
CAR
T cell
anti-FITC
CAR
Zanamivir-FITC conjugate
virus neuraminidase
virus
infected
cell

FIGURE 13

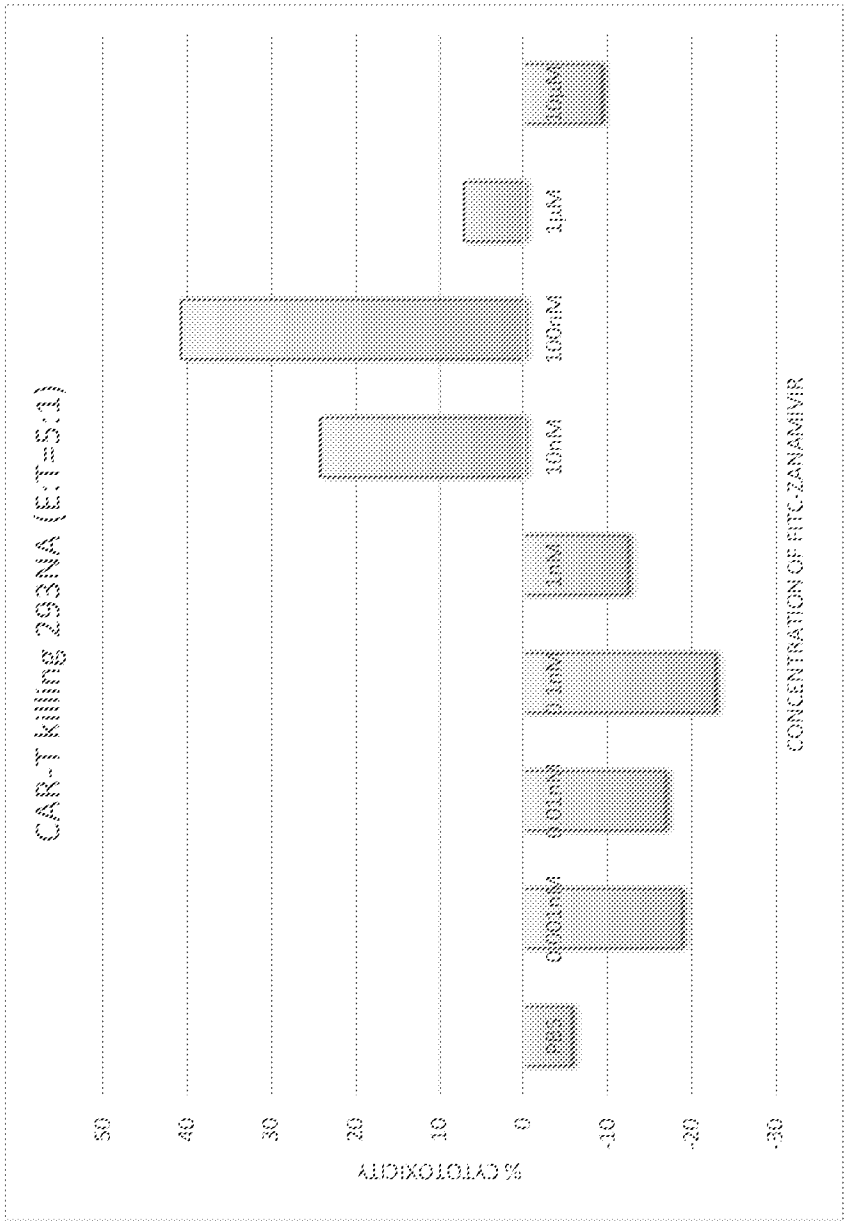
CAR-T killing 293NA (E:T=5:1)
% CYTOTOXICITY
60
40
30
20
10
0
-10
-20
-30
DMSO
0.01nM
0.1nM
1nM
10nM
100nM
1μM
10μM
CONCENTRATION OF PITAVASTATIN

FIGURE 14 A

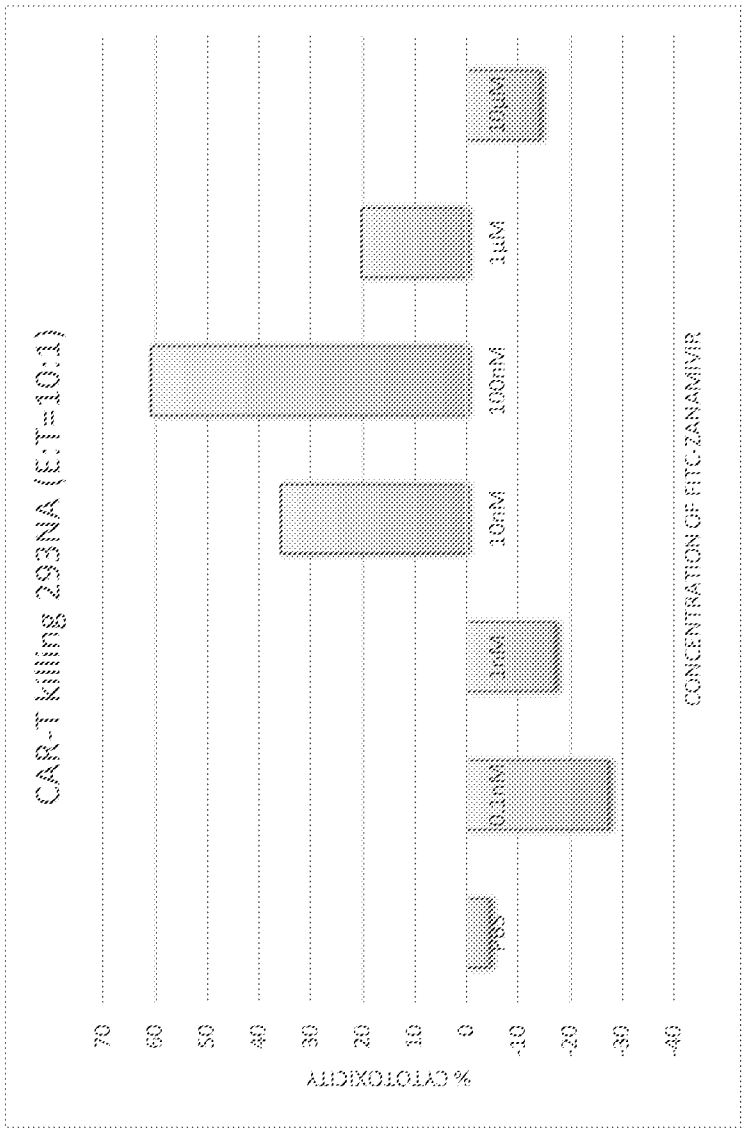
CAR-T killing 293NA (E:T=10:1)
% CYTOTOXICITY
70
60
50
40
30
20
10
0
-10
-20
-30
-40
CONCENTRATION OF FITC-ZANAMIVIR
100μM
1μM
100nM
10nM
1nM
0.1nM
0pM

FIGURE 14 B

No binding of Zanamivir-FITC to normal 293T cells

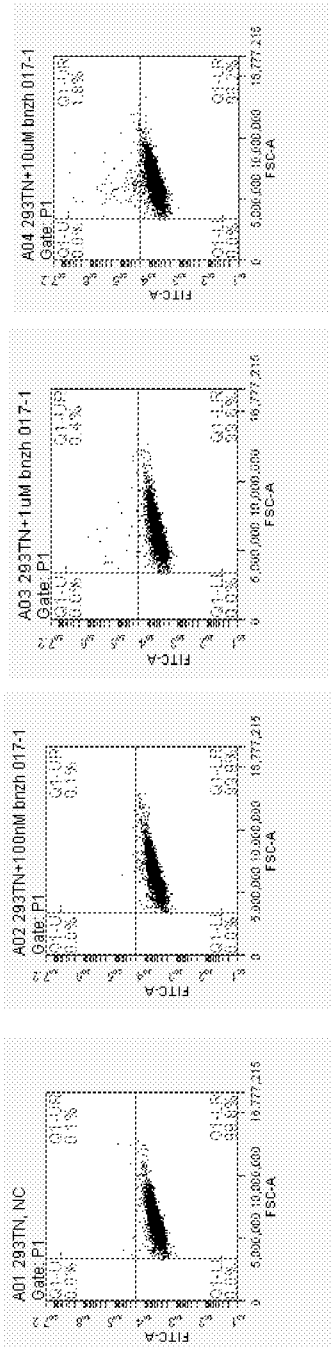

Adaptor Concentration	0	100nM	1uM	10uM
% binding to 293T	0.1%	0.1%	0.4%	1.8%

FIGURE 15

LDH Killing of Negative Controls		
	10nM	100nM
HEK-293 + FITC-zanamivir	-1.90	-2.77
293NA + EC17	5.65	3.65
293NA + Free zanamivir	-1.69	2.46

The cytotoxicity against NA is specifically induced by Zanamivir-FITC

FIGURE 16

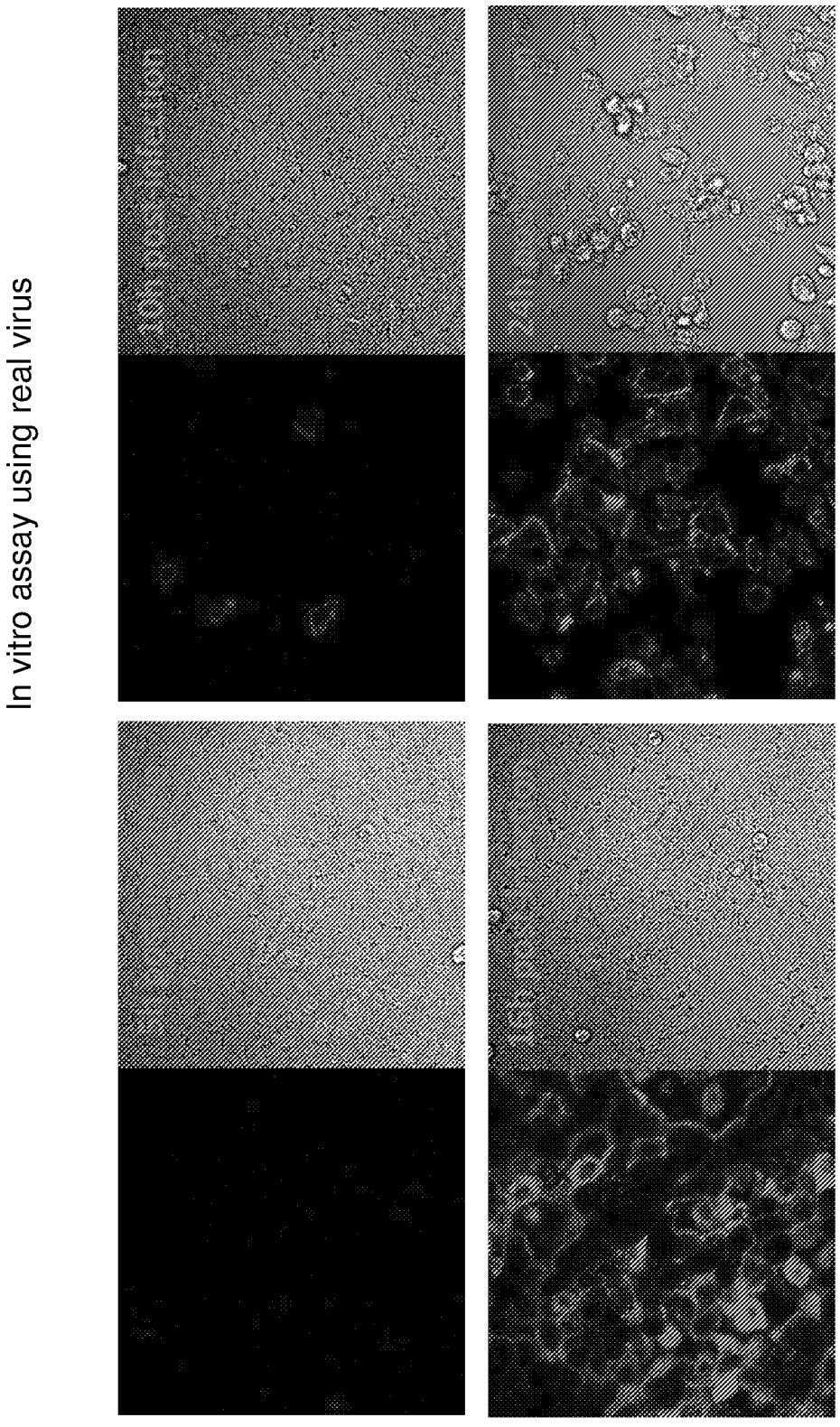

FIGURE 17

LDH assay of CAR-T Killing Influenza Infected MDCK

- T cell : MDCK = 10 : 1
- Co-cultured for 18 hours
- Maximum killing: 10%.

CAR-T : Infected MDCK = 10 : 1
Co-cultured for 7 hours 100nM adaptor causes 8.4% killing.
No killing for non-infected MDCK

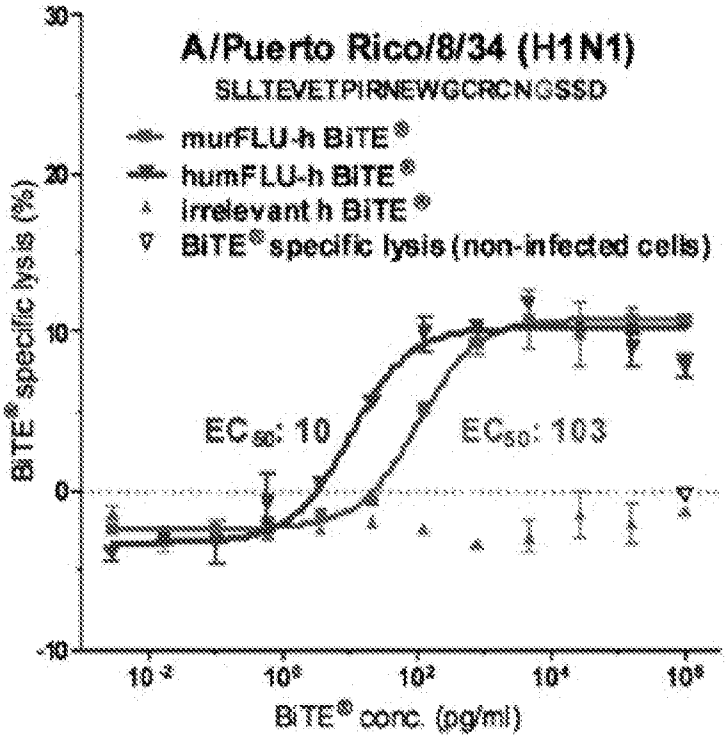

Pendzialek, J. etc. Antiviral Res. May;141:155-164.

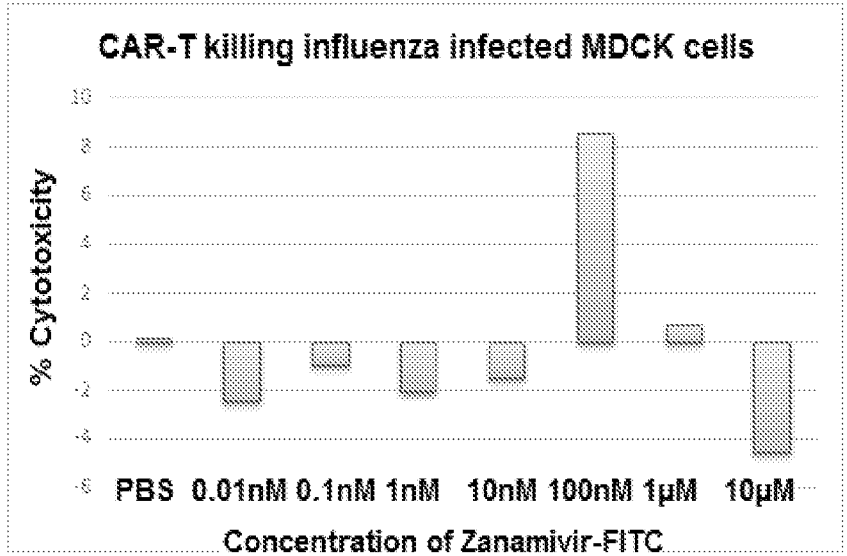

Our experimental results

FIGURE 18

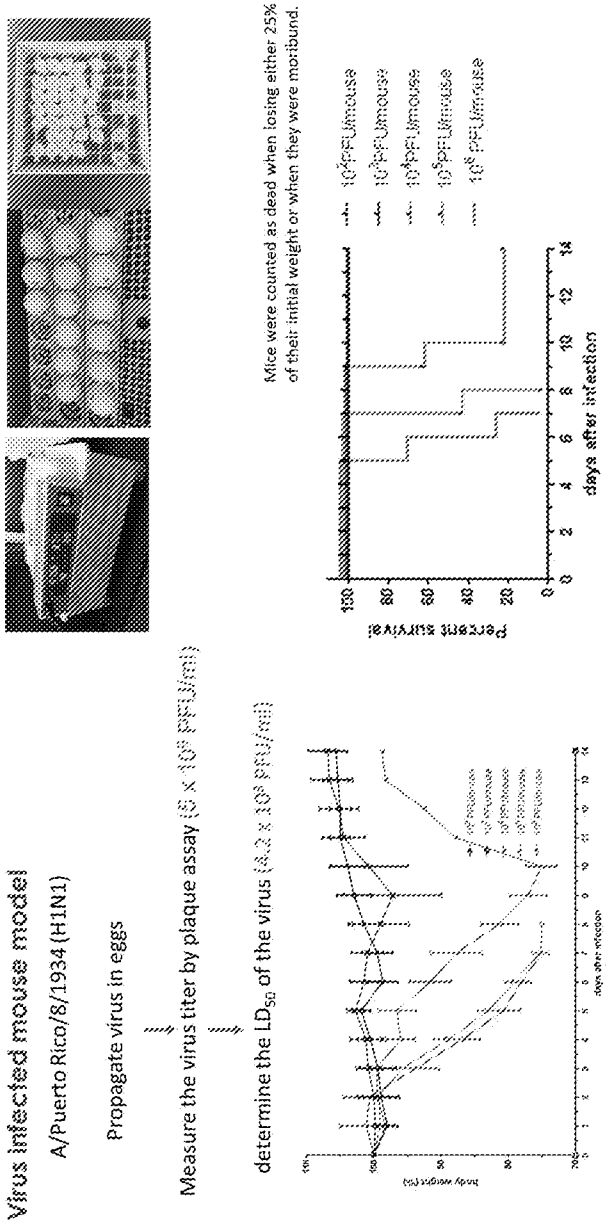
Virus infected mouse model
A/Puerto Rico/8/1934 (H1N1)
Propagate virus in eggs
Measure the virus titer by plaque assay (5 x 10⁶ PFU/ml)
determine the LD50 of the virus (4.2 x 10⁵ PFU/ml)
Mice were counted as dead when losing either 25% of their initial weight or when they were moribund.
Percent survival
days after infection
10⁴ PFU/mouse
10⁵ PFU/mouse
10⁶ PFU/mouse
10⁷ PFU/mouse
10⁸ PFU/mouse

FIGURE 19

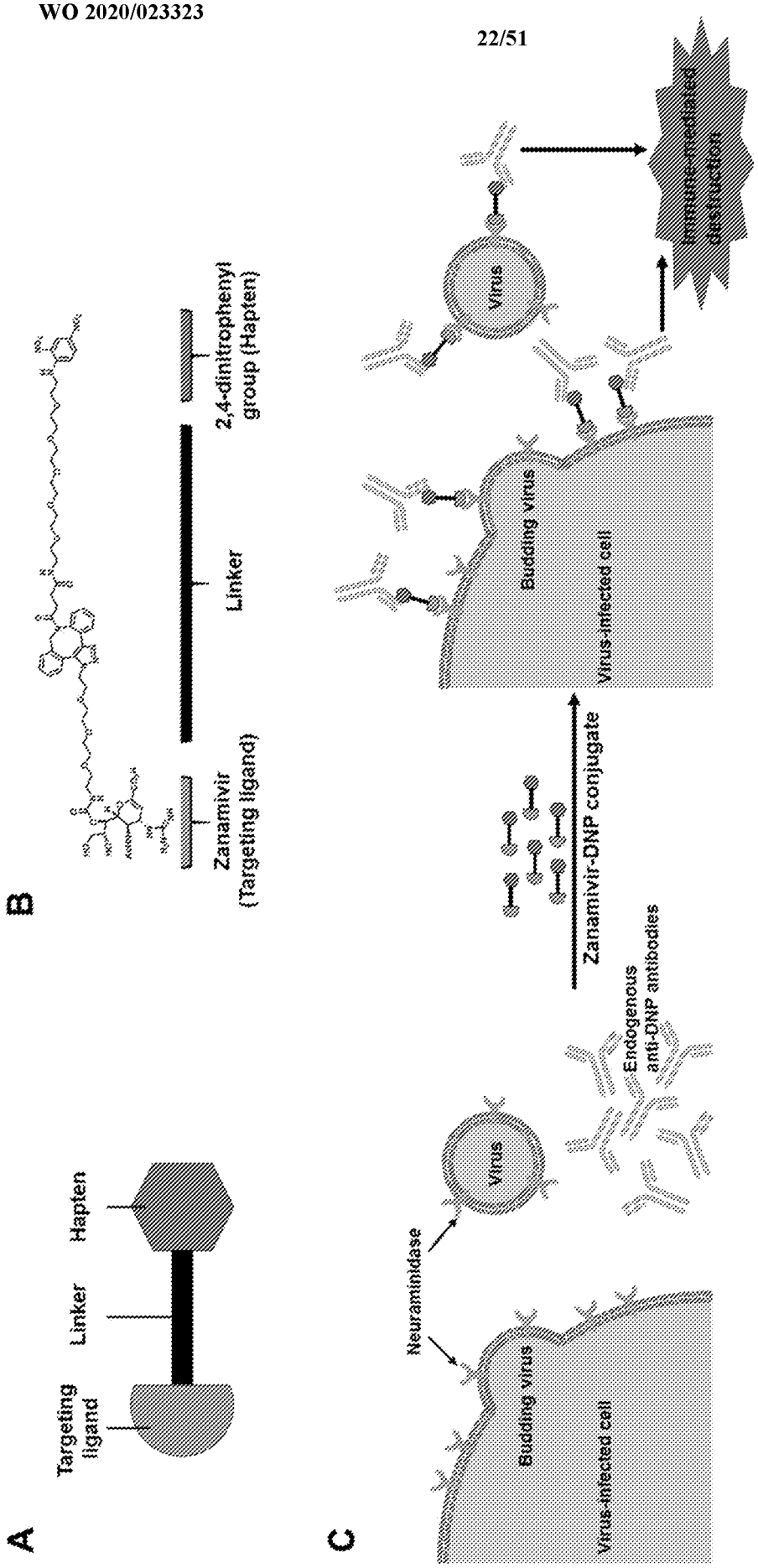
A
Targeting ligand
Linker
Hapten
B
Zanamivir (Targeting ligand)
Linker
2,4-dinitrophenyl group (Hapten)
C
Neuraminidase
Virus
Budding virus
Virus-infected cell
Endogenous anti-DNP antibodies
Zanamivir-DNP conjugate
Virus
Budding virus
Virus-infected cell
Immune-mediated destruction

FIGURE 20 A-C

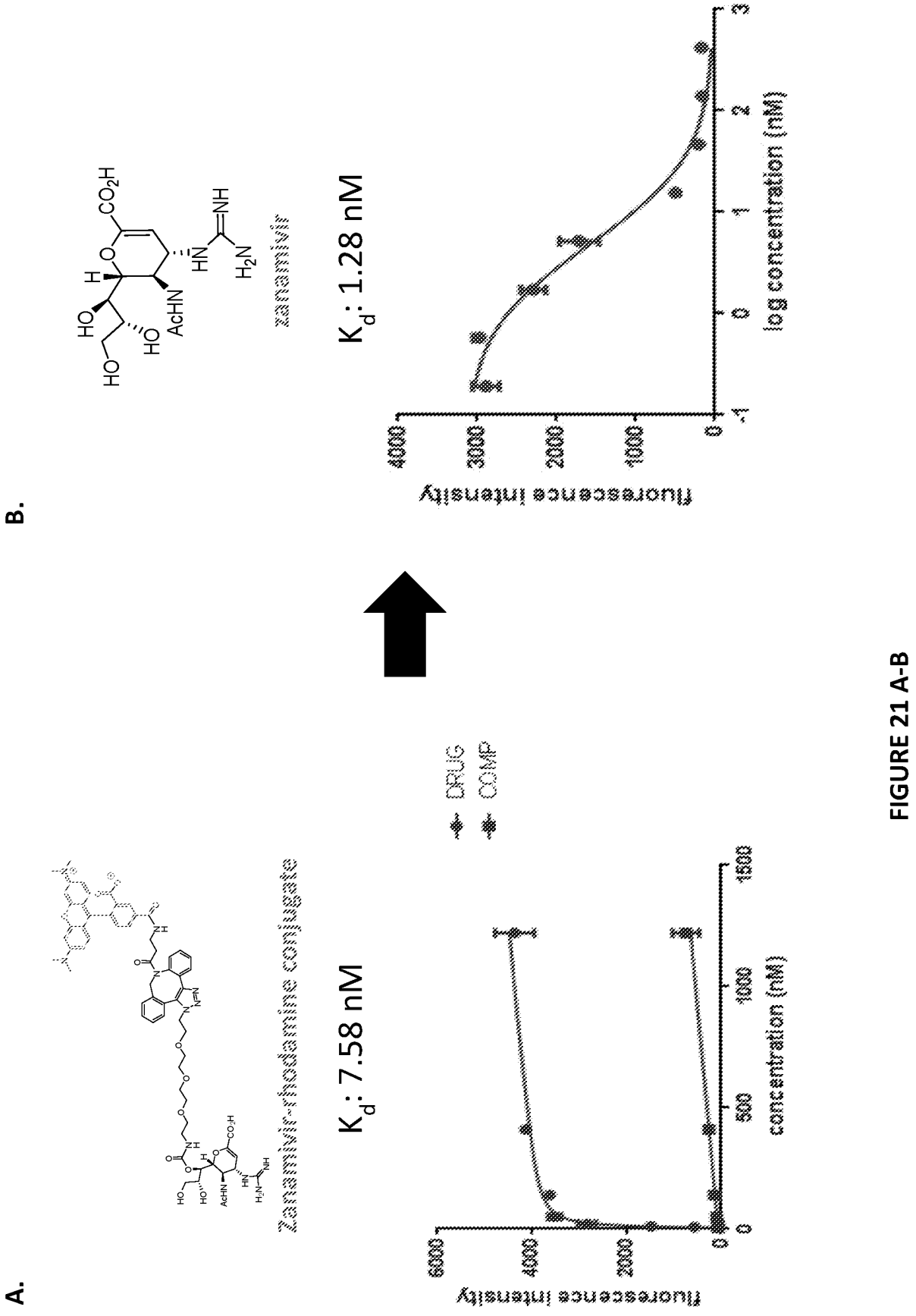
B.
zanamivir
K_d: 1.28 nM
fluorescence intensity
log concentration (nM)
A.
Zanamivir-rhodamine conjugate
K_d: 7.58 nM
DRUG
COMP
fluorescence intensity
concentration (nM)

FIGURE 21 A-B

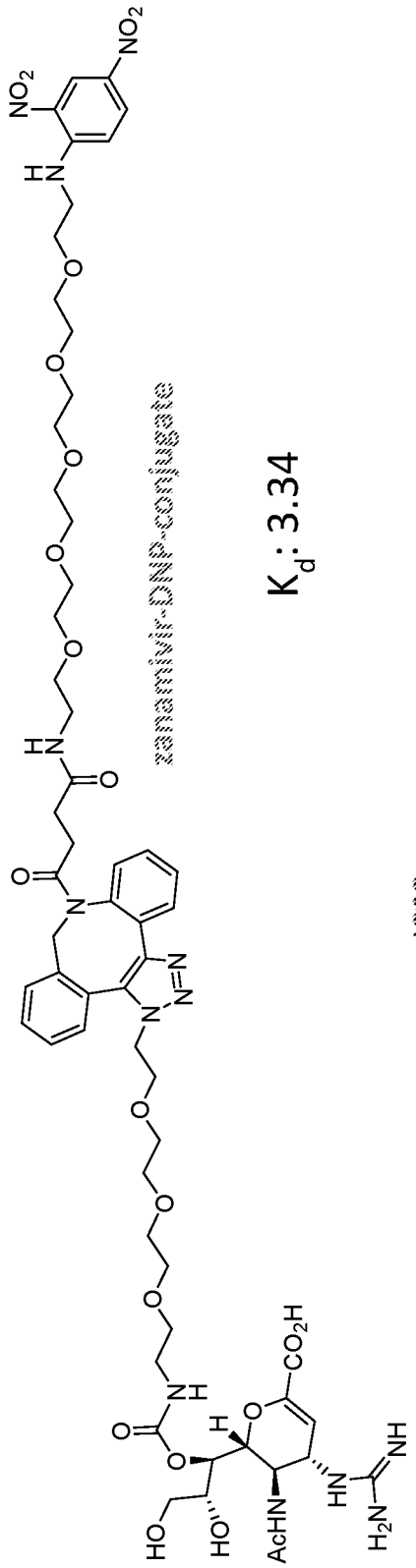

K_d: 3.34

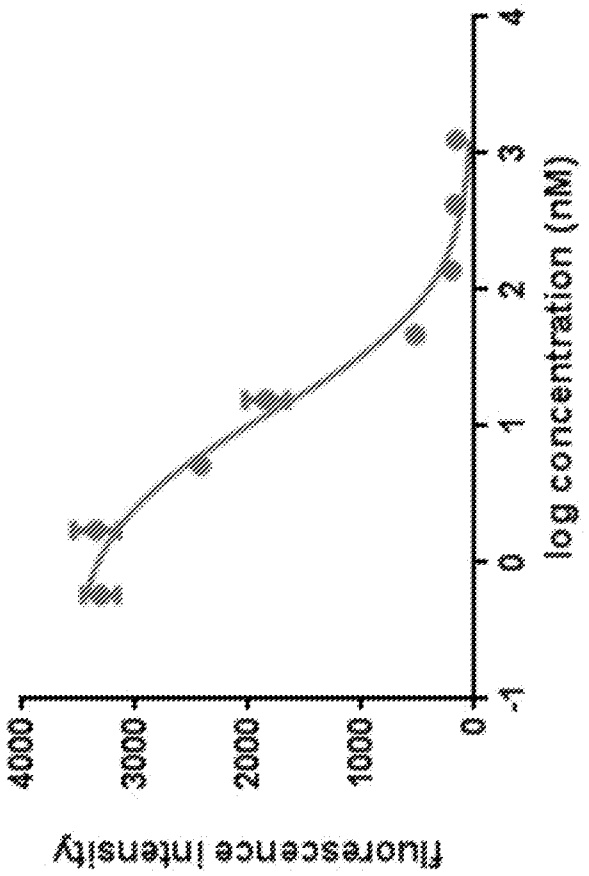

FIGURE 21 C.

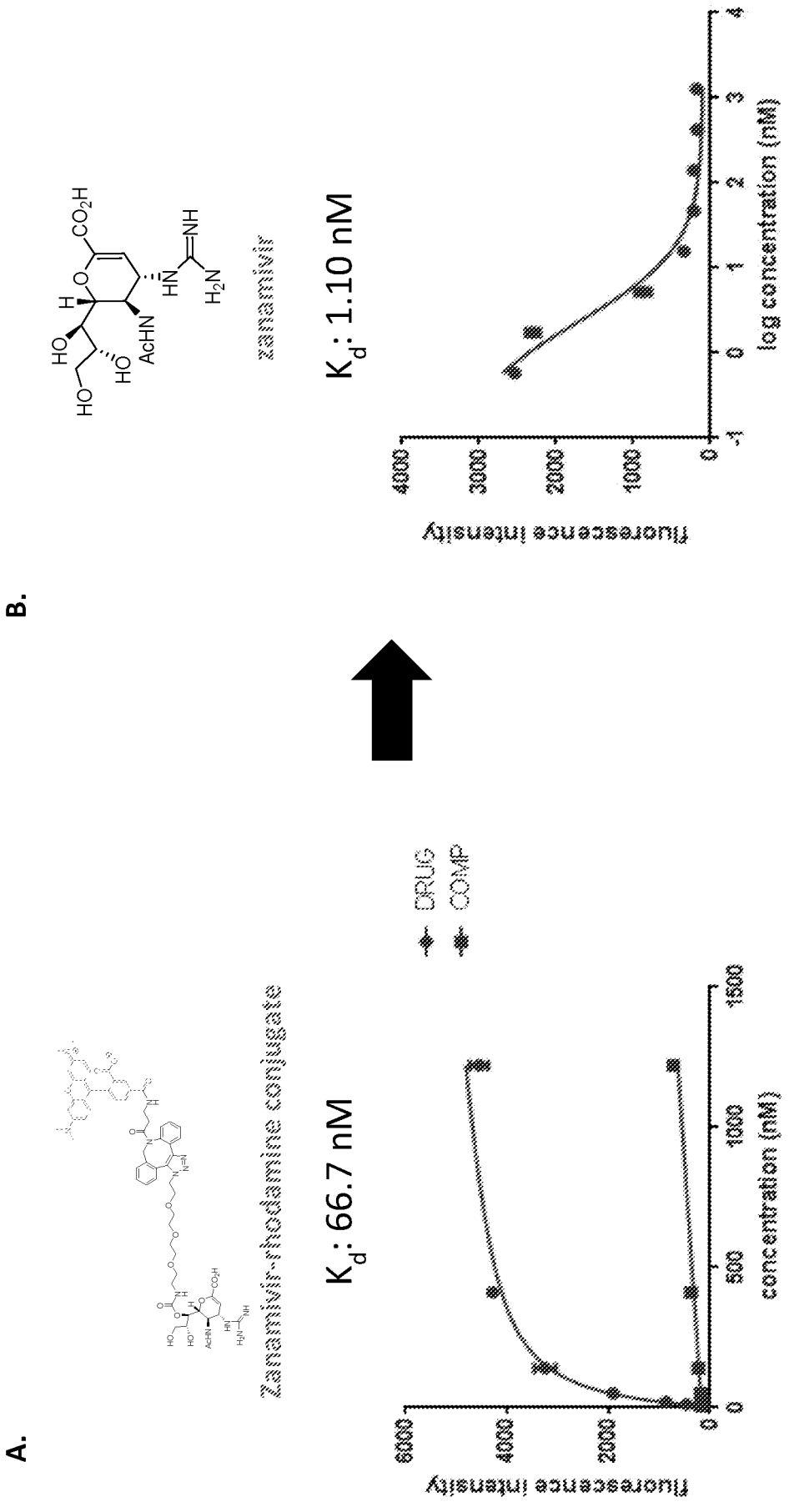
A.
Zanamivir-rhodamine conjugate
DRUG
COMP
K_d: 66.7 nM
fluorescence intensity
concentration (nM)
B.
zanamivir
K_d: 1.10 nM
fluorescence intensity
log concentration (nM)

FIGURE 22 A-B

C.

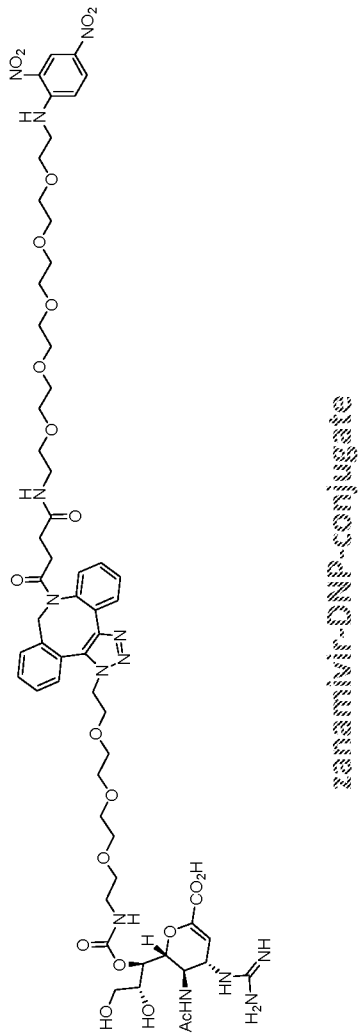

zanamivir-DNP-conjugate

K_d: 9.56 nM

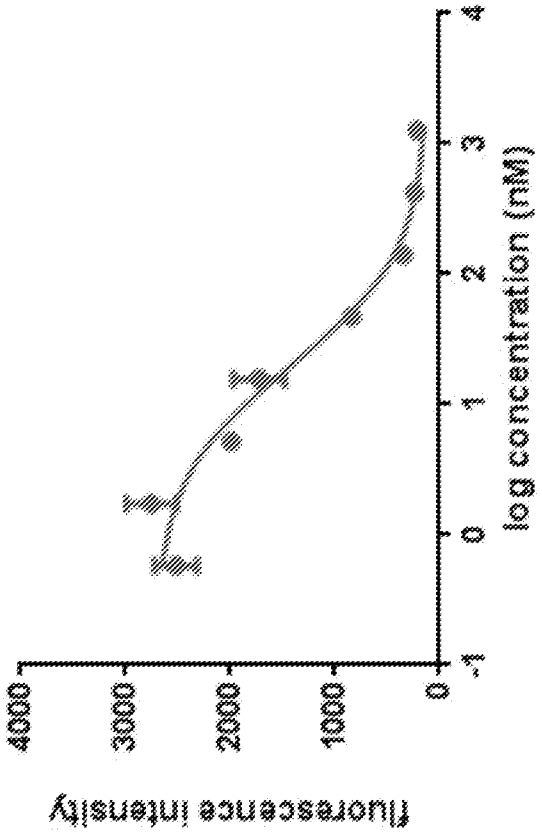

FIGURE 22 C

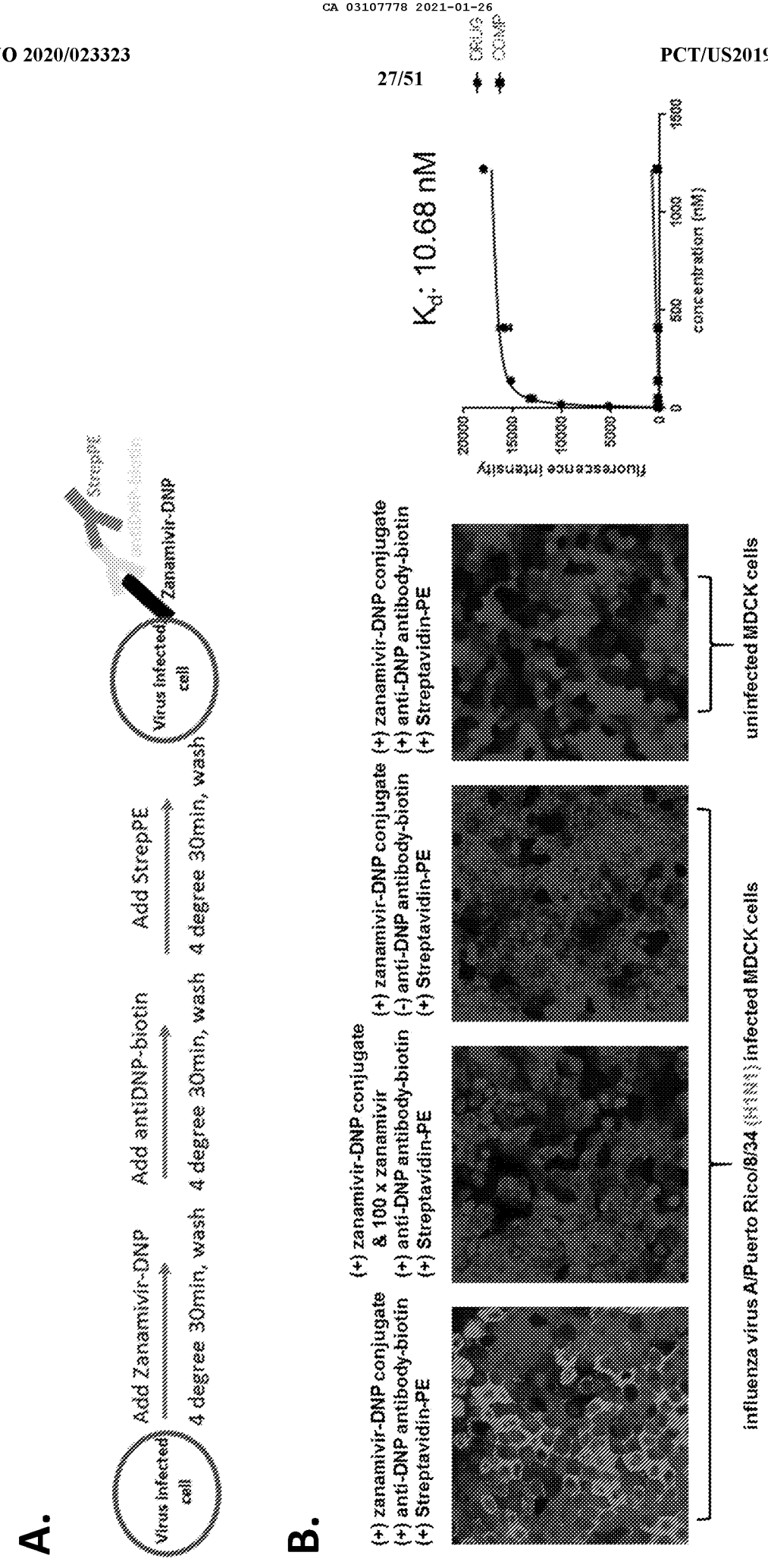
A.
Virus infected cell
Add Zanamivir-DNP
4 degree 30min, wash
Add antiDNP-biotin
4 degree 30min, wash
Add StrepPE
4 degree 30min, wash
Zanamivir-DNP
StrepPE
B.
(+) zanamivir-DNP conjugate
(+) anti-DNP antibody-biotin
(+) Streptavidin-PE
(+) zanamivir-DNP conjugate & 100 x zanamivir
(+) anti-DNP antibody-biotin
(+) Streptavidin-PE
(+) zanamivir-DNP conjugate
(-) anti-DNP antibody-biotin
(+) Streptavidin-PE
(+) zanamivir-DNP conjugate
(+) anti-DNP antibody-biotin
(+) Streptavidin-PE
influenza virus A/Puerto Rico/8/34 infected MDCK cells
uninfected MDCK cells
K_d: 10.68 nM
fluorescence intensity
concentration (nM)
CBUS
CDNP

FIGURE 23 A-B

A.

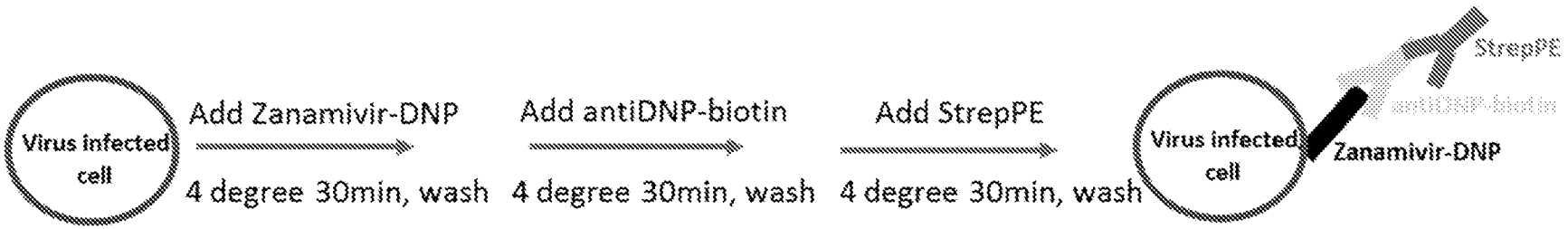

B.

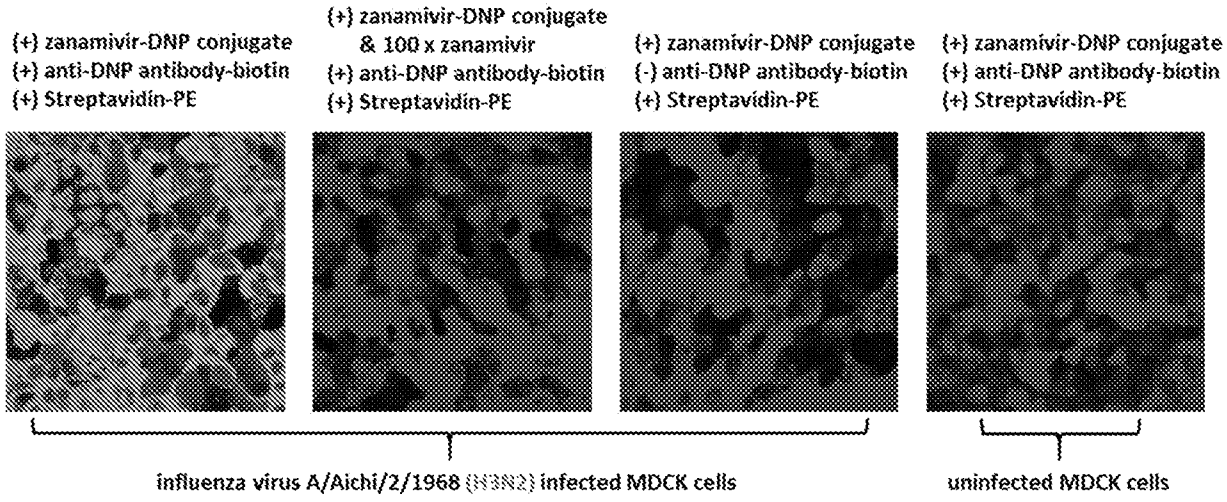

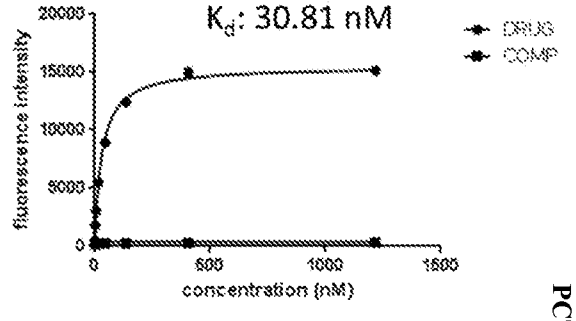

FIGURE 24 A-B

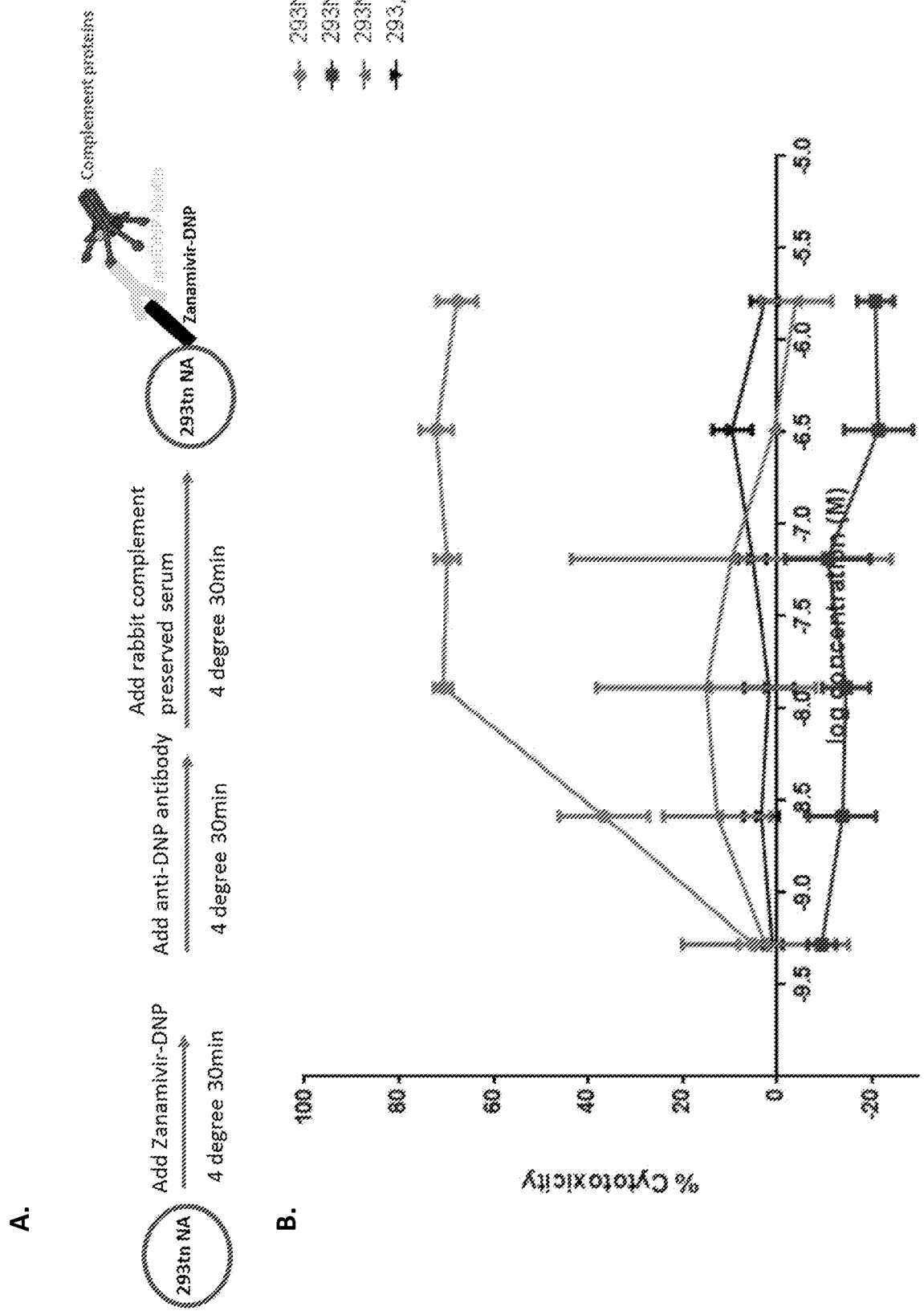
A.
293tn NA
Add Zanamivir-DNP
4 degree 30min
Add anti-DNP antibody
4 degree 30min
Add rabbit complement
preserved serum
4 degree 30min
293tn NA
Zanamivir-DNP
Complement proteins
B.
293NA, drug
293NA, competition
293NA, w/o antibody
293, (-) NA, drug
% Cytotoxicity
100
80
60
40
20
0
-20
-5.0
-5.5
-6.0
-6.5
-7.0
-7.5
-8.0
-8.5
-9.0
-9.5
log concentration (M)

FIGURE 25 A-B

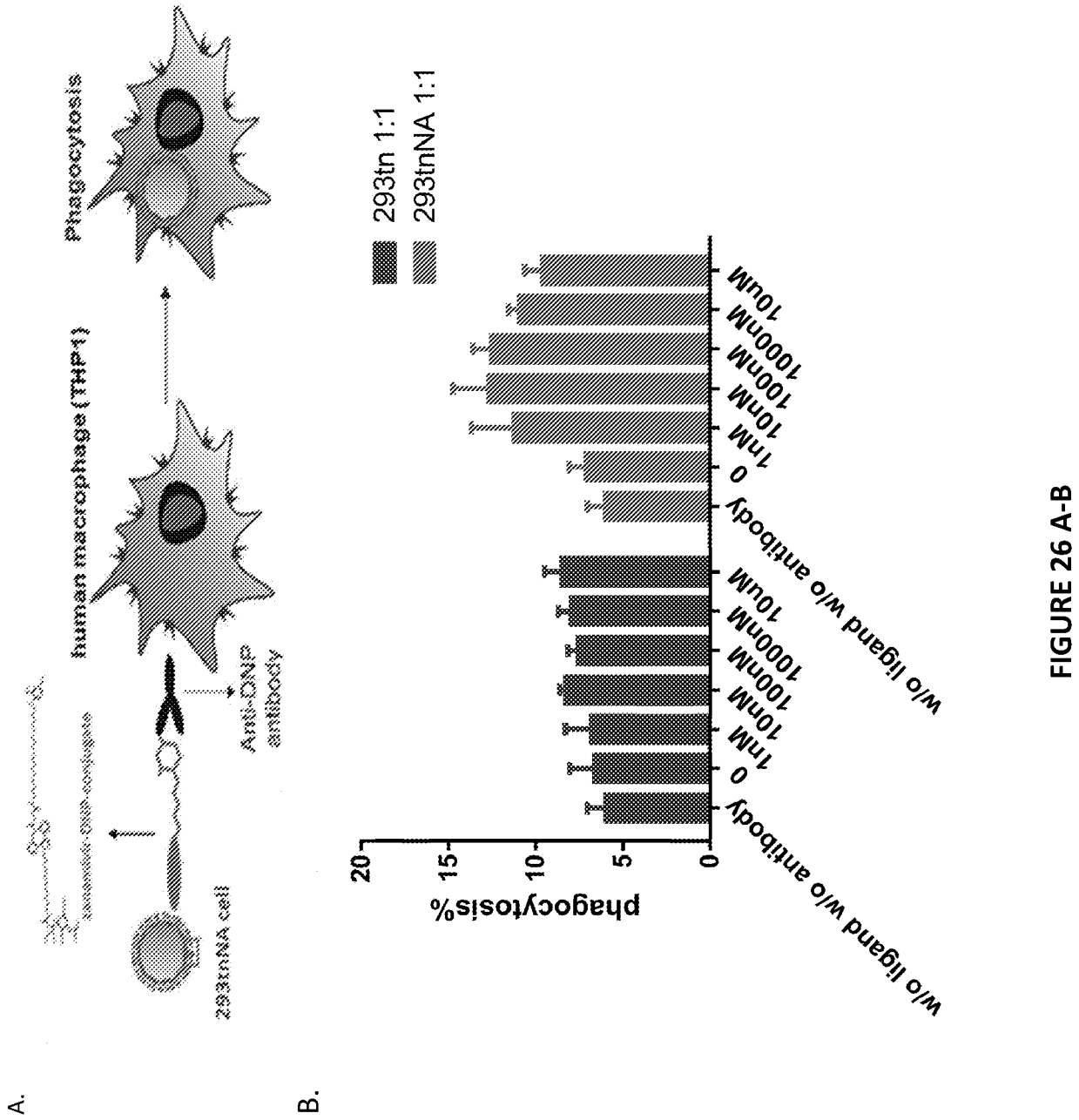
A.
293tnNA cell
human macrophage (THP1)
Phagocytosis
Anti-ONP antibody
B.
293tn 1:1
293tnNA 1:1
phagocytosis%
20
15
10
5
0
w/o ligand w/o antibody
0
1nM
10nM
100nM
1000nM
10uM
w/o ligand w/o antibody
0
1nM
10nM
100nM
1000nM
10uM

FIGURE 26 A-B

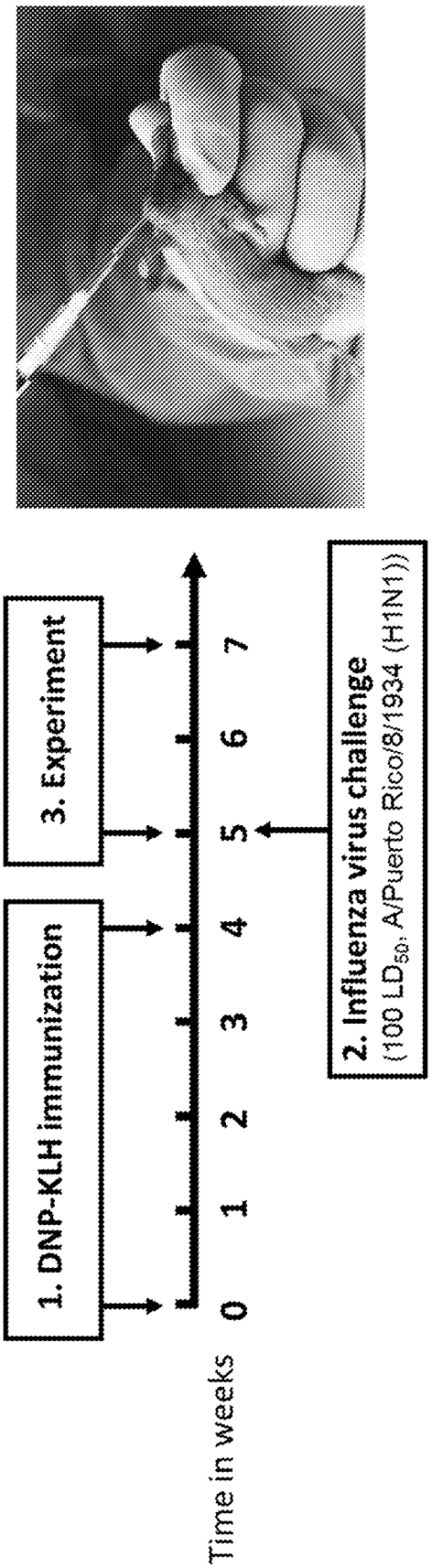
1. DNP-KLH immunization
3. Experiment
2. Influenza virus challenge
(100 LD_{50}, A/Puerto Rico/8/1934 (H1N1))
Time in weeks
0
1
2
3
4
5
6
7

FIGURE 27

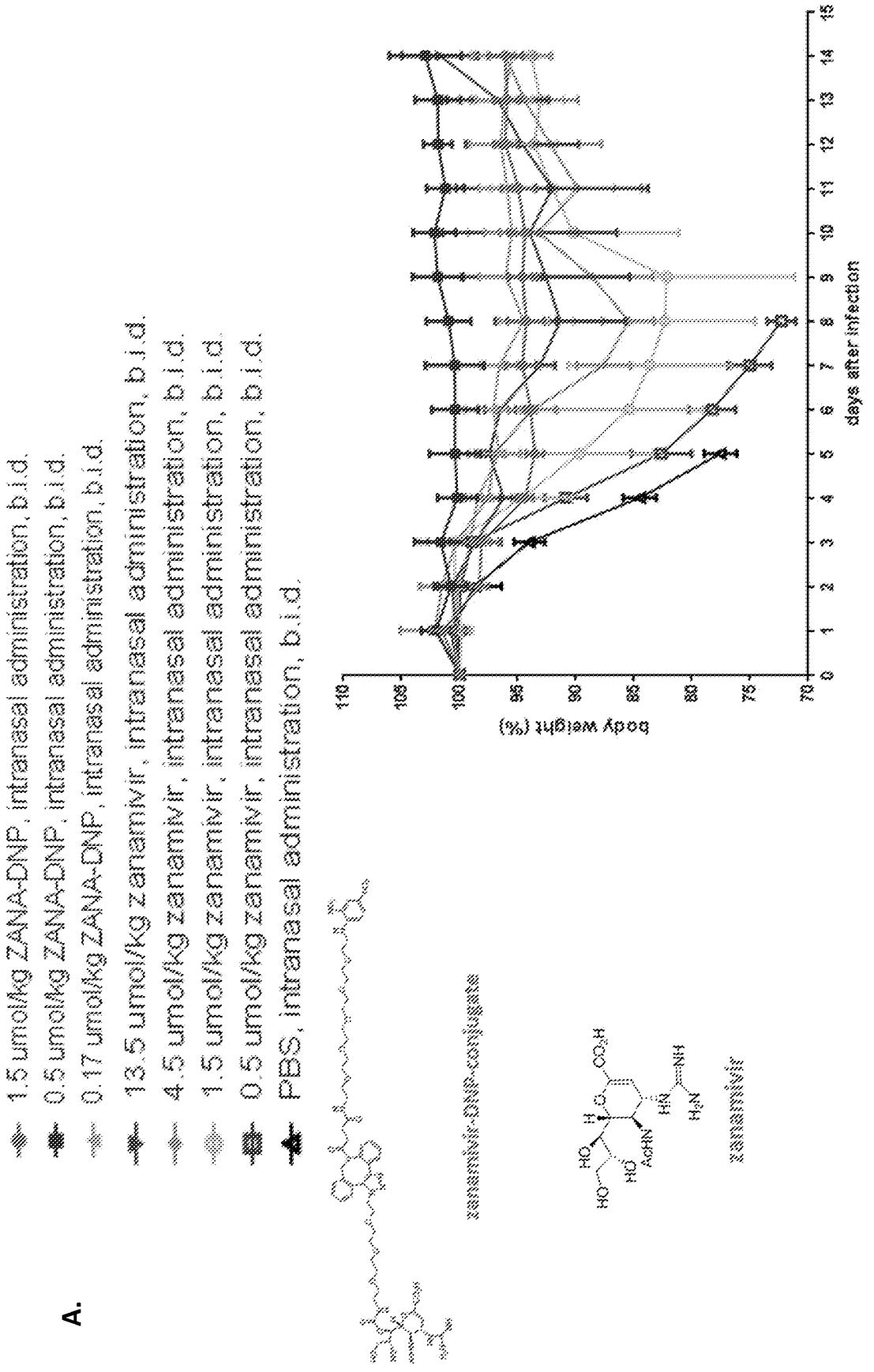
A.
1.5 umol/kg ZANA-DNP, intranasal administration, b.i.d.
0.5 umol/kg ZANA-DNP, intranasal administration, b.i.d.
0.17 umol/kg ZANA-DNP, intranasal administration, b.i.d.
13.5 umol/kg zanamivir, intranasal administration, b.i.d.
4.5 umol/kg zanamivir, intranasal administration, b.i.d.
1.5 umol/kg zanamivir, intranasal administration, b.i.d.
0.5 umol/kg zanamivir, intranasal administration, b.i.d.
PBS, intranasal administration, b.i.d.
body weight (%)
days after infection
zanamivir-DNP-conjugate
zanamivir

FIGURE 28A

B.

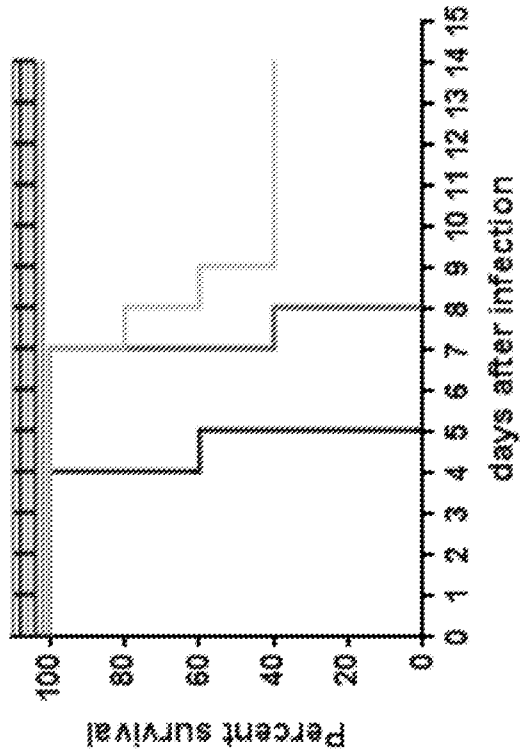
Percent survival
100
80
60
40
20
0
0 1 2 3 4 5 6 7 8 9 10 11 12 13 14 15
days after infection

FIGURE 28B

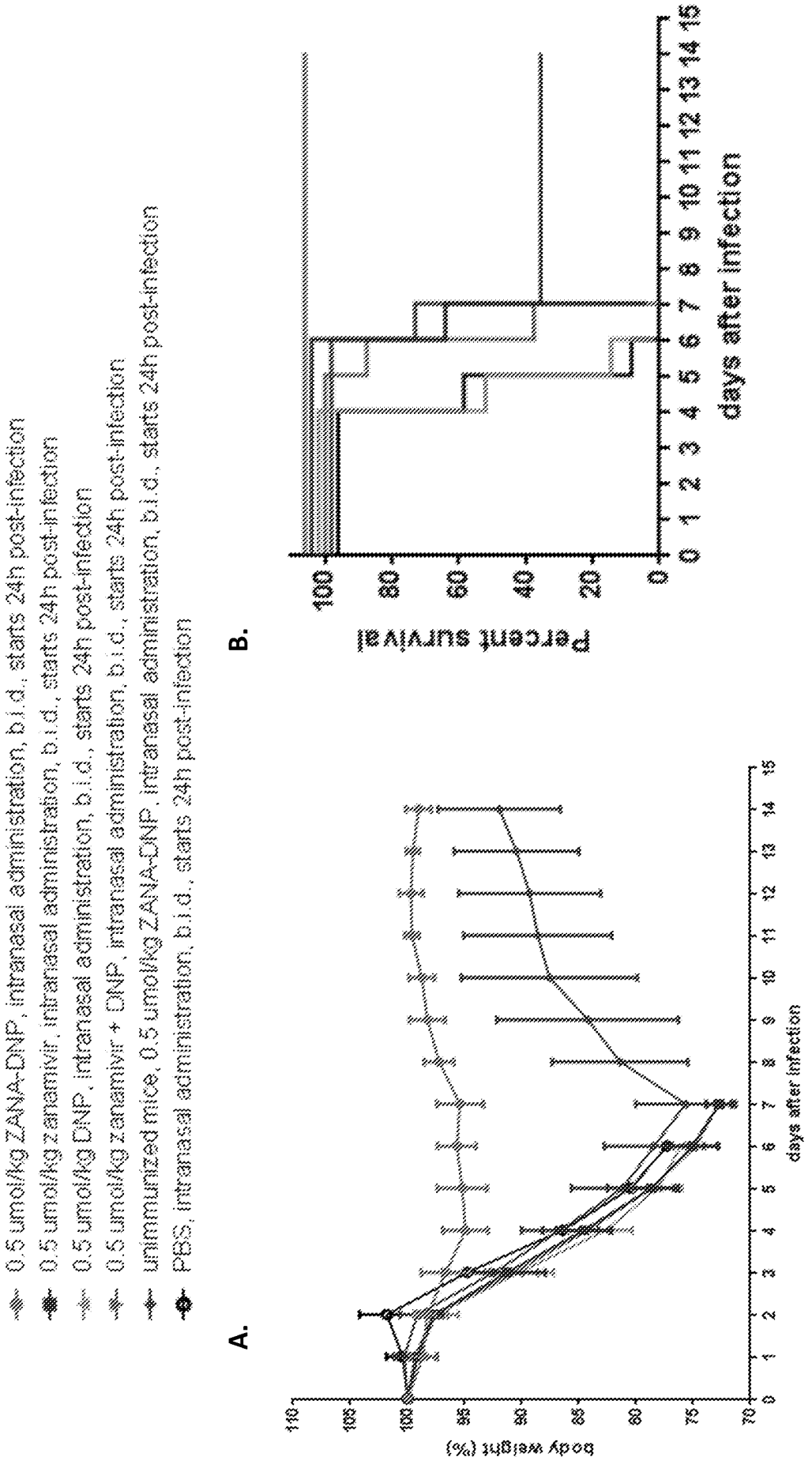
0.5 umol/kg ZANA-DNP, intranasal administration, b.i.d., starts 24h post-infection
0.5 umol/kg zanamivir, intranasal administration, b.i.d., starts 24h post-infection
0.5 umol/kg DNP, intranasal administration, b.i.d., starts 24h post-infection
0.5 umol/kg zanamivir + DNP, intranasal administration, b.i.d., starts 24h post-infection
unimmunized mice, 0.5 umol/kg ZANA-DNP, intranasal administration, b.i.d., starts 24h post-infection
PBS, intranasal administration, b.i.d., starts 24h post-infection
A.
body weight (%)
days after infection
B.
Percent survival
days after infection

FIGURE 29 A-B

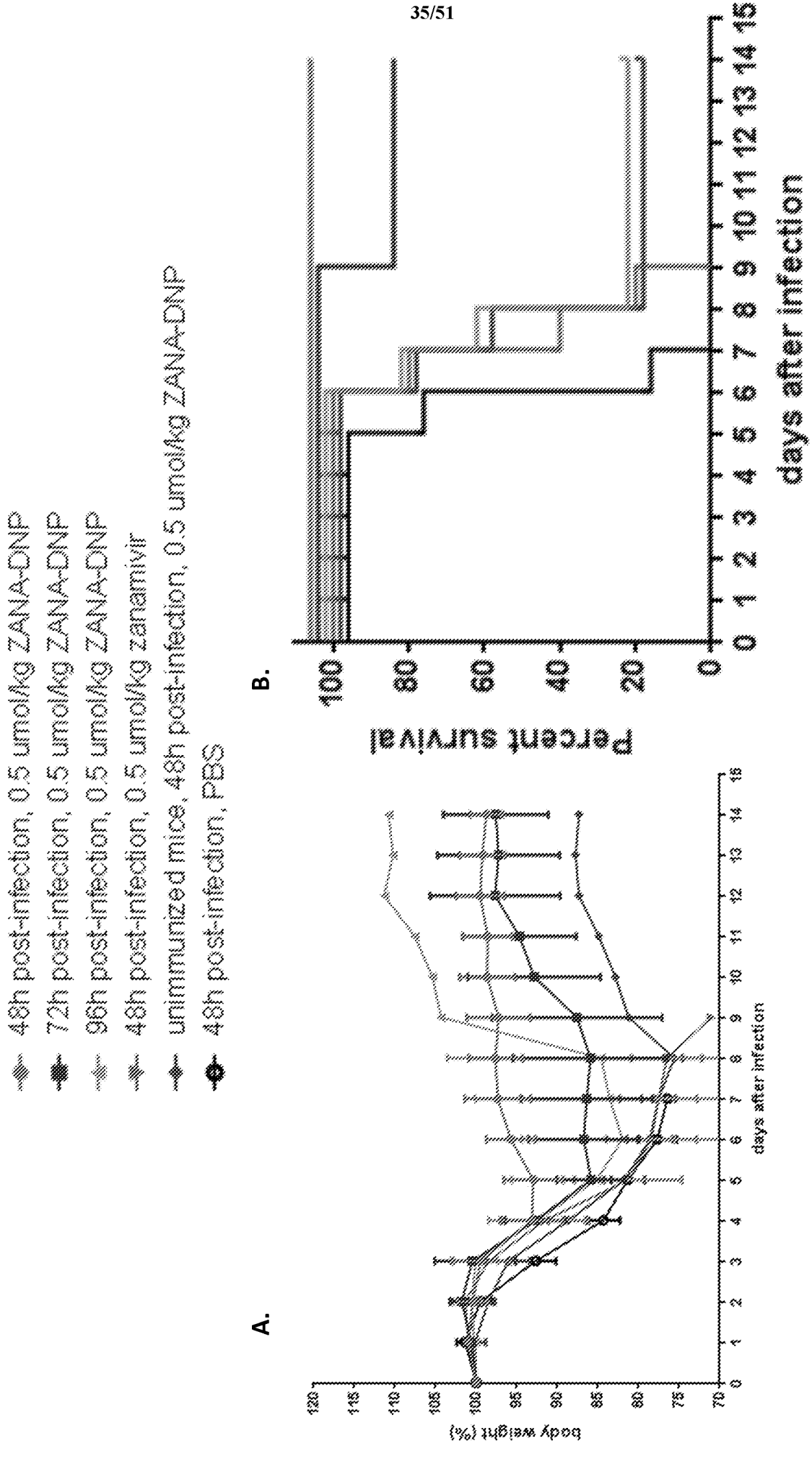
48h post-infection, 0.5 umol/kg ZANA-DNP
72h post-infection, 0.5 umol/kg ZANA-DNP
96h post-infection, 0.5 umol/kg ZANA-DNP
48h post-infection, 0.5 umol/kg zanamivir
unimmunized mice, 48h post-infection, 0.5 umol/kg ZANA-DNP
48h post-infection, PBS
A.
body weight (%)
days after infection
B.
Percent survival
days after infection

FIGURE 30 A-B

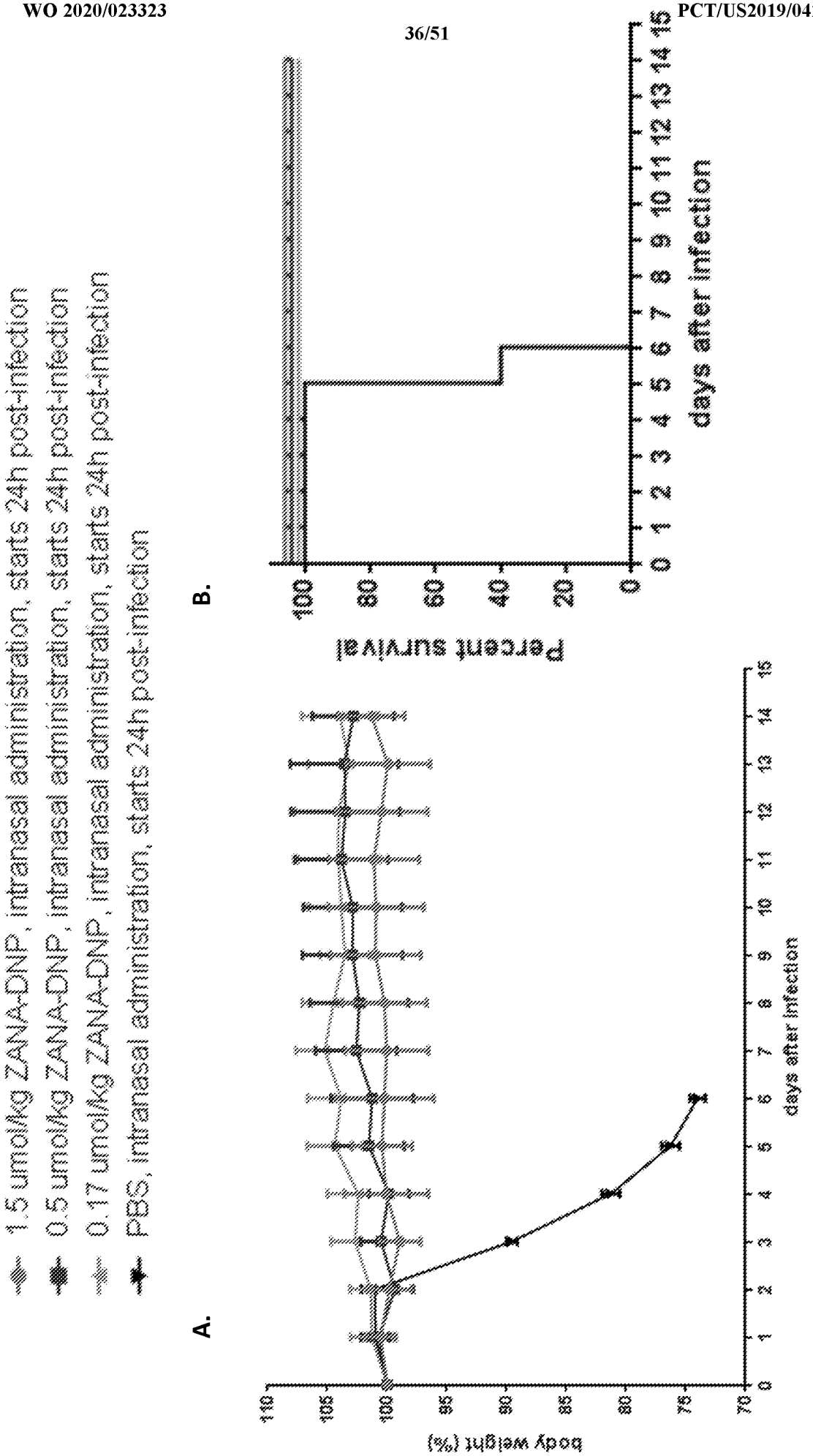
1.5 umol/kg ZANA-DNP, intranasal administration, starts 24h post-infection
0.5 umol/kg ZANA-DNP, intranasal administration, starts 24h post-infection
0.17 umol/kg ZANA-DNP, intranasal administration, starts 24h post-infection
PBS, intranasal administration, starts 24h post-infection
A.
body weight (%)
days after infection
B.
Percent survival
days after infection

FIGURE 31A-B

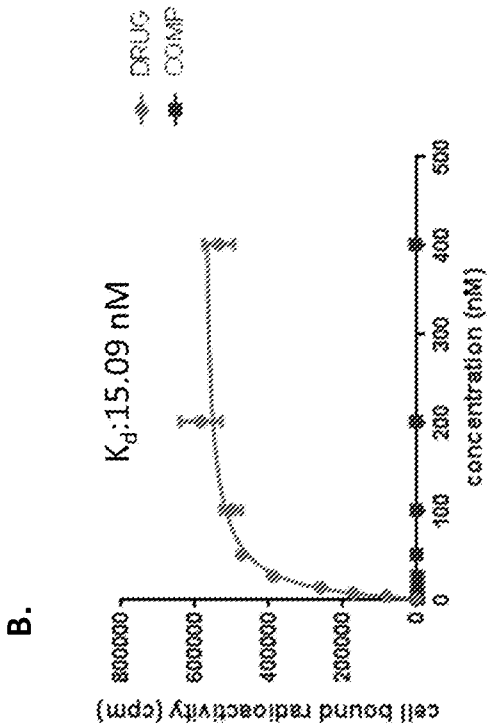
B.
DRUG
COMP
K_d:15.09 nM
cell bound radioactivity (cpm)
800000
600000
400000
200000
0
0
100
200
300
400
500
concentration (nM)

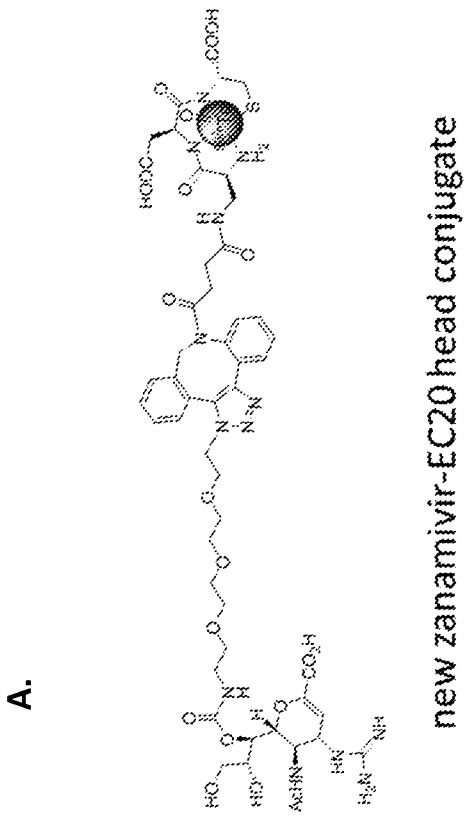
A.
new zanamivir-EC20 head conjugate

FIGURE 32A-B

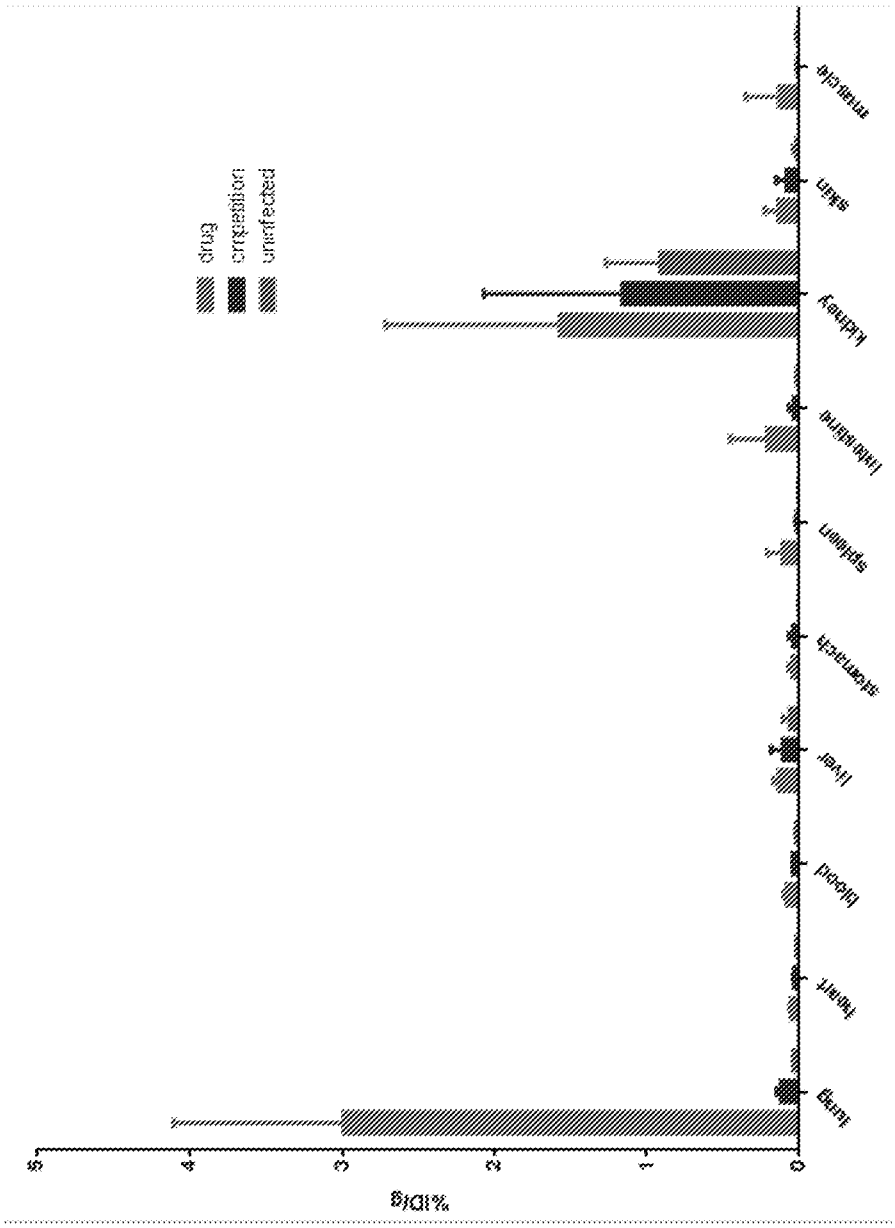
drug
organism
uninfected
%IDIg
0
2
4
6
Brain
Heart
Muscle
Skin
Bone
Liver
Spleen
Kidney
Intestine
Stomach

FIGURE 32 C

zanamivir-EC20 head

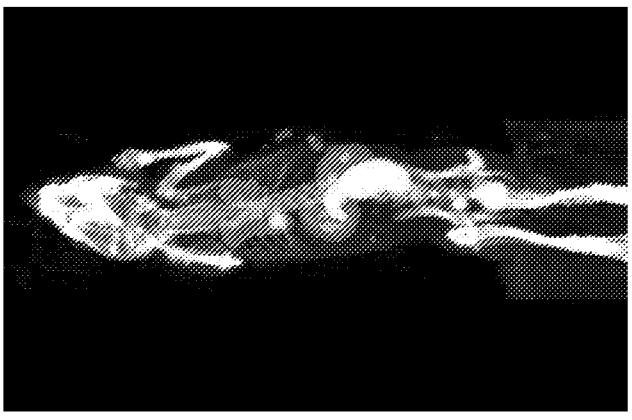

zanamivir-EC20 head
+100 x zanamivir

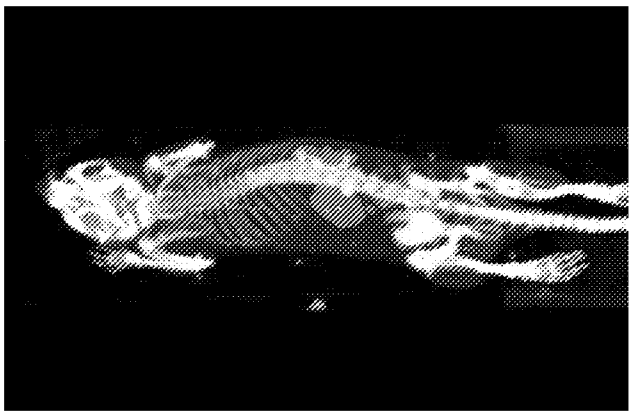

FIGURE 32D

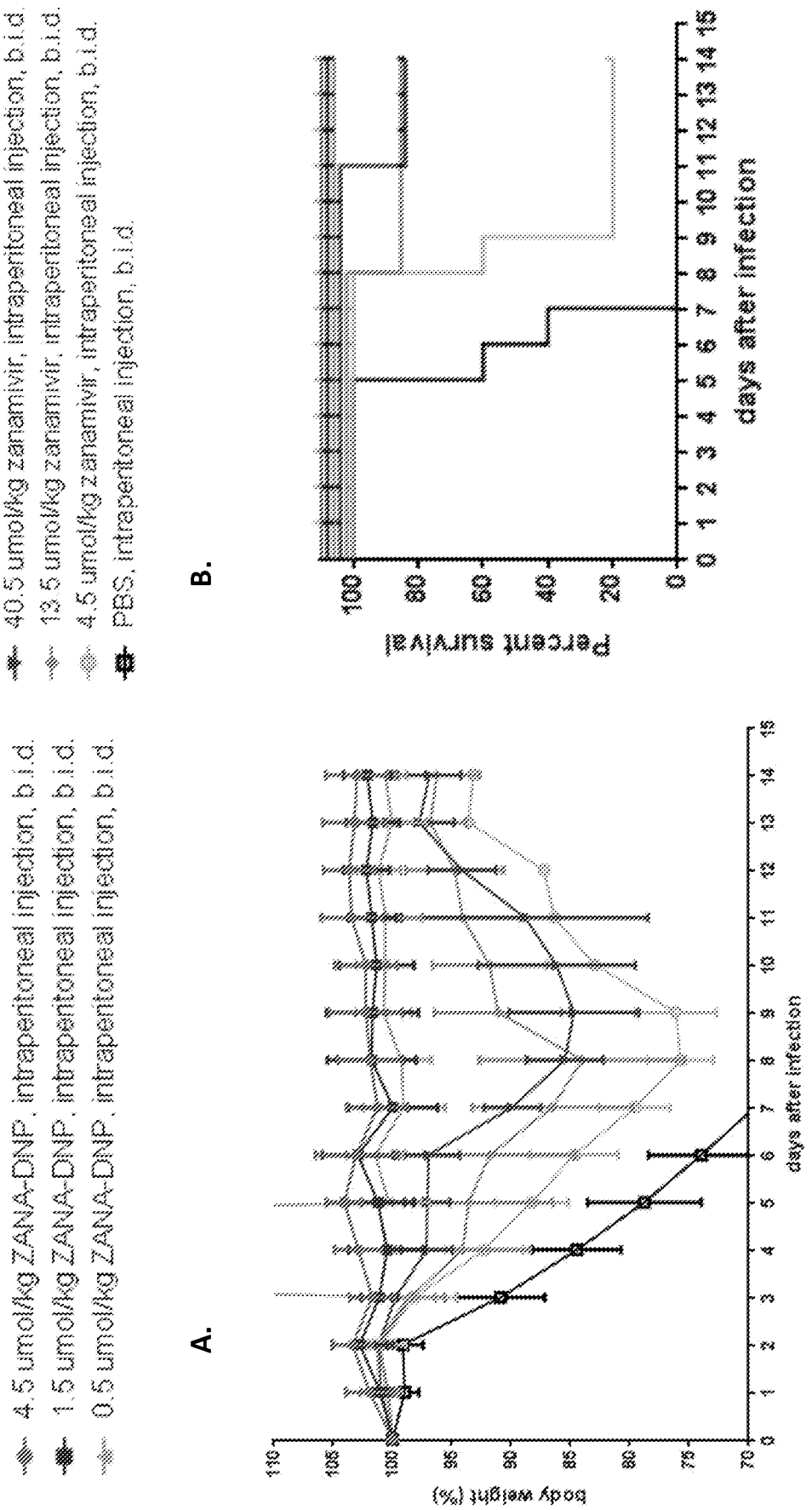
4.5 umol/kg ZANA-DNP, intrapentoneal injection, b.i.d.
1.5 umol/kg ZANA-DNP, intrapentoneal injection, b.i.d.
0.5 umol/kg ZANA-DNP, intrapentoneal injection, b.i.d.
A.
body weight (%)
days after infection
40.5 umol/kg zanamivir, intraperitoneal injection, b.i.d.
12.5 umol/kg zanamivir, intraperitoneal injection, b.i.d.
4.5 umol/kg zanamivir, intraperitoneal injection, b.i.d.
PBS, intraperitoneal injection, b.i.d.
B.
Percent survival
days after infection

FIGURE 33A-B

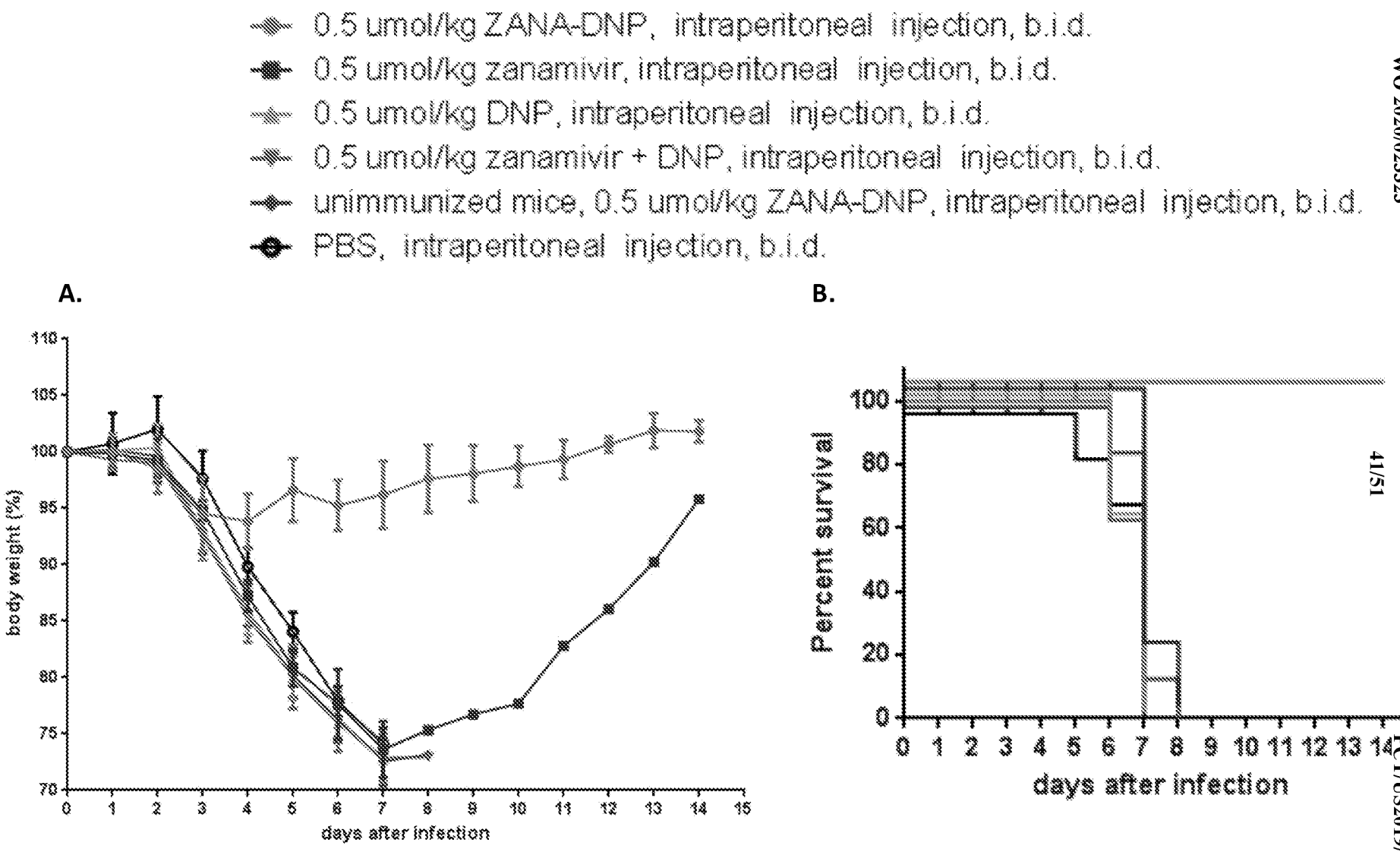

FIGURE 34 A-B

CA 03107778 2021-01-26

PCT/US2019/042715

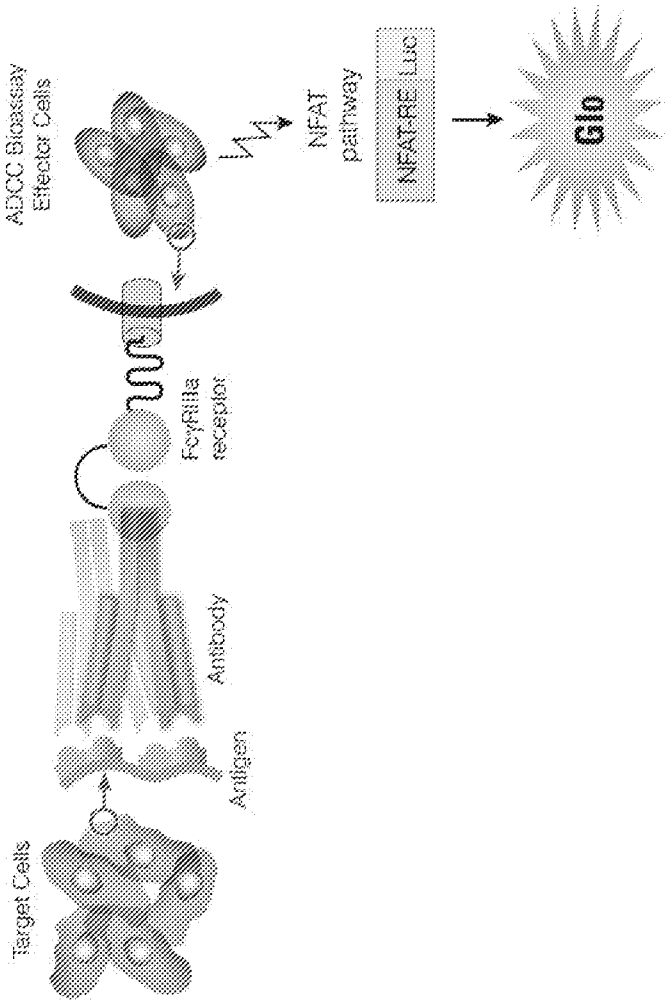
ADCC Bioassay
Effector Cells
NFAT
pathway
NFAT-RE Luc
Glo
FcγRIIIa
receptor
Antibody
Antigen
Target Cells

FIGURE 35A

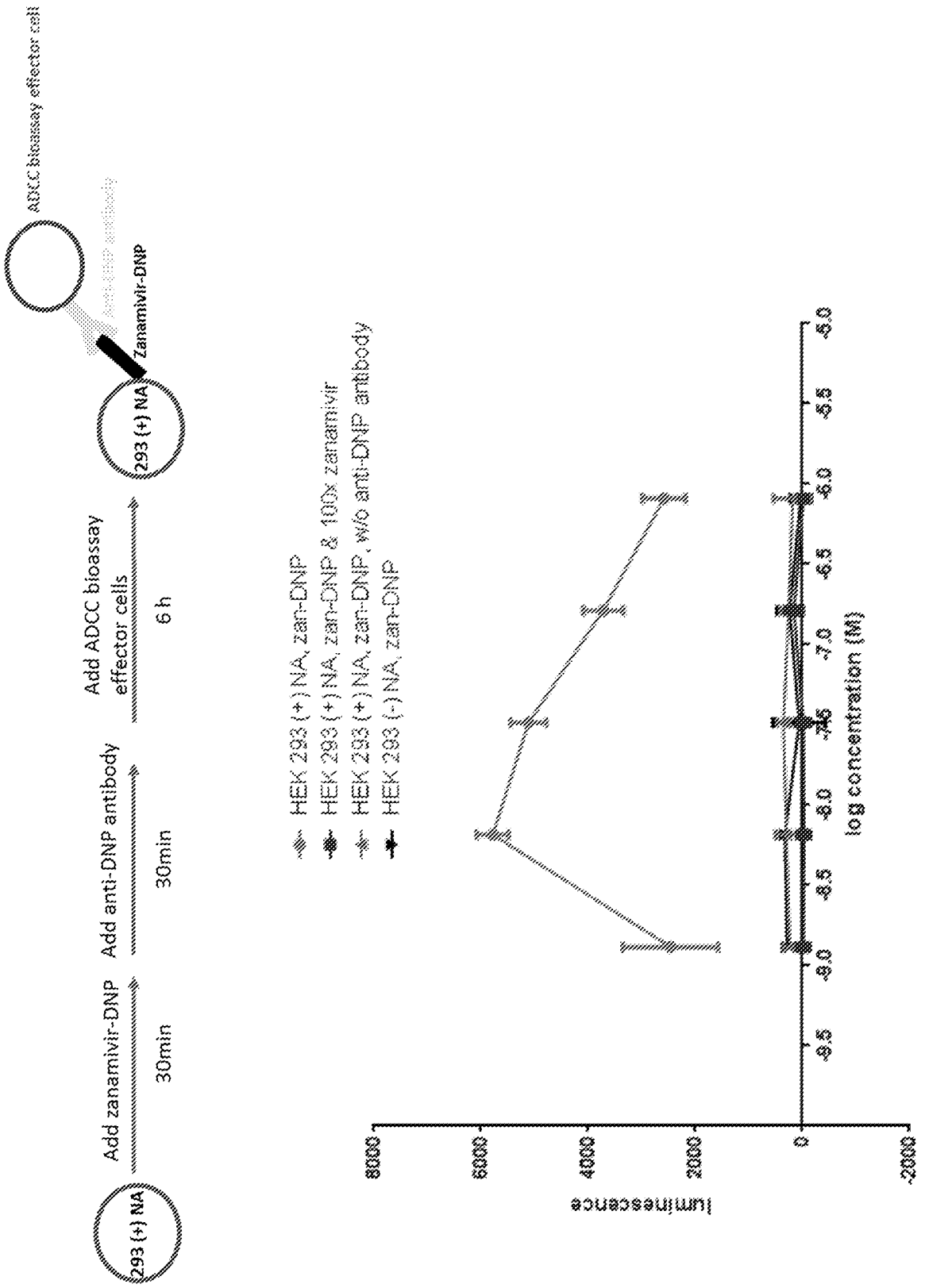
ADCC bioassay effector cell
Zanamivir-DNP
293 (+) NA
Add zanamivir-DNP
30min
293 (+) NA
Add anti-DNP antibody
30min
Add ADCC bioassay effector cells
6 h
HEK 293 (+) NA, zan-DNP
HEK 293 (+) NA, zan-DNP & 100x zanamivir
HEK 293 (+) NA, zan-DNP, w/o anti-DNP antibody
HEK 293 (-) NA, zan-DNP
luminescence
8000
6000
4000
2000
0
-2000
-9.5
-9.0
-8.5
-8.0
-7.5
-7.0
-6.5
-6.0
-5.5
-5.0
log concentration (M)

FIGURE 35B

A/Puerto Rico/8/34 (H1N1)
zanamivir
EC50: 1.9 nM
zanamivir-DNP conjugate
EC50: 1.7 nM
absorbance 450nm
log concentration (nM)
A
A/Aichi/2/1968 (H3N2)
zanamivir
EC50: 3.7 nM
zanamivir-DNP conjugate
EC50: 7.6 nM
absorbance 450nm
log concentration (nM)
B

FIGURE 36 A-B

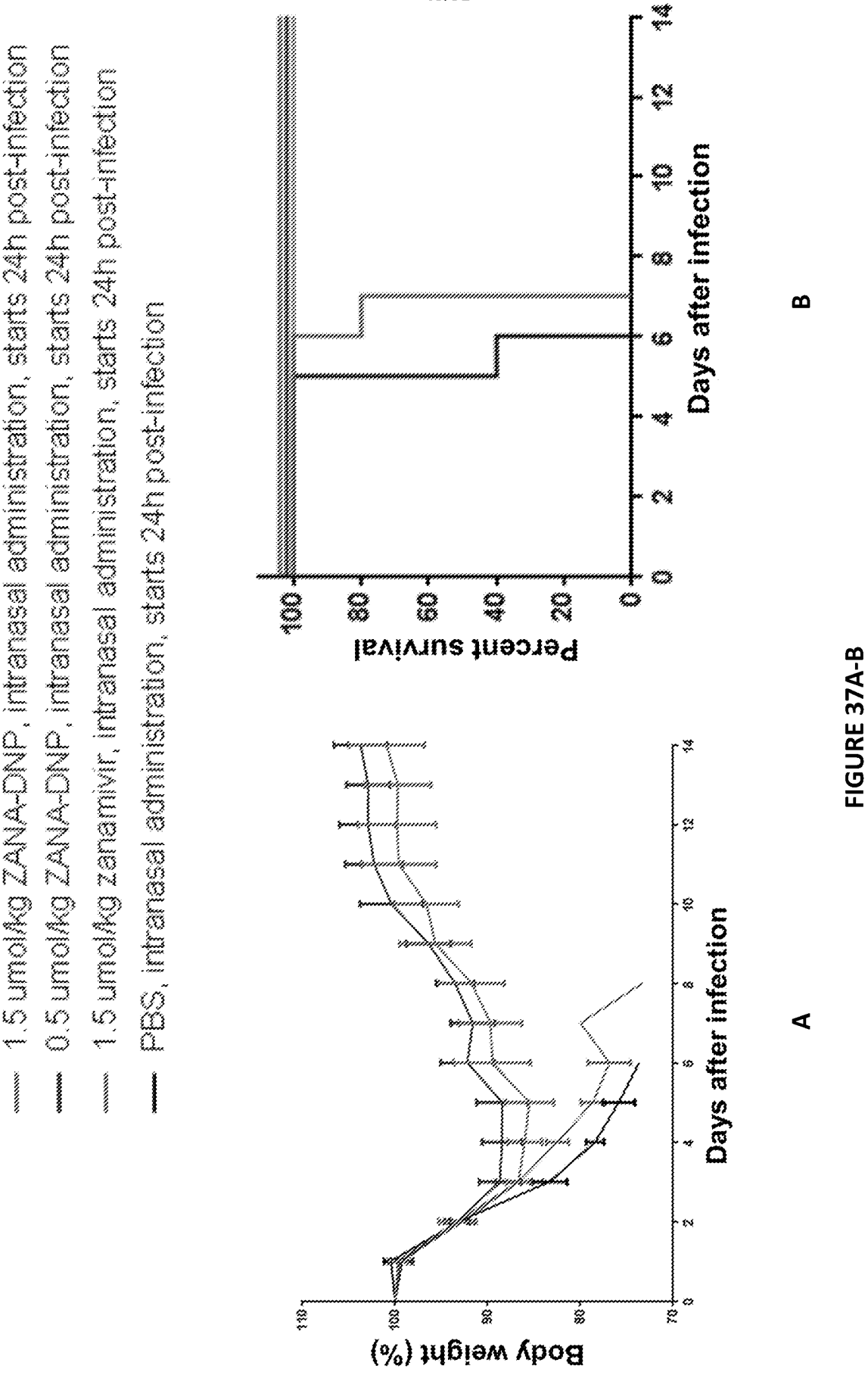
1.5 umol/kg ZANA-DNP, intranasal administration, starts 24h post-infection
0.5 umol/kg ZANA-DNP, intranasal administration, starts 24h post-infection
1.5 umol/kg zanamivir, intranasal administration, starts 24h post-infection
PBS, intranasal administration, starts 24h post-infection
Body weight (%)
Days after infection
A
Percent survival
Days after infection
B

FIGURE 37A-B

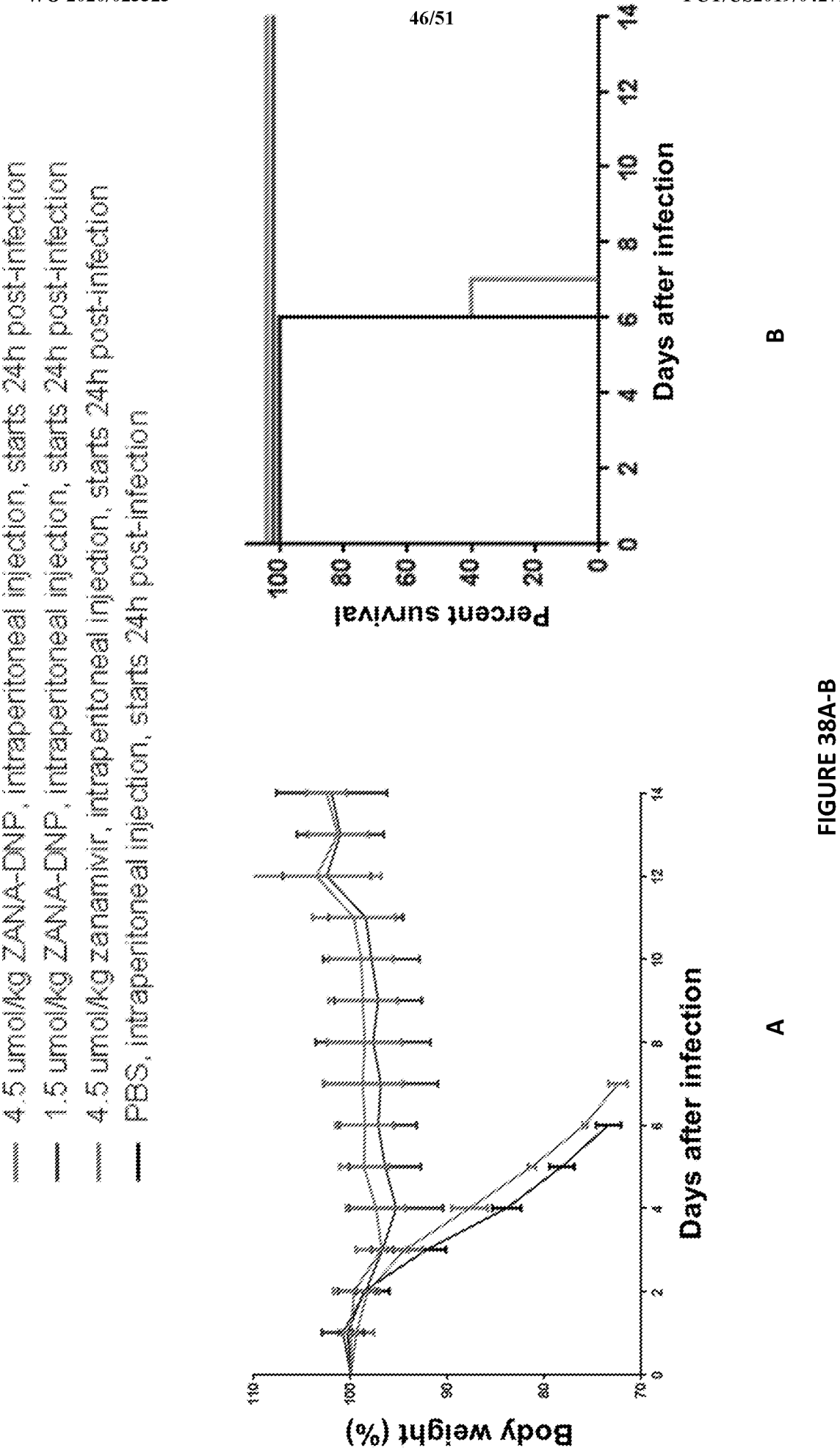
4.5 umol/kg ZANA-DNP, intraperitoneal injection, starts 24h post-infection
1.5 umol/kg ZANA-DNP, intraperitoneal injection, starts 24h post-infection
4.5 umol/kg zanamivir, intrapentoneal injection, starts 24h post-infection
PBS, intraperitoneal injection, starts 24h post-infection
Body weight (%)
Days after infection
A
Percent survival
Days after infection
B

FIGURE 38A-B

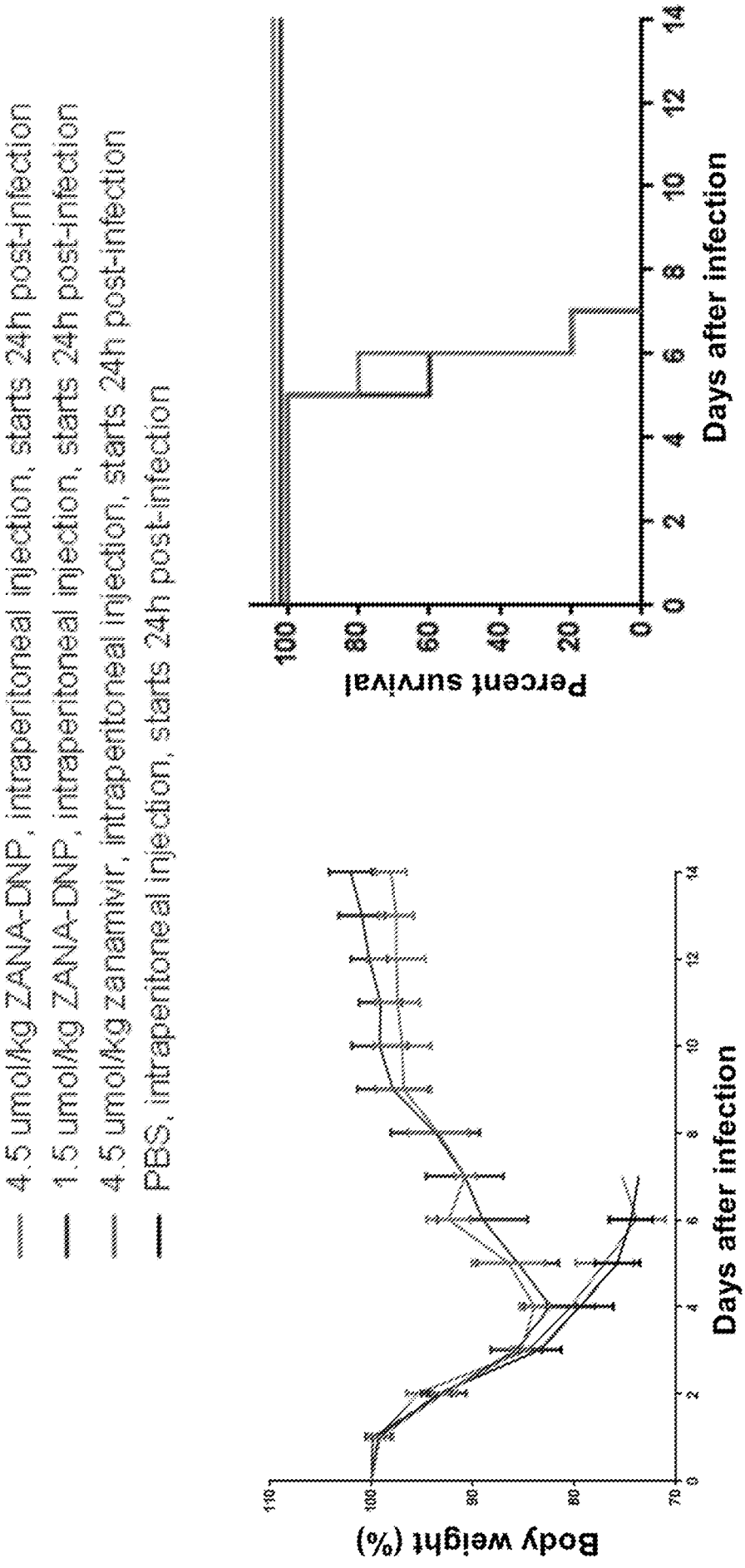
4.5 umol/kg ZANA-DNP, intraperitoneal injection, starts 24h post-infection
1.5 umol/kg ZANA-DNP, intraperitoneal injection, starts 24h post-infection
4.5 umol/kg zanamivir, intraperitoneal injection, starts 24h post-infection
PBS, intraperitoneal injection, starts 24h post-infection
Body weight (%)
Days after infection
A
Percent survival
Days after infection
B

FIGURE 39A-B

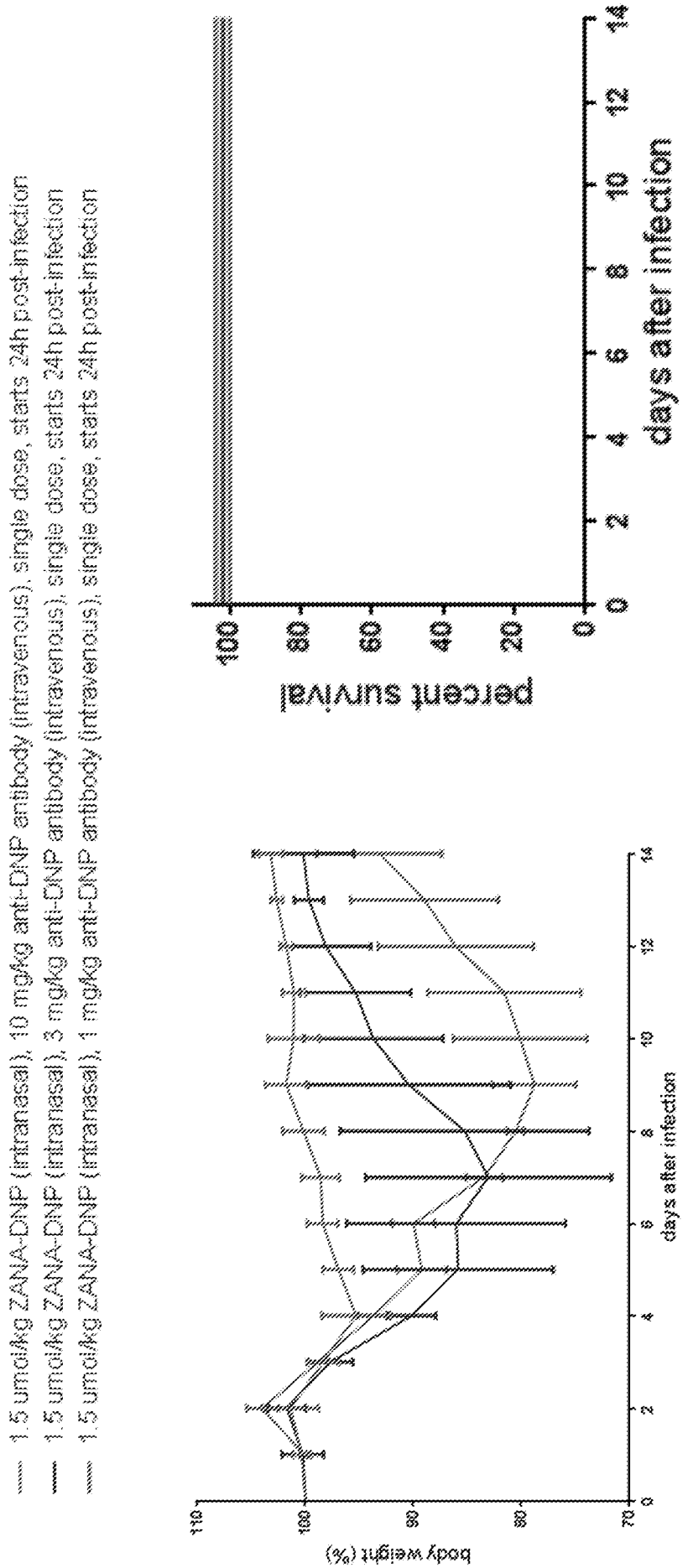
1.5 umol/kg ZANA-DNP (intranasal), 10 mg/kg anti-DNP antibody (intravenous), single dose, starts 24h post-infection
1.5 umol/kg ZANA-DNP (intranasal), 3 mg/kg anti-DNP antibody (intravenous), single dose, starts 24h post-infection
1.5 umol/kg ZANA-DNP (intranasal), 1 mg/kg anti-DNP antibody (intravenous), single dose, starts 24h post-infection
body weight (%)
days after infection
percent survival
days after infection
A
B

FIGURE 40 A-B

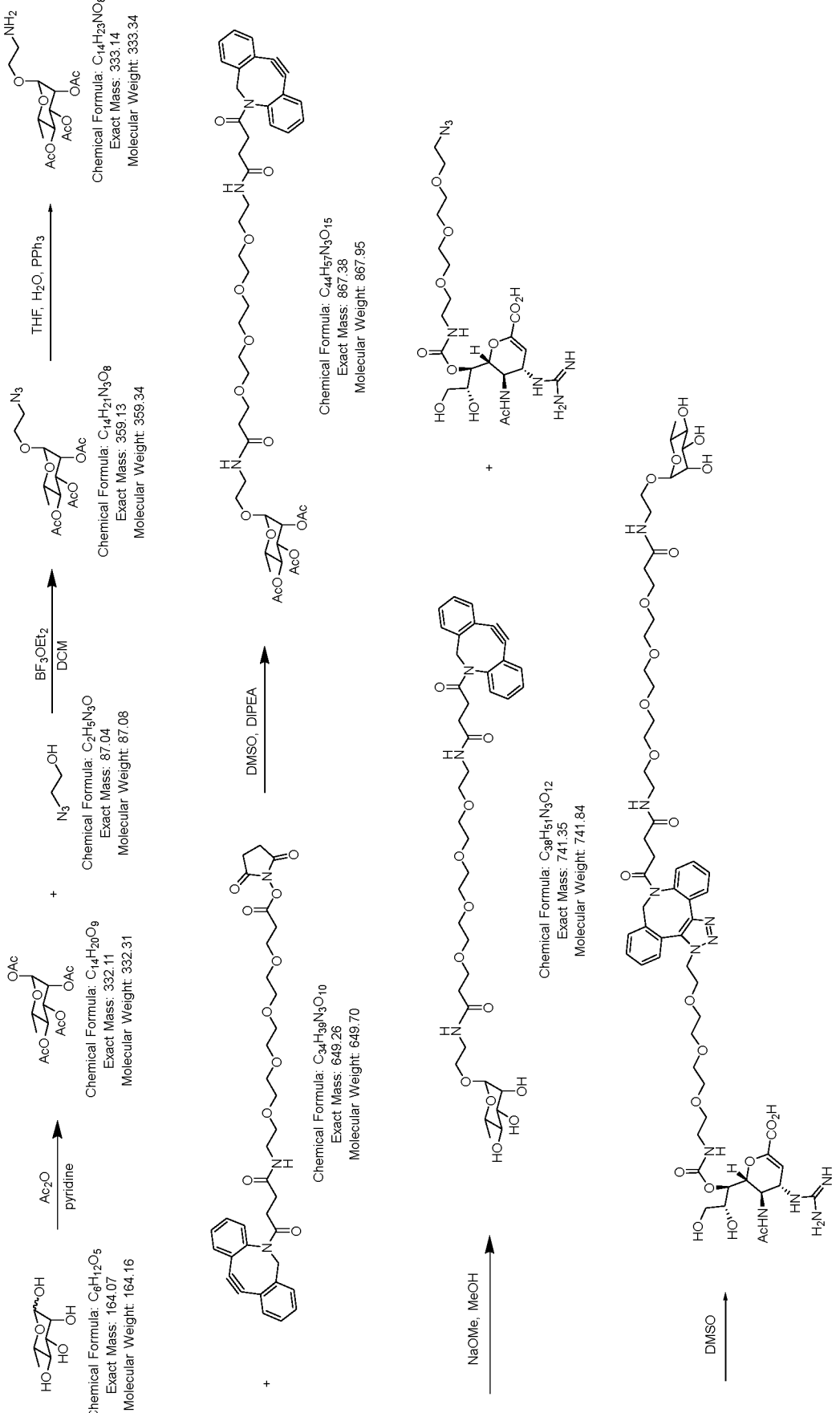
Ac2O
pyridine
BF3OEt2
DCM
THF, H2O, PPh3
DMSO, DIPEA
NaOMe, MeOH
DMSO
Chemical Formula: C6H12O5
Exact Mass: 164.07
Molecular Weight: 164.16
Chemical Formula: C14H20O9
Exact Mass: 332.11
Molecular Weight: 332.31
Chemical Formula: C2H5N3O
Exact Mass: 87.04
Molecular Weight: 87.08
Chemical Formula: C14H21N3O8
Exact Mass: 359.13
Molecular Weight: 359.34
Chemical Formula: C14H23NO8
Exact Mass: 333.14
Molecular Weight: 333.34
Chemical Formula: C34H39N3O10
Exact Mass: 649.26
Molecular Weight: 649.70
Chemical Formula: C44H57N3O15
Exact Mass: 867.38
Molecular Weight: 867.95
Chemical Formula: C38H51N3O12
Exact Mass: 741.35
Molecular Weight: 741.84

FIGURE 41

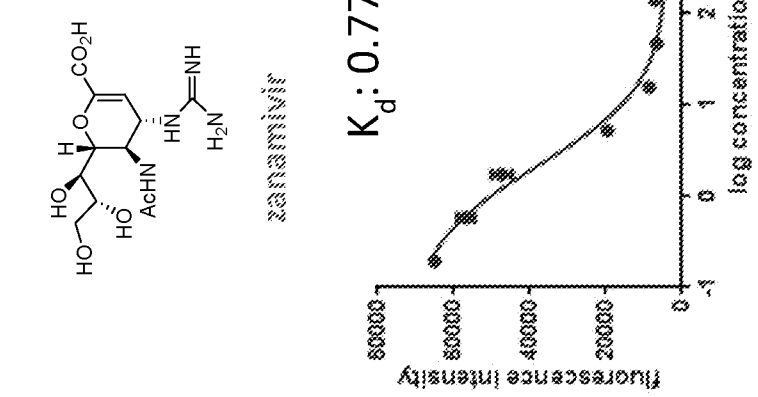
zanamivir
K_d: 0.77 nM
fluorescence intensity
log concentration (nM)
A

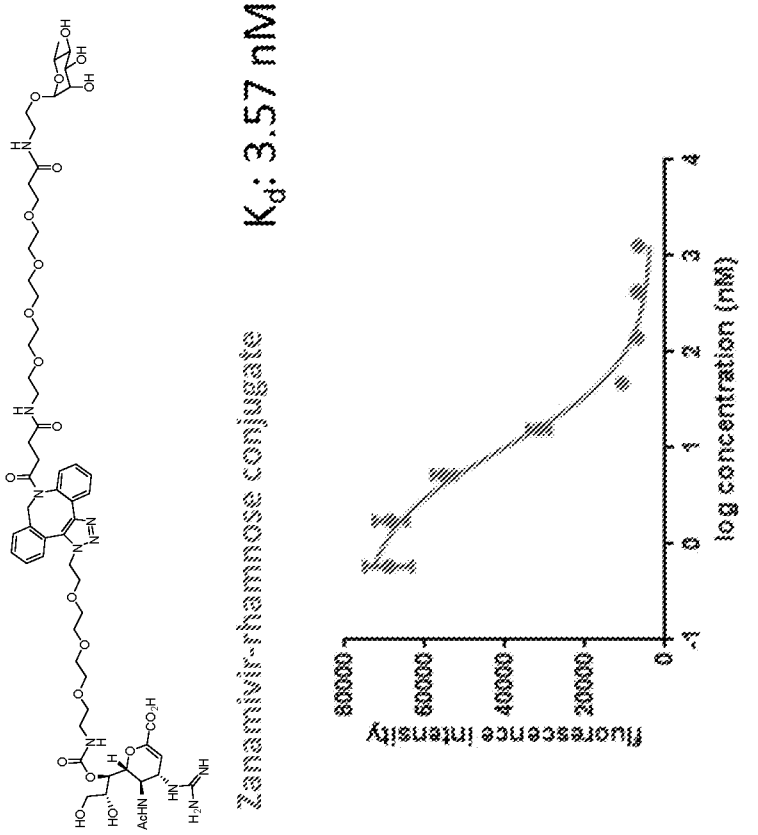
zanamivir-rhamnose conjugate
K_d: 3.57 nM
fluorescence intensity
log concentration (nM)
B

FIGURE 42A-B

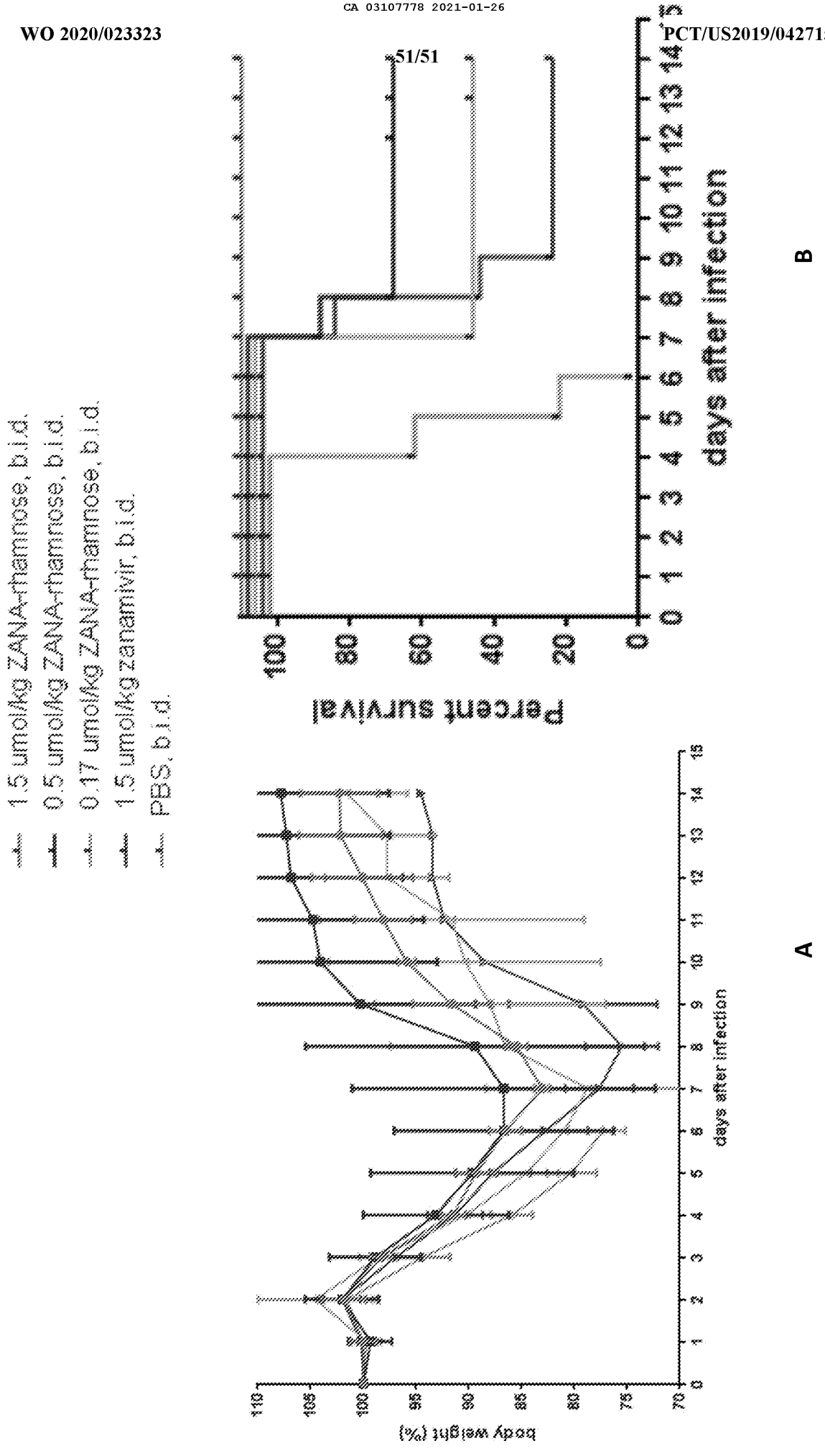
1.5 umol/kg ZANA-rhamnose, b.i.d.
0.5 umol/kg ZANA-rhamnose, b.i.d.
0.17 umol/kg ZANA-rhamnose, b.i.d.
1.5 umol/kg zanamivir, b.i.d.
PBS, b.i.d.
Percent survival
days after infection
B
body weight (%)
days after infection
A

FIGURE 43A-B

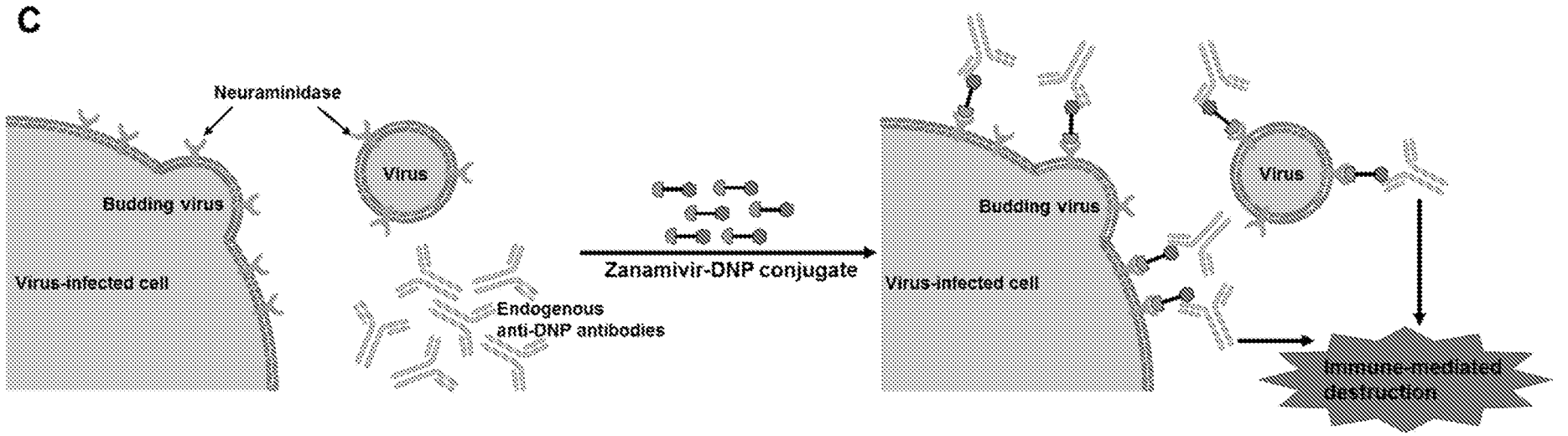
C
Neuraminidase
Virus
Budding virus
Virus-infected cell
Endogenous
anti-DNP antibodies
Zanamivir-DNP conjugate
Budding virus
Virus
Virus-infected cell
Immune-mediated
destruction

FIGURE 20C